Horizontal Shear Strength at the Interface of the Concrete Beams Cast in Two Time Stages

مقاومة القص الأفقي على الواجهة البينية للعارضات الخرسانية المصبوبة في مرحلتين زمنيتين مختلفتين

by

HATEM ADY ABUSHAABAN

Dissertation submitted in fulfilment

of the requirements for the degree of

MSc STRUCTURAL ENGINEERING

at

The British University in Dubai

December 2020

DECLARATION

I warrant that the content of this research is the direct result of my own work and that any use made in it of published or unpublished copyright material falls within the limits permitted by international copyright conventions.

I understand that a copy of my research will be deposited in the University Library for permanent retention.

I hereby agree that the material mentioned above for which I am author and copyright holder may be copied and distributed by The British University in Dubai for the purposes of research, private study or education and that The British University in Dubai may recover from purchasers the costs incurred in such copying and distribution, where appropriate.

I understand that The British University in Dubai may make a digital copy available in the institutional repository.

I understand that I may apply to the University to retain the right to withhold or to restrict access to my thesis for a period which shall not normally exceed four calendar years from the congregation at which the degree is conferred, the length of the period to be specified in the application, together with the precise reasons for making that application.

____

Signature of the student

COPYRIGHT AND INFORMATION TO USERS

ABSTRACT

Composite concrete is a method of construction that uses both precast and cast in situ concrete to produce a structural element. In framing big slabs areas, the use of precast slabs and beams is being an economical way of construction. The best procedure is to employ beams of inverted T section, which bottom flange will act as a ledge to seat the precast slab. Topping concrete slab is then cast on top of the precast slabs and beams. It is cleaner and safer than the full cast in place construction. This kind of construction which is cast in two stages at different times reduces the quantities of formworks at site and reduces the back propping which in some cases is required to be extended below to multiple levels according to the expected construction loading. Accordingly, more clear spaces for lower levels will be available so that other site activities can be accomplished to complete the job faster with less building materials and reduced risk levels.

The bond strength between the precast concrete part and the cast in place part is essential to provide the monolithic behavior for the composite concrete members. The integrated monolithic behavior is achieved only if all forces including the horizontal shear are fully transferred at the interface. From the structural normal practice, the word “interface” means the plane between two different materials; such as concrete to steel or concrete to concrete that is cast in stages at different ages. This interface which is studied in this dissertation is that the plane between the precast and the cast in situ parts of the composite concrete beams.

The rough surface of the precast beam part, aggregate interlock, concrete strength and the steel bars crossing the interface between the cast in place and precast parts are the main factors that affect the horizontal shear strength of the that interface.

The international design codes propose semi empirical equations to determine the horizontal shear strength considering adhesion, friction caused by normal stress and friction caused by interface steel rebar clamping stress. Usually the experimental tests are done on series of specimens of small size and in some other cases, are done on small sized composite beams of short span that can be accommodated in a concrete testing facility.

The small specimens testing somehow reduced the level of reliability of the results. Accordingly, there is a considerable difference in the proposed interface shear strength limits between the different structural design codes.

This dissertation presents a study of four composite beams with different sections, properties and reinforcement that were experimented for shear friction in a previous research. The beams are modeled using a 3D finite element software. A shear friction design hand calculation is provided as well using the provisions and equations proposed by the code of practice.

The dissertation provides a comparison between simplified code approach, 3D finite element model and results from the experimental work published by Anil Patnaik at 1992.

الملخص

يعتبر البناء الخرساني المركب طريقة بناء تستخدم كل من الخرسانة مسبقة الصب والخرسانة المصبوبة في الموقع لإنتاج العنصر الإنشائي. إنه أنظف وأكثر أماناً من البناء المصبوب بالكامل في الموقع. إن استخدام هذا النظام لإنشاء بلاطات الأسقف ذات المساحات الكبيرة يعتبر نظاماً إنشائياً اقتصادياً. الطريقة المثالية هي بتوظيف العوارض على شكل الحرف T مقلوباً، حيث ستعمل الحافة السفلية كمقعد استناد لترتكز عليها البلاطة مسبقة الصب. يتم بعد ذلك صب الجزء العلوي فوق الألواح والعوارض سابقة الصب. هذا النوع من البناء الذي يتم صبه على مرحلتين في أوقات مختلفة يقلل من كمية قوالب الصب المطلوبة ويقلل أيضاً من عدد الدعامات الخلفية التي تتطلب في بعض الحالات تثبيتها في طوابق سفلية متعددة وفقًا لأحمال البناء المتوقعة. وبالتالي، ستتوفر مساحات أكبر في تلك الطوابق بحيث يمكن إنجاز أنشطة البناء الأخرى لإكمال العمل بشكل أسرع و بأقل مواد بناء وبأقل خطورة.

تعتبر قوة الرابطة بين الجزء الخرساني المسبق الصب والجزء المصبوب في المكان أمراً ضرورياً لتحقيق السلوك المتكامل للعناصر الخرسانية المركبة. يتم تحقيق هذا السلوك فقط إذا انتقلت جميع القوى بما فيها قوه القص الأفقي بشكل كامل من خلال الواجهة. كلمة "واجهة" في المجال الهندسي تعني السطح البيني بين مادتين مختلفتين؛ مثل الخرسانة إلى الصلب أو الخرسانة إلى الخرسانة التي تصب على مراحل في أزمنة مختلفة. في هذا البحث سيكون التركيز على الواجهة بين جزئي العارضة الخرسانية المركبة.

يعد السطح الخشن لجزء العارضة مسبقة الصب، والتشابك الكلي للركام مع باقي المكونات الخرسانية، وقوة الخرسانة و مقاومتها للضغط، والقضبان الحديدية التي تعبر الواجهة بين الجزء المصبوب في مكانه و الجزء الخرساني المسبق الصب من العوامل الرئيسية التي تؤثر على مدى مقاومة قوى القص الأفقية لتلك الواجهة.

تقترح أكواد التصميم العالمية معادلات استنباطية لتحديد قوة القص الأفقية مع الأخذ بعين الاعتبار عوامل الالتصاق والاحتكاك الناجم عن الإجهاد المتعامد والاحتكاك الناجم عن إجهاد تثبيت حديد التسليح للواجهة. عادةً ما يتم إجراء الاختبارات التجريبية على سلسلة من عينات الاختبار صغيرة الحجم، وفي بعض الأحيان يتم اختبار العارضات المركبة ذات المقطع الصغير و ذات الطول القصير والتي يمكن استيعابها في منشأة اختبار الخرسانة. اختبارات العينات هذه إلى حد ما خفضت مستوى موثوقية النتائج. و وفقاً لذلك، هناك فرق كبير في حدود قوة القص الأفقي للواجهة المقترحة بين أكواد التصميم الإنشائي المختلفة.

تقدم هذه الرسالة دراسة لأربعة نماذج لعارضات مركبة مختلفة المقاطع و الخواص و حديد التسليح والتي تم اختبارها عملياً لاحتكاك القص في بحث سابق. يتم نمذجة العارضة باستخدام برنامج نموذج العناصر المحدودة ثلاثي الأبعاد، ويتم عرض النتائج ومقارنتها بالتجربة التي تم إجراؤها مسبقاً. و سوف يتم أيضاً تقديم حسابات يدوية لتصميم احتكاك القص باستخدام الأحكام والمعادلات المقترحة بواسطة كود الممارسة الإنشائي.

سوف تقدم الرسالة مقارنة بين المقاربة المبسطة للكود الإنشائي و برنامج نموذج العناصر المحدودة ثلاثي الأبعاد و نتائج التجارب العملية التي قام أنيل باتنايك بنشرها عام 1992.

ACKNOWLEDGEMENTS

I would like to express my sincere appreciation to my advisor Professor Abid Abu-Tair for his guidance and continued support throughout the research. Professor Abid was the main source of teaching, advising and guiding me for my whole program of the masters in structural engineering.

I am also very thankful to my friends; the graduate students and colleagues for their help and valuable advices and suggestions throughout the research process.

I am very grateful to my father and mother who raised me to have the confidence and faith to achieve my goals in life.

The special thanks and appreciation go to my wife who supported me from the beginning to take this challenge. She was beside me through all times with patience, support and love.

TABLE OF CONTENTS:

1. **INTRODUCTION**……1
1.1 Mechanical Properties and Behavior of Concrete and Steel……3
1.1.1 Concrete Behavior in Uniaxial Stress State……3
Concrete Properties in Compression……3
Concrete Properties in Tension……5
1.1.2 Concrete Behavior in Biaxial Stress State……5
1.1.3 Reinforcing Steel Properties……6
1.2 Horizontal Shear in Composite Sections……7

2. **LITERATURE REVIEW**……8
2.1 Introduction……8
2.2 Shear-Friction Hypothesis……10
2.3 The Experimental Evaluation of The Interface Shear Strength……15
2.3.1 Push-off Test……17
2.4 Determination of the Horizontal Shear Failure……25
2.5 Maximum Slip……25
2.6 Surface Preparation……25
2.7 Development Analysis of the horizontal Shear Stresses……27
2.8 Shear-Friction Design Expressions – Historical Development……28
2.8.1 Anderson (1960)……29
2.8.2 Hanson (1960)……29
2.8.3 Mattock and Kaar (1961)……29
2.8.4 Grossfield and Birnstiel (1962)……30
2.8.5 Saemann and Washa (1964)……30
2.8.6 Gaston and Kriz (1964)……30
2.8.7 Birkeland and Birkeland, (1966)……31
2.8.8 Badoux and Hulsbos (1967)……31
2.8.9 Birkeland (1968)……32
2.8.10 Mast (1968)……32
2.8.11 Hofbeck, Ibrahim and Mattock (1969)……33
2.8.12 Mattock and N.M. Hawkins (1972)……33
2.8.13 Mattock (1974)……34
2.8.14 Hermansen and Cowan (1974)……35
2.8.15 Cowan and Cruden (1975)……35

2.8.16 Mattock, Li and Wang (1976)……35
2.8.17 Raths (1977)……36
2.8.18 Shaikh (1978)……36
2.8.19 Loov (1978)……37
2.8.20 Mattock (1981)……38
2.8.21 Vecchio and Collins (1986)……38
2.8.22 Walraven, Frenay and Pruijssers (1987)……39
2.8.23 Mattock (1988)……40
2.8.24 Mau and Hsu (1988)……41
2.8.25 Anil Patnaik (1992)……41
2.8.26 Loov and Patnaik (1994)……41
2.8.27 Mattock (1994)……42
2.8.28 Valluvan, Kreger and Jirsa (1999)……43
2.8.29 Patnaik (2000)……43
2.8.30 Mattock (2001)……44
2.8.31 Patnaik (2001)……45
2.8.32 Kahn and Mitchell (2002)……46
2.8.33 Gohnert (2003)……46
2.8.34 Mansur, Vinayagam and Tan (2008)……47
2.8.35 Harries, Zeno & Shahrooz (2012)……48
2.8.36 Sneed, Wermager & Krc (2016)……49

2.9 Horizontal Shear Design Requirements – Code Provisions……50

2.9.1 Shear-Friction Provisions of ACI 318-11 Code of Practice……50
2.9.2 Shear-Friction Provisions of Eurocode 2 (2004)……55
2.9.3 Shear-Friction Provisions of PCI Design Handbook (2010)……57
2.9.4 Shear-Friction Provisions of AASHTO LRFD Bridge Design Specifications (2007)….58

3. RESEARCH METHODOLOGY……61

3.1 Introduction……61
3.2 Research Approach and Strategy……61
3.3 Long Flange and Short Flange……66

4. RESEARCH RESULTS……………………………………………………………………………………………………69

4.1 Introduction……………………………………………………………………………………………………..69

4.2 Shear Stresses……………………………………………………………………………………………….69

4.2.1 Beam 2 – Horizontal Shear Stress Contour Range (S13)…………………………………71

4.2.2 Beam 8 – Horizontal Shear Stress Contour Range (S13)…………………………………73

4.2.3 Beam 9 – Horizontal Shear Stress Contour Range (S13)…………………………………75

4.2.4 Beam 10 – Horizontal Shear Stress Contour Range (S13)………………………………77

4.3 Hand Calculations for the Beam Horizontal Shear……………………………………………79

5. DISCUSSION OF THE RESULTS……………………………………………………………………………94

5.1 Introduction……………………………………………………………………………………………………..94

5.2 Composite Concrete Beams – Horizontal Shear Stress Comparative Tables and Charts………94

6. SUMMARY AND CONCLUSION…………………………………………………………………………99

6.1 Composite Concrete Beams – Horizontal Shear Stress Comparison Conclusion……99

6.2 Design Recommendations…………………………………………………………………………..100

6.3 Recommendation for Future Research…………………………………………………………..101

7. REFERENCES…………………………………………………………………………………………………..102

LIST OF FIGURES:

Figure 1.1: Typical detail of a T shape composite concrete beam cast in two stages at different times……1
Figure 1.2: Behavior of the loaded composite concrete beam according to the quality of the interface and surface preparation……2
Figure 1.3: Typical stress-strain curves for normal weight concrete……4
Figure 1.4: Typical stress-strain curves for lightweight concrete……4
Figure 1.5: Concrete strength in biaxial stress case……5
Figure 1.6: Typical stress-strain curves for steel reinforcement……6
Figure 1.7: Typical horizontal shear in composite concrete beam, PCI Design Handbook 2010……7
Figure 2.1: Shear interfaces in a composite concrete beam cast in stages……9
Figure 2.2: Examples of the interface reinforcement……9
Figure 2.3: Illustration of the main applications of the shear-friction theory in structures.11
Figure 2.4: Shear Friction Hypothesis……12
Figure 2.5: Load transfer mechanisms at the shear interface……13
Figure 2.6: Contribution of adhesion, shear-friction and shear reinforcement……14
Figure 2.7: Push-off Test Setup……15
Figure 2.8 Composite Girder / Beam Test Setup……16
Figure 2.9: Push-off specimens by Hanson, Anderson & Mast……17
Figure 2.10: Typical shear-slip curves for different interface conditions, Hanson, 1960……18
Figure 2.11: Push-off specimens details, Hofbeck, Ibrahim and Mattock, 1969……19
Figure 2.12: Typical load-slip curves of the push-off specimens, Hofbeck, Ibrahim and Mattock, 1969……20
Figure 2.13: Shear transfer test specimens; (a) push-off; (b) pull-off; (c) modified push-off, Mattock and Hawkins, 1972……20
Figure 2.14: Typical push-off specimens with orthogonal and parallel reinforcement Mattock, 1974……21

Figure 2.15: Typical shear stress-slip curves for specimens with parallel reinforcement Mattock, 1974……………………………………………………………………………………………..22

Figure 2.16: Geometry of the push-off specimens, Walraven and Reinhardt, 1981……………..23

Figure 2.17: Push-off test setup, a loaded specimen and the electrical strain gauges…………..23

Figure 2.18: Cold joint specimen before concrete casting………………………………………………..24

Figure 2.19: The steel cage with strain gauges fixed……………………………………………………….25

Figure 2.20: Surface preparation & Roughness……………………………………………………………….26

Figure 2.21: Development of horizontal shear stresses in concrete beams…………………………..27

Figure 2.22: Shear-friction reinforcement inclined to the shear plane………………………………..34

Figure 2.23: The effect of concrete compressive strength on the shear strength…………………39

Figure 2.24: Cement matrix and aggregates effect………………………………………………………….40

Figure 2.25: Generally observed structure of a crack plane (Sphere model)…………………………40

Figure 2.26: Shear friction of concrete and steel components of two test specimens, with different steel grades………………………………………………………………………………………49

Figure 2.27: Tension in shear friction reinforcement according to Mattock, 1974………………..52

Figure 2.28: Compression in reinforcement where shear friction does not apply………………..53

Figure 2.29: Intended surface at the joint between old and new concrete…………………………56

Figure 3.1: Modeling of the beam-2 by using the Solid element………………………………………62

Figure 3.2: Modeling of the beam-8 by using the Solid element………………………………………63

Figure 3.3: Modeling of the beam-9 by using the Solid element………………………………………64

Figure 3.4: Modeling of the beam-10 by using the Solid element……………………………………65

Figure 3.5: Horizontal shear failure mode for beams with full length flange………………………66

Figure 3.6: Horizontal shear failure mode for beams with short-discontinued flange…………67

Figure 4.1: Horizontal shear stress diagram for a simply supported beam subjected to a concentrated load……………………………………………………………………………………………70

Figure 4.2: Horizontal shear stress contour S13 – Beam 2………………………………………………..71

Figure 4.3: Horizontal shear stress contour S13 at the interface of Beam 2 –0.13mm slip….71

Figure 4.4: Horizontal shear stress contour S13 at the interface of Beam 2 –0.5mm slip……72

Figure 4.5: Horizontal shear stress contour S13 at the interface of Beam 2 –failure slip........72
Figure 4.6: Horizontal shear stress contour S13 – Beam 8...73
Figure 4.7: Horizontal shear stress contour S13 at the interface of Beam 8 –0.13mm slip........73
Figure 4.8: Horizontal shear stress contour S13 at the interface of Beam 8 –0.5mm slip..........74
Figure 4.9: Horizontal shear stress contour S13 at the interface of Beam 8 –failure slip...........74
Figure 4.10: Horizontal shear stress contour S13 – Beam 9..75
Figure 4.11: Horizontal shear stress contour S13 at the interface of Beam 9 –0.13mm slip.......75
Figure 4.12: Horizontal shear stress contour S13 at the interface of Beam 9 –0.5mm slip.........76
Figure 4.13: Horizontal shear stress contour S13 at the interface of Beam 9 –failure slip..........76
Figure 4.14: Horizontal shear stress contour S13 – Beam 10..77
Figure 4.15: Horizontal shear stress contour S13 at the interface of Beam 10 – 0.13mm slip....77
Figure 4.16: Horizontal shear stress contour S13 at the interface of Beam 10 –0.5mm slip.......78
Figure 4.17: Horizontal shear stress contour S13 at the interface of Beam 10 – failure slip.......78
Figure 4.18: Reinforcement elevation of Beam-2..79
Figure 4.19: Reinforcement section of Beam-2...79
Figure 4.20: Reinforcement elevation of Beam-8..83
Figure 4.21: Reinforcement section of Beam-8...83
Figure 4.22: Reinforcement elevation of Beam-9..86
Figure 4.23: Beam-9 sections with and without a topping flange...86
Figure 4.24: Reinforcement elevation of Beam-10..90
Figure 4.25: Beam-10 sections with and without a topping flange..90
Figure 5.1: Horizontal shear stress / slip approach comparison chart – Beam-2..........................95
Figure 5.2: Horizontal shear stress / slip approach comparison chart – Beam-8..........................96
Figure 5.3: Horizontal shear stress / slip approach comparison chart – Beam-9..........................97
Figure 5.4: Horizontal shear stress / slip approach comparison chart – Beam-10........................98

LIST OF TABLES:

Table 2.1: Coefficient of friction as recommended by the (ACI 318-11)……………………………51

Table 2.2: Values of λ for lightweight concrete based on equilibrium density, (ACI 318-11)……………………………………………………………………………………………….53

Table 2.3: Values of λ for lightweight concrete based on composition of aggregates, (ACI 318-11)……………………………………………………………………………54

Table 2.4: Maximum shear strength v_u along the shear plane, (ACI 318-11)…………………….55

Table 2.5: Coefficients of friction and cohesion, (EN 1992-1-1, 2004)………………………………56

Table 2.6: Recommended shear-friction coefficients, (PCI Design Handbook, 2010)………..58

Table 2.7: Recommended shear-friction coefficients, (AASHTO LRFD Specs, 2007)………...60

Table 3.1: Properties of the Test Beams (Geometry and Reinforcement)………………………….67

Table 3.2: Properties of the Test Beams (Material Strength and Loading)…………………………68

Table 5.1: Beam 2 – Horizontal Shear Values Comparison…………………………………………………94

Table 5.2: Beam 8 – Horizontal Shear Values Comparison…………………………………………………95

Table 5.3: Beam 9 – Horizontal Shear Values Comparison…………………………………………………96

Table 5.4: Beam 10 – Horizontal Shear Values Comparison…………………………………………………97

1. INTRODUCTION

The composite concrete beam is a beam cast in stages at different times. Usually, that beam consists of a precast concrete web and a cast in place topping which is cast as a part of the slab supported on the beam. A cold joint is developed along the interface between the beam parts. In order for composite concrete beams to act as a monolithic structure and shear stresses fully transferred through the beam, the surface preparation of the interface must be done perfectly considering the intentional roughening and well cleaning of the surface. After curing completes for the concrete, a bond will be developed between the new cast in place concrete and the precast concrete. Figure 1.1 illustrates the typical detail of a T shape composite concrete beam with a web and a flange sections cast in two stages at different ages.

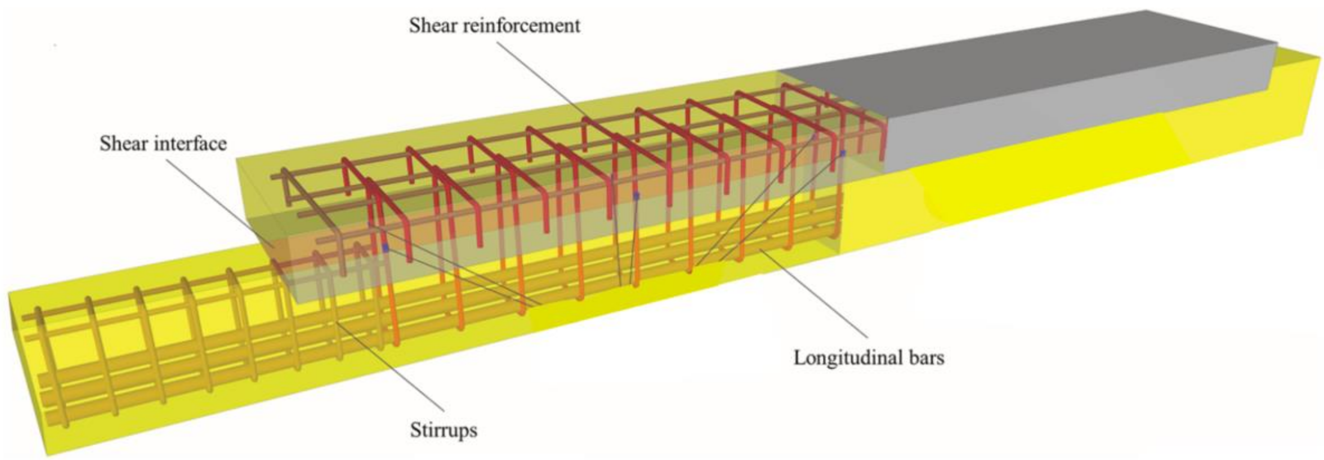

Fig. 1.1 – Typical detail of a T shape composite concrete beam cast in two stages at different times.

The strong interface bond and the aggregate interlock should give the required monolithic behavior of the final beam (Fig. 1.2a). That strong bond will allow all forces to be fully transferred across the well-prepared interface (Fig. 1.2b). In case of loading a composite concrete beam with a weak bond, there will be a high opportunity for interface failure. That failure causes slippage and separation between the two parts cast at different ages (Fig. 1.2c). Accordingly, the precast web and the flange will behave separately to resist the loads (Fig. 1.2d). The shear ties or stirrups crossing the interface are proved experimentally that they increase the capacity of the composite section and are recommended to be used by the international structural codes.

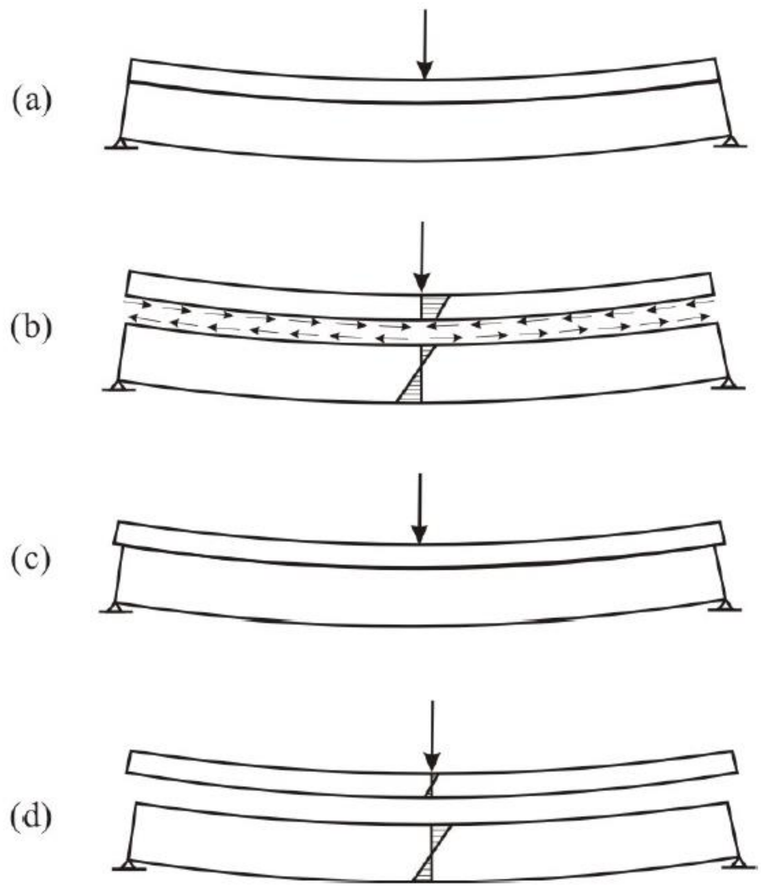

Fig. 1.2 - Behavior of the loaded composite concrete beam according to the quality of the interface and surface preparation.

1.1. MECHANICAL PROPERTIES AND BEHAVIOR OF CONCRETE AND STEEL

Since the two main materials used in the production of the composite concrete beams are the concrete and the steel, an explanation for the mechanical properties of each material will be presented.

Performance of a structure that is subjected to loading depends on the stress-strain relationship of the material from which that structure is made. Reinforced concrete is composed of concrete and steel. The steel stress strain relation is well known, while the concrete as a non-homogeneous material has different properties in compression and tension.

The interaction between steel and concrete including the bond between both materials is so important to study a reinforced concrete specimen.

1.1.1 Concrete Behavior in Uniaxial Stress State

- **Concrete Properties in Compression**

The compressive stress-strain curve of the concrete is very important because concrete is basically used in compression. This curve is generated by proper strain measurements in tests or on the beams' compression side. Figure 1.3 illustrates typical curves resulted from 28 days old uniaxial compressive tests of normal weight concrete. The curves are somehow similar, they are straight in the first elastic zone in which the stress-strain relation is proportional. The curve then starts to move horizontally at the maximum stress which is the concrete compressive strength at a strain value 0.002 to 0.003. For light weight concrete, the strain values are from 0.003 to 0.0035. As the compressive strength is higher, the strain will be larger, figure 1.4.

The modulus of elasticity of concrete E_c which is the slope of the straight elastic part of the stress-strain curve is bigger when the concrete strength is larger. As per the ACI 318-11, the elasticity modulus E_c can be calculated from the following equations:

1) For normal weight concrete

$$E_c = 4700\sqrt{f_c'}$$

2) For concrete weight w_c is ranging between 1440 and 2560 kg/m^3

$$E_c = 0.043\,(w_c)^{1\,1/2}\sqrt{f_c'}$$

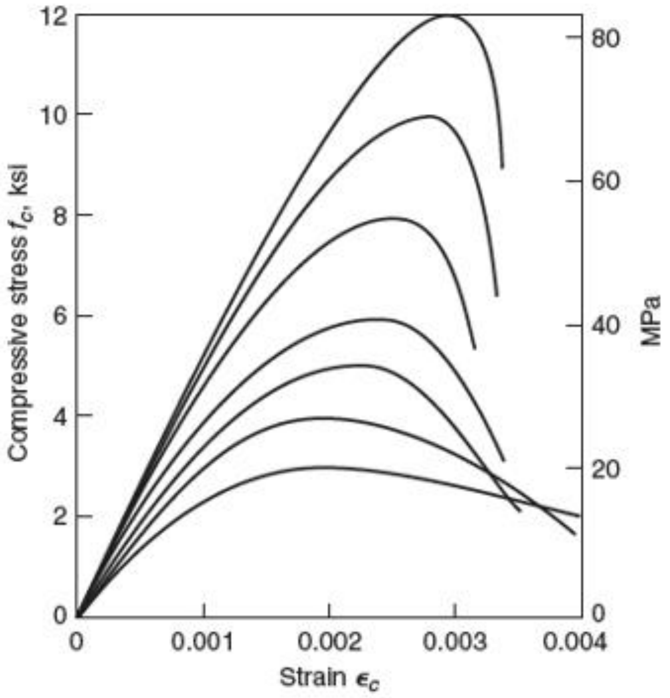

Fig. 1.3 - Typical stress-strain curves for normal weight concrete

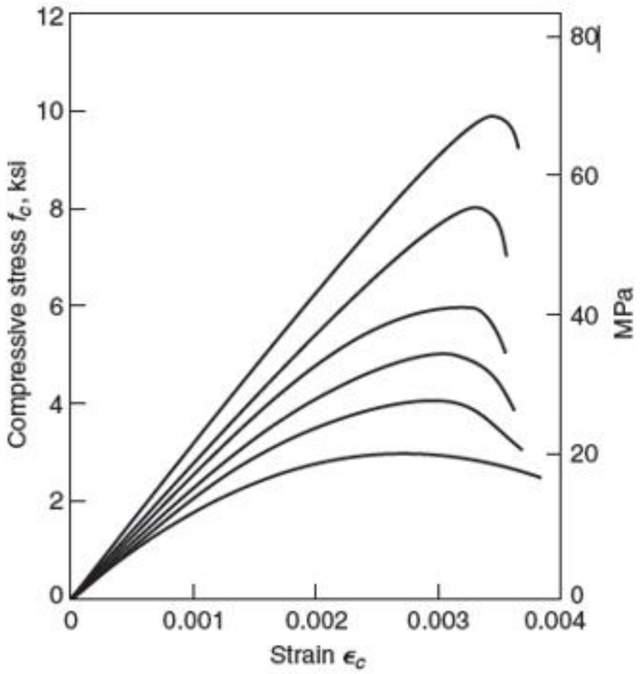

Fig. 1.4 - Typical stress-strain curves for lightweight concrete

- **Concrete Properties in Tension**

The concrete behavior in compression is the most important, however its behavior in tension is also of an interest. The cracks on the tension side of reinforced concrete flexural elements rely on the tensile strength and the concrete fracture properties. Moreover, shear and torsion cause tensile stresses in the concrete. To expect the concrete tensile strength is so important as the concrete member behavior changes after cracking.

According to ACI 318-11 code, the tensile strength of concrete in flexure (modulus of rupture f_r) is about 10 to 15 percent of the compressive strength and it is equal to $0.62.\sqrt{f'_c}$ for normal weight concrete and if the yield stress f_y of the steel reinforcement is greater than 550 MPa then the value of the concrete modulus of rupture will be reduced to $0.41.\sqrt{f'_c}$.

1.1.2 Concrete Behavior in Biaxial Stress State

In most cases, concrete is subjected to stresses in different directions at the same time. For example, beams are usually subjected to biaxial shear and compression stresses simultaneously. That combined stress can be either compression or tension. Although continuous research takes place, there is no general theory of the concrete strength under biaxial or triaxial stresses and the concrete strength cannot be calculated reasonably. The main reason for that is the nonhomogeneous concrete nature. Testing is the only trusted way to determine the concrete strength for the biaxial stress state. An interaction diagram is the presentable illustration for the concrete strength test results under combined stress as shown in figure 1.5.

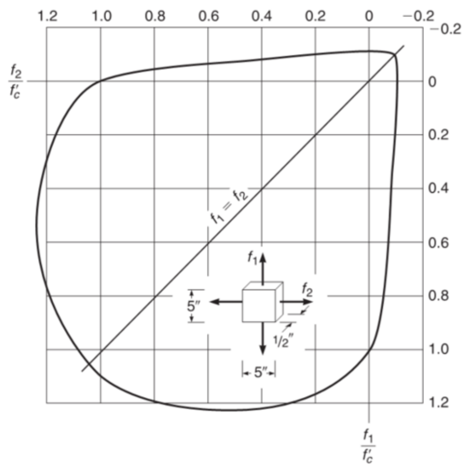

Fig. 1.5 – Concrete strength in biaxial stress case

1.1.3 Reinforcing Steel Properties

The two main properties which are required to describe the steel reinforcement characteristics are the yield strength and the modulus of elasticity of the steel E_s.

The maximum stress that can be reached by the steel within the elastic zone of the stress-strain curve is known as the yield strength f_y. This stress corresponds to a strain of a value of 0.01.

The modulus of elasticity E_s is the slope of the straight initial part of the steel stress-strain curve, and it is typically considered equals 200,000 MPa for all steel reinforcement but not applicable for the prestressing steel. Typical steel stress-strain curve is shown in figure 1.6. The right part of the figure shows the initial stress-strain curve while the left part of the figure shows the complete steel stress-strain curve, and both curves are 10 times magnified for more clarity.

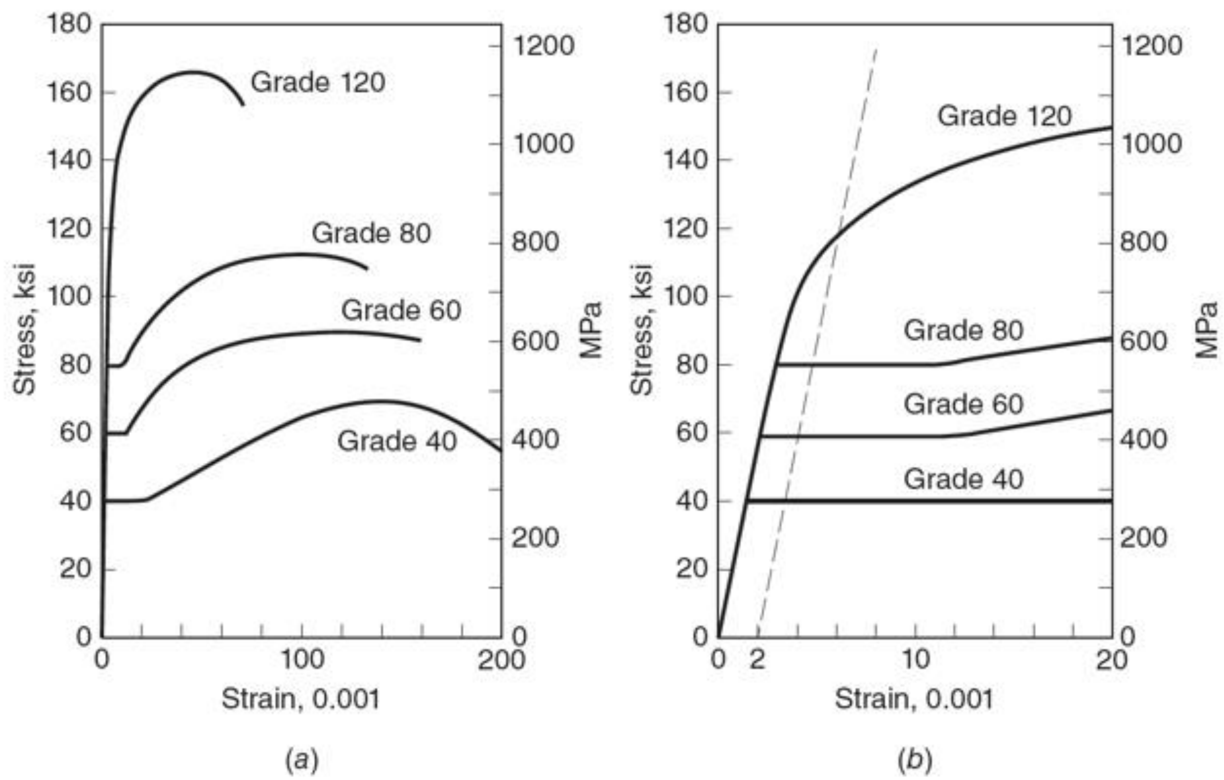

Fig. 1.6 – Typical stress-strain curves for steel reinforcement

1.2. Horizontal Shear in Composite Sections

The perfect behavior of the composite concrete beam section is achieved if the interface is clean, free of laitance and the intentional roughening for the surface is done. Steel reinforcement may be required to be provided and embedded in both parts of the beam depending on the shear force value.

The horizontal longitudinal shear force which is required to be resisted is equal to the force in the top part of the beam. Compression force is at the positive moment sections, and tension force is at the negative moment sections. This force can be evaluated from the concrete stress block as shown in figure 1.7 and considering the shear friction equations and limits from the code.

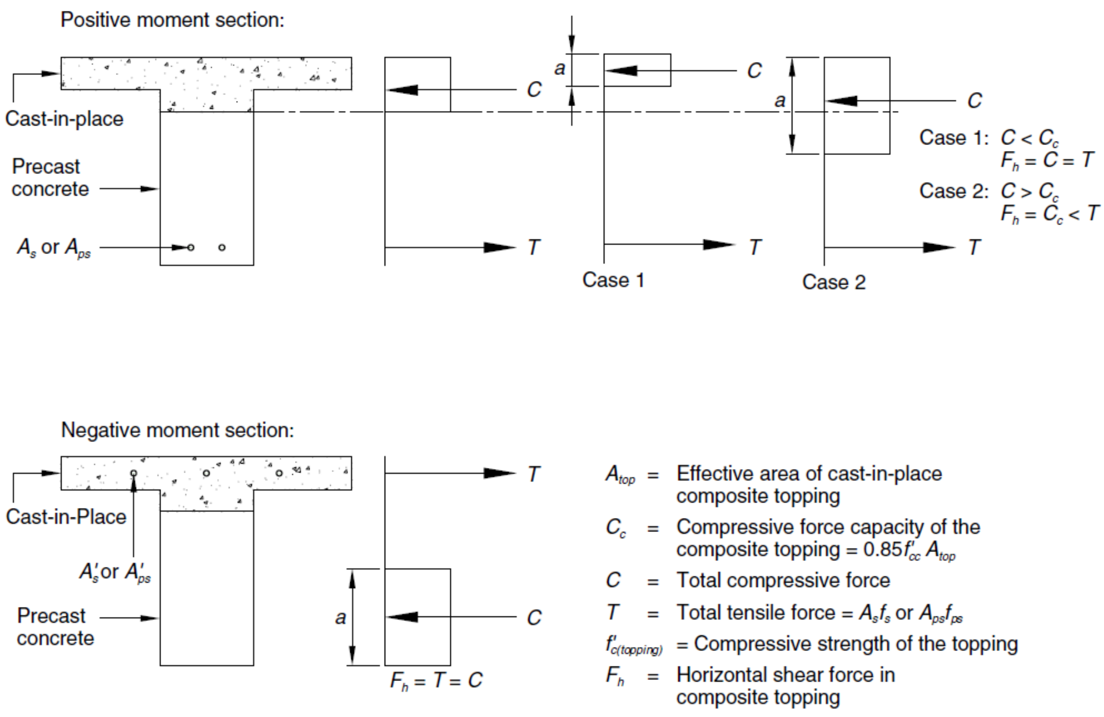

Fig. 1.7 – Typical horizontal shear in composite concrete beam, PCI Design Handbook 2010.

2. LITERATURE REVIEW

2.1 Introduction

A lot of trials for jointing a cast in place concrete with a precast concrete were done and documented since 1950s. This approach is being increasingly used in the bridges and the building structures. For bridges, the lower web part of the composite beam should be the precast part which the topping slab is then cast on it. In the building structures, the same concept is followed, however in most of the cases, the lower precast part of the beam is used to support precast slabs and steel beams and the topping cast in place part is then cast on top of that precast concrete. This construction method is useful because of different reasons; such as to decrease the labor at site, reduce the shuttering materials and back propping. This leads to a more economical, safer and faster construction. The quality assurance and quality control shall be precisely performed.

The researchers thought that if the surface of the precast concrete part is free of laitance, artificially roughened and well cleaned of dust, then this will provide the required adhesion to joint with the new cast in place concrete. Others relied on that intentionally roughened surface in addition to a shear key along that side of the previously cast concrete which is provided to avoid the lateral displacements. There are also researchers studied and experimented the effect of providing steel stirrups basically for the beam shear resistance and to reinforce the concrete diagonal tension as well. Some others stated that stirrups are to be provided to resist all the horizontal shear at the interface. The word “interface” here means the plane between the two different concrete materials that are cast in two time stages. Based on the last-mentioned opinion, the adhesion between the cast in place slab part and precast beam is neglected completely no matter the surface roughness. This approach is so conservative, and the related design would not be economical, so most of the research relied on a compromise theory that considers the effect of adhesion, friction and the steel reinforcement crossing the interface.

The composite action of a beam cast in stages at different times tends to develop shear stresses along the interface, and there should be a proper shear transfer to achieve a safe behavior of the composite beam-slab to resist the proposed loads. Figure 2.1 illustrates the possible interfaces of a typical concrete beam cast in stages at different ages.

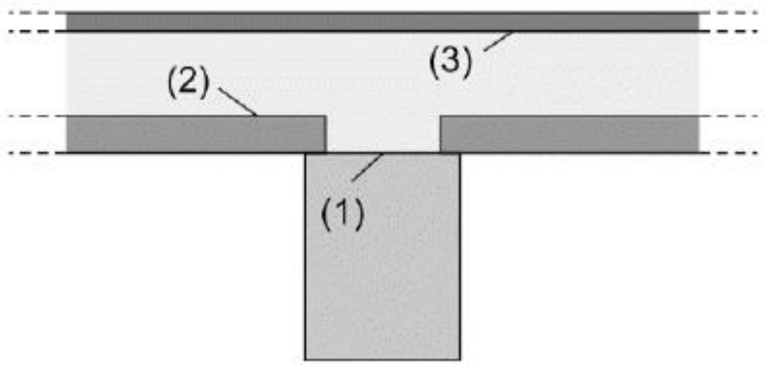

(1) Interface between a precast beam and cast in place slab.
(2) Interface between precast element and cast in situ concrete.
(3) Interface between existing structure and strengthening layer.

Fig. 2.1 – Shear interfaces in a composite concrete beam cast in stages.

If the applied shear force exceeds the capacity of the interface, then steel reinforcement shall be involved in the form of stirrups, dowels, lattice girders or studs crossing the interface and well anchored at both sides of the concrete in order to resist those forces. Some of the common examples of the interface reinforcement are shown in figure 2.2.

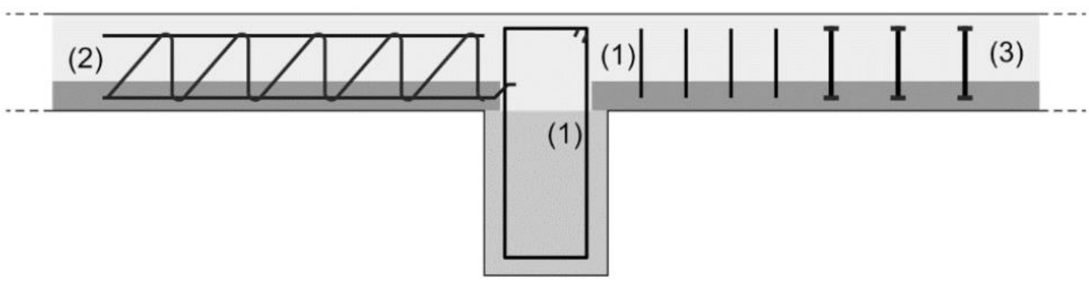

(1) Stirrups and dowels.
(2) Lattice girders.
(3) Studs.

Fig. 2.2 – Examples of the interface reinforcement.

In this literature review, the shear-friction hypothesis, the development of the theoretical and experimental methods, procedures and then design equations to evaluate the horizontal shear at the interface of concrete beams cast in stages at different ages are explained within the following classification.

- Shear-Friction Hypothesis.
- The Experimental Evaluation of The Interface Shear Strength.
- Analysis of the Development of Horizontal Shear Stresses.
- Shear-Friction Design Expressions – Historical Development.
- Horizontal Shear Design Requirements – Code Provisions.

2.2 Shear-Friction Hypothesis

Most structural issues in the precast buildings are about the shear interfaces. It is usually found in corbels, beam ledges, and structural members installed and cast in more than one stage at different times. By jointing the precast and cast in situ concrete parts together, a cold joint would be formed along that interface.

For concrete to steel and concrete to concrete interfaces, shear failure should be studied as slippage along the plane with the maximum shear at the interface between both sides. Examples like beam to column corbel, beam to a beam ledge, column to footing, a beam cast on top of a hardened concrete column and steel support subjects to shear forces are also categorized as shear friction cases which require an investigation and checking during the design of the connections.

The CIRSOC 201 (2005) – Argentinian design code introduced illustration of the possible applications of shear-friction in several members of a structure as shown in figure 2.3.

The shown applications are covering the most known applications in the industry where the composite construction is used and considered.

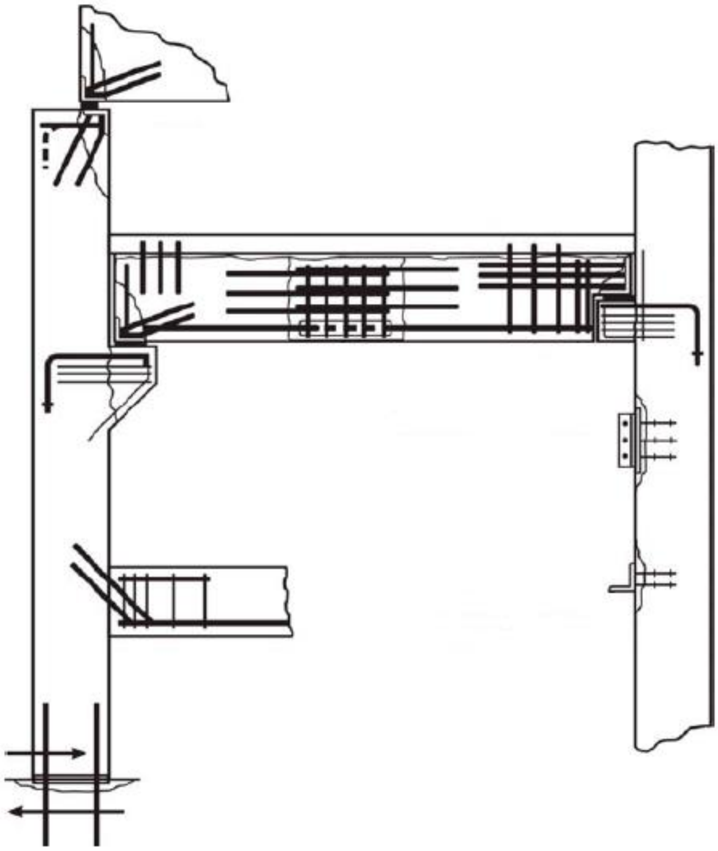

Fig. 2.3 - Illustration of the main applications of the shear-friction theory in structures, (CIRSOC 201 – 2005)

For concrete beams cast in two stages where it is required to behave like monolithic structure, the shear forces should be completely transferred across the joint line. This shear force (V) tends to slipping and sliding. The developed friction between the two parts resists those forces. If the surface at the joint is rough, more friction resistance is developed. The value of frictional force which resists the slippage is (μ.P) which resulted from the external clamping force (P). If the shear force increased than the resisting force, then separation of the beam parts will happen. If steel stirrups are extending from the lower beam part up through the joint and anchored in the upper part, then the beam separation causes tension force (T) in the reinforcement. This tension force at the reinforcement will develop an equal external clamping force (P) on the concrete because the reinforcement is well anchored at the two beam sides. A frictional resistance shall be developed at the construction joint line.

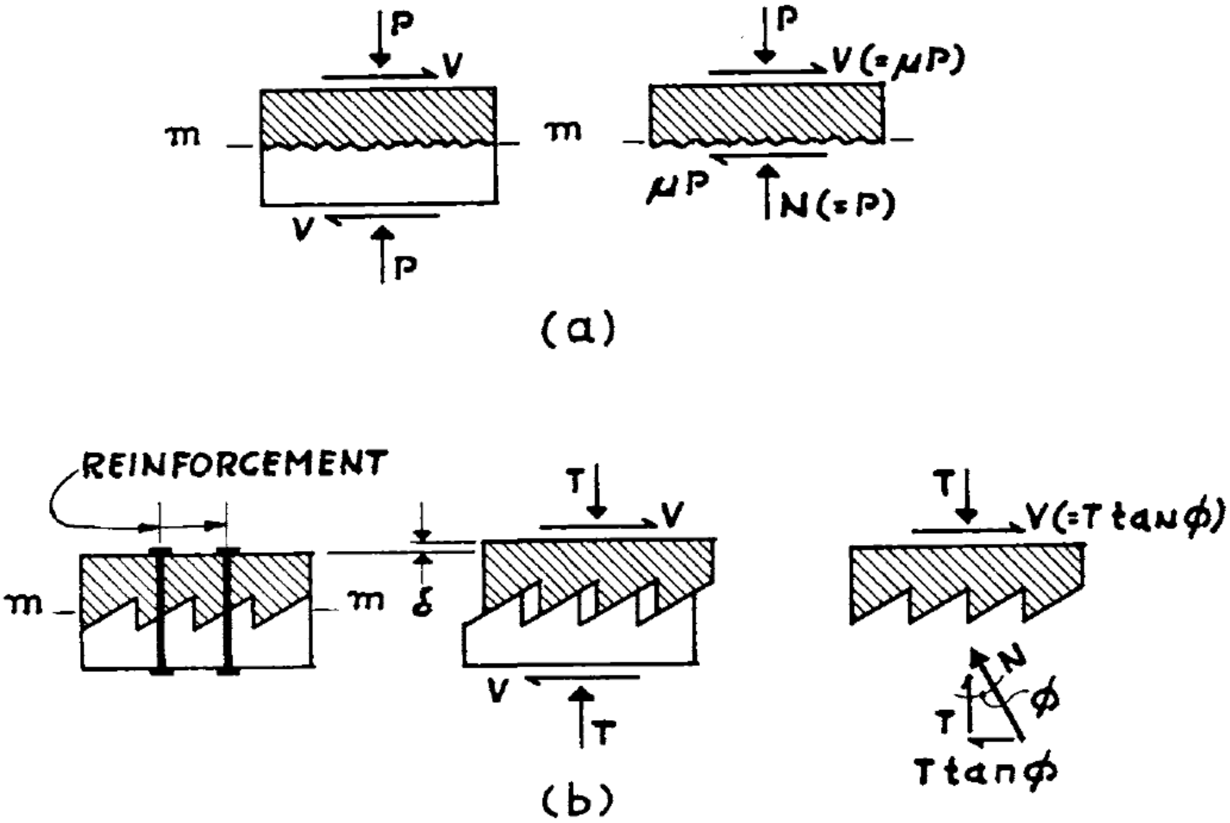

Fig. 2.4 – Shear Friction Hypothesis,
(Birkeland & Birkeland, 1966)

The interface roughness can be seen as series of frictionless fine sawtooth ramps with a slope of tan ϕ. To achieve equilibrium of the system in figure 2.4, the developed tension force in the reinforcement on the interface due to separation T is equal to the external clamping force P, and accordingly μ.P = T.tan ϕ. In case, the steel crossing the interface is stressed to the yield strength f_y, clamping stress σ_n is then equivalent to the reinforcement index ($\rho_v.f_y$). The ultimate shear resistance at the construction joint is happening at the yield of the steel reinforcement $T_u = A_{vf}.f_y$. Hence, the shear resistance equation at the interface is:

$$V_u = A_{vf}.\, f_y.\, \tan \phi$$

$$v_u = \frac{V_u}{A_g} = \rho_v.\, f_y.\, \tan \phi = \rho_v.\, f_y.\, \mu$$

Where,

tan $\phi = \mu$ (friction coefficient).

v_u = ultimate shear stress.

A_g = gross area of the interface.

A_{vf} = area of reinforcement across the interface.

ρ_v = The ratio of the steel reinforcement at the interface.

f_y = The yield stress of the reinforcement.

tan ϕ = 1.70 for monolithic concrete.

= 1.40 for artificially roughened construction joints.

= 0.80 to 1.0 for ordinary construction joints and for concrete to steel interfaces.

According to the load transfer mechanism explanation by Zilch and Reinecke (2001), in figure 2.5, there are three load carrying mechanisms describe the shear strength at the interface of a composite concrete beam cast in two stages at different times:

(a) adhesion;

(b) shear-friction;

(c) Interface shear reinforcement.

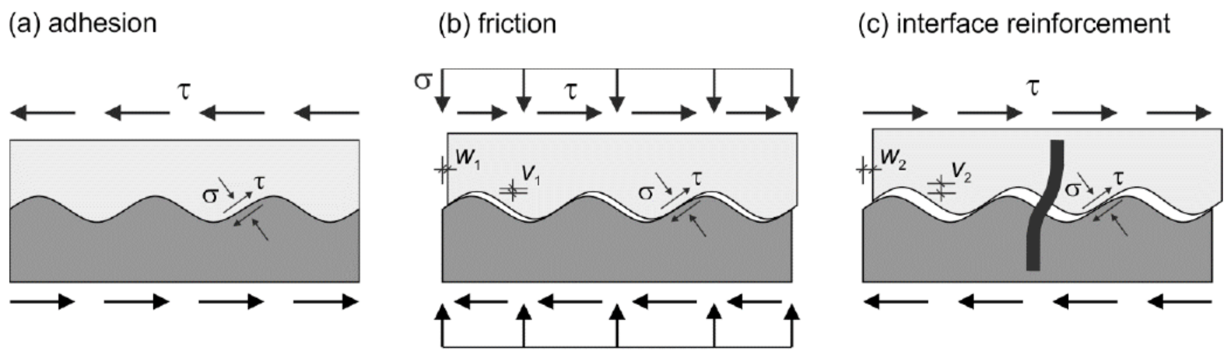

Fig. 2.5 – Load transfer mechanisms at the shear interface

The adhesion is generated by the chemical bond between the two concrete parts cast at different ages. The bond will be dissipated after reaching the upper limit of the load applied as shown in figure 2.6, which illustrates the shear stress-slip relation for each of the participating stress components. The shear stress is then transferred at the interface by shear-friction and aggregate interlock if it is subjected to compression. As the load increases, the movement or slip increases relatively, and the reinforcement will be tensioned till it reaches the yield. Shear reinforcement will develop compression and shear force will transfer by friction. The shear reinforcement shall be subjected to shear force due to the slippage which is known as the dowel action.

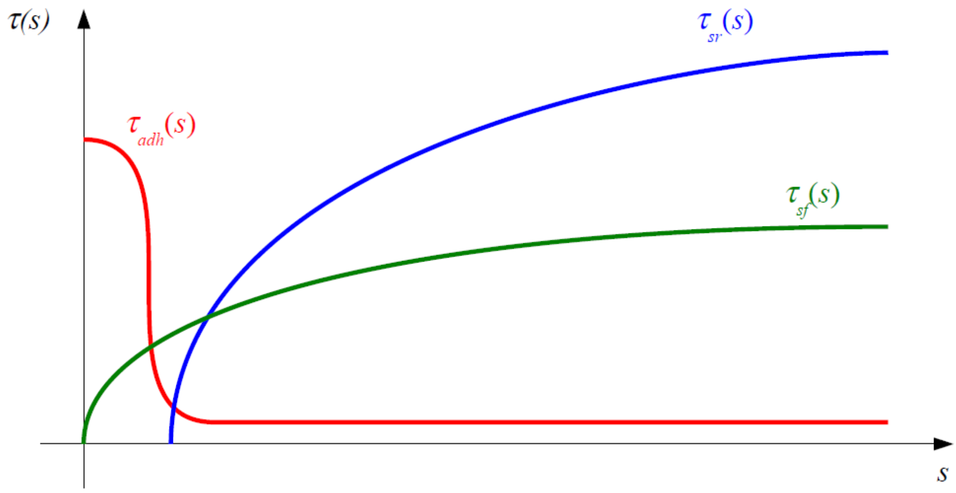

Fig. 2.6 – Contribution of adhesion, shear-friction and shear reinforcement, Zilch and Reinecke (2001)

The shear strength at the shear plane for a concrete beam cast in two stages $\tau(s)$, with a relative displacement (s), is obtained by the following equation:

$$\tau\ (s) = \tau_{adh}(s) + \tau_{sf}(s) + \tau_{sr}(s)$$

where,

τ_{adh} (s) is the adhesion component participated to the shear stress.

τ_{sf} (s) is shear-friction component participated to the shear stress.

τ_{sr} (s) is shear reinforcement component participated to the shear stress.

The hypothesis of shear-friction as described above is considered the basis of the horizontal shear research and studies till date as well as the provisions of shear-friction in the international structural design codes.

2.3 The Experimental Evaluation of The Interface Shear Strength

There are two main testing methods to evaluate the horizontal shear capacity of a section. One of them depends on testing specimens and the other depends on testing a complete beam. Both are effective and reliable experimental methods to evaluate the shear capacity at the interface of the composite concrete.

The Push-off shear test method which consider the testing of concrete specimens is being used for quite long time till today. Other shear testing procedures of similar kind are also being used at the time being, all of them are of the same purpose but the used equipment and the sizes of the specimens are somehow different. Figure 2.7 shows the push-off test setup.

Fig. 2.7 – Push-off Test Setup

The girder or beam test is an experimental procedure to test the horizontal shear capacity for a real composite beam but with limitation to the size, weight and span which are smaller in scale as per the capability of the testing facility. This tested composite girder is in flexure and should be designed in such a way that the horizontal shear at the beam interface reaches high values at forces less than maximum flexural capacity.

It gives results close to the real cases as the testing is being done on a composite concrete beam even if smaller in size than the normal sized beam used in the real building construction. It was recorded that slip values which can be reached in the beam test are always higher than those of the push-off specimens before the bond is failed. Figure 2.8 shows the girder test setup.

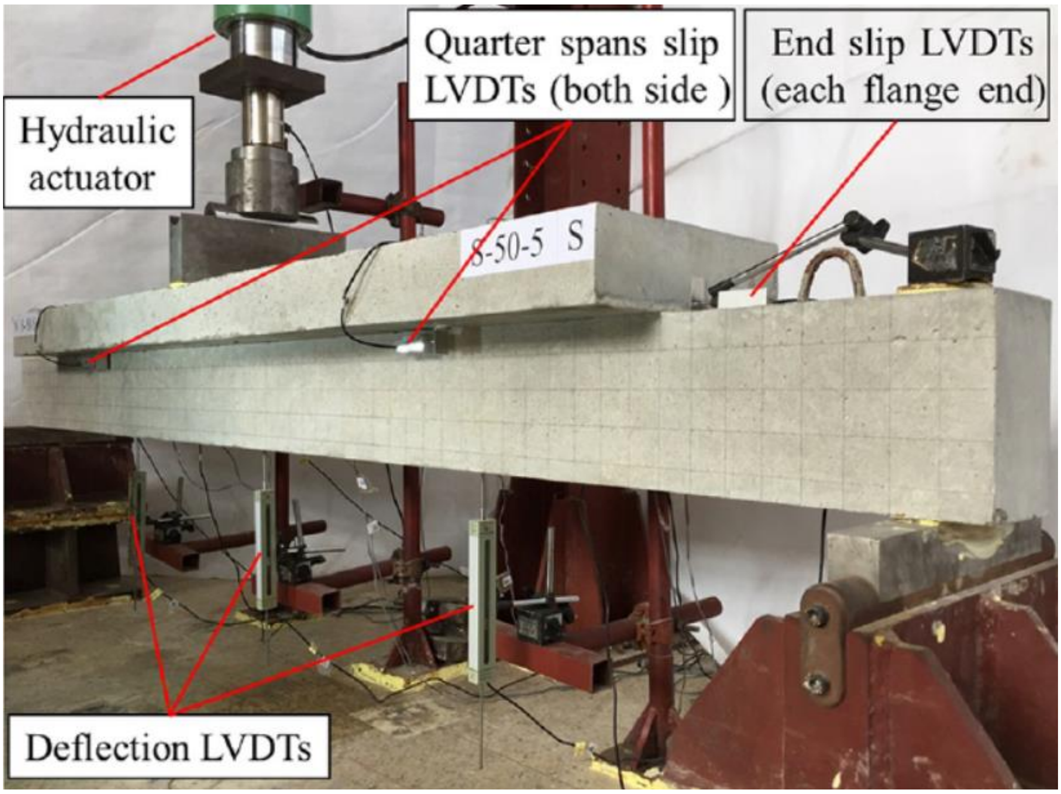

Fig. 2.8 – Composite Girder / Beam Test Setup

In the following section, the push-off test will be further explained along with previous related testing done by effective researchers who relied on push-off specimens testing in developing proposals of design equation to determine the horizontal shear capacity of composite sections. However, in the next chapter of this dissertation I will consider modeling and shear-friction design for four beams that were tested experimentally in a separate previous research.

2.3.1 Push-off Test

The push-off test is a shear test which determines the strength at the interfaces of concrete to concrete beam parts where the steel bars are crossing the interface. It was also referred to as the L-shaped test.

A hydraulic machine with certain load capacity is used for testing the concrete specimens. There are two procedures adopted for implementing the push-off tests, the first was considering a precast part and a cast in place beam part which is cast after the precast part is getting hardened and gaining the required design strength. The other procedure of the push-off test is considering both beam parts are precast, the extended reinforcement is welded, and concrete is placed at the joint between both beam part. The load is applied until the cracks are formed along the shear interface.

The push-off testing was first used by Anderson (1960), Hanson (1960), Mast (unpuplished), and Birkeland & Birkeland (1966), see figure 2.9.

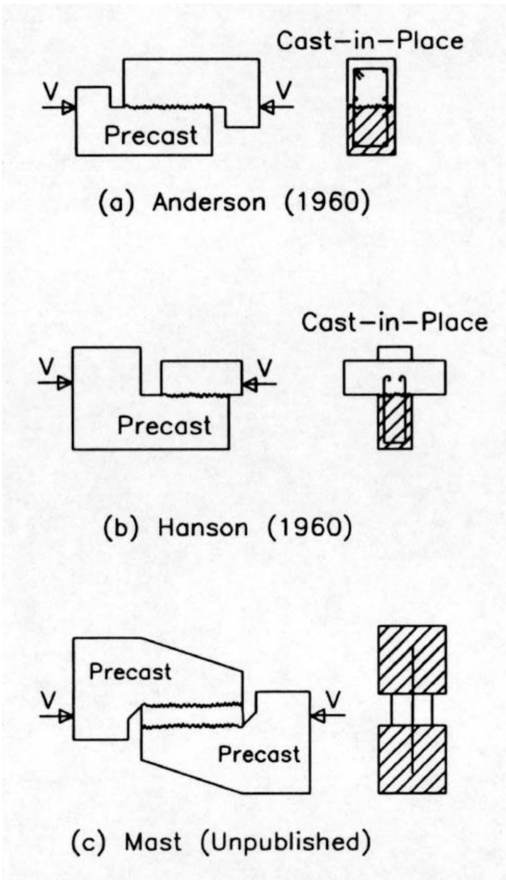

Fig. 2.9 – Push-off specimens by Hanson, Anderson & Mast

Hanson (1960) tested 62 specimens with different surface condition of the interface and reinforcement ratios. Following are the surfaces states which where experimented.

Rough surface, that was done intentionally. Some of these specimens were aggregate bared after casting and cement paste removed from the aggregate.

Smooth surface, the surface was made smooth at the time of casting. Some of these specimens were aggregate bared after casting.

Bonded surface, where no trials made to change the interface state, and the new concrete was cast on top of the dry surface.

Unbonded surface, where a silicone paint was applied to prevent the bond between the new concrete and the hardened concrete.

The nature of failure as resulted in the push-off tests done by Hanson is illustrated in the shear – slip curves shown in figure 2.10. Those curves show the shear – deformation typical relationships for the different interface conditions.

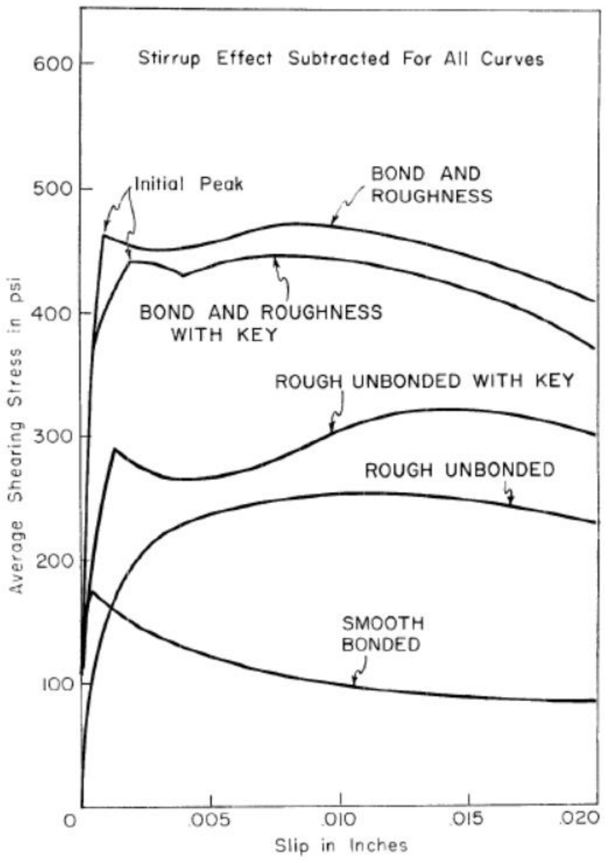

Fig. 2.10 – Typical shear-slip curves for different interface conditions, Hanson (1960)

Hofbeck *et al*. (1969) performed thirty-eight push-off concrete specimens to study the shear transfer across the shear plane. Some of the specimens were pre-cracked and others were without pre-existing cracks at the shear plane. Different concrete compressive strength values were investigated to determine its effect on the shear transfer strength. Some specimens were tested considering no dowel action between the stirrups and the surrounding concrete at the interface shear plane by providing rubber sleeves around the steel bars.

Cracking of the specimens which are initially uncracked was done by placing the specimen horizontally in a hydraulic testing device. Line load then was added to the opposite sides and increased in increments till cracks formed at the shear plane.

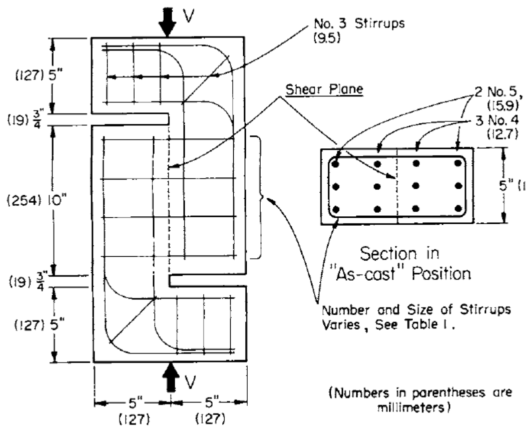

Fig. 2.11 – Push-off specimens details,

(Hofbeck, Ibrahim and Mattock, 1969)

The shear test was done in the same device and the specimens were oriented vertically as shown in figure 2.11, and then loaded concentrically with increments till failure.

The slip along the shear plane was measured after each increase in the load. A load slip curves were generated for both types of specimens – with and without pre-existing cracks – as shown in figure 2.12. It is obvious that the pre-cracked specimens have movement from the beginning of loading, while the specimens which are initially uncracked will have some movement after applying higher loads.

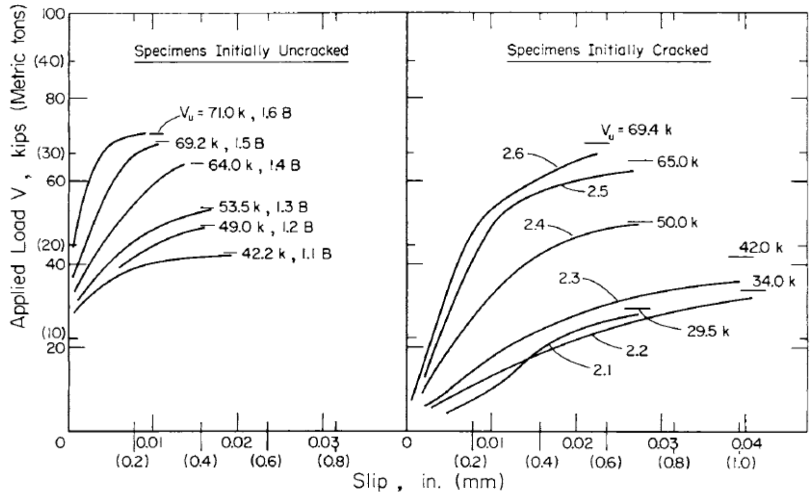

Fig. 2.12 – Typical load-slip curves of the push-off specimens,
(Hofbeck, Ibrahim and Mattock, 1969)

Mattock and Hawkins, (1972) studied the factors affecting the shear transfer strength such as the shear plane characteristics, steel bars characteristics, concrete compressive strength which were tested by applying the push-off test on specimens that are monolithically cast, the researchers also studied the effect of the direct stresses which are acting either parallel or transverse to the shear plane by applying the pull-off test and the modified push-off test on the specimens as illustrated in figure 2.13.

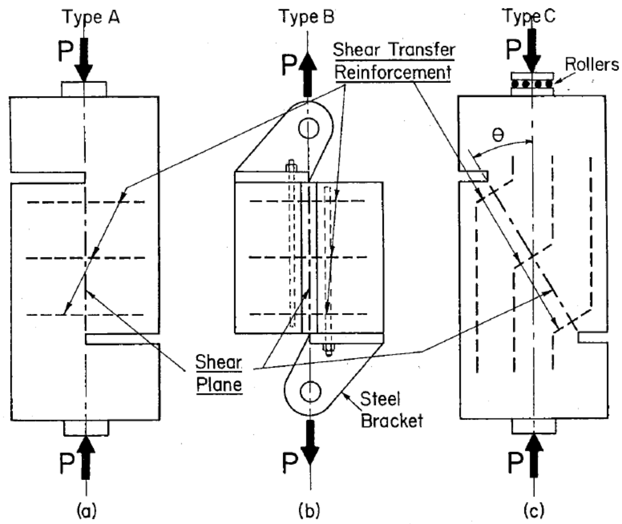

Fig. 2.13 – Shear transfer test specimens; (a) push-off; (b) pull-off; (c) modified push-off,
(Mattock and Hawkins, 1972)

Sixty-Six specimens divided to Ten series were used for the three types testing; Push-off, pull-off and modified push-off tests were done on initially cracked and initially uncracked specimens with different concrete strength and steel reinforcement. The values of shear strength for the tests support the hypothesis of shear friction.

Mattock (1974) studied the shear transfer behavior of concrete having reinforcement at an angle to the shear plane. Two series of specimens having parallel reinforcement and three series with orthogonal reinforcement were tested, figure 2.14. Some series of specimens were initially cracked and the others were uncracked at the beginning of the push-off shear test. One value of concrete compressive strength was used for all specimens, 4000 psi (27.6 MPa).

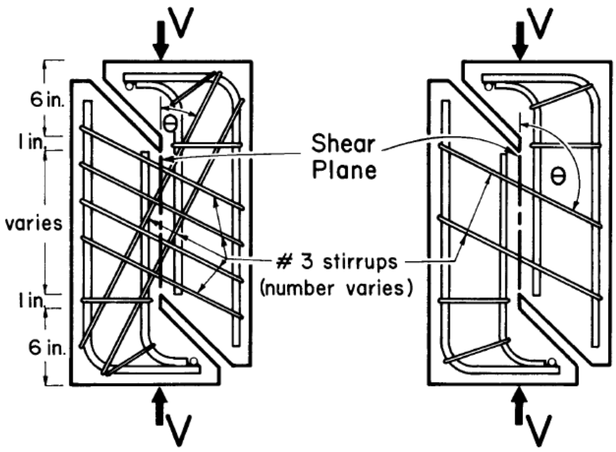

Fig. 2.14 – Typical push-off specimens with orthogonal and parallel reinforcement, (Mattock, 1974)

The load was applied and increased at about 35 increments till failure occurred. slippage was measured by mechanical gauges after each load increment. The initially cracked specimens started to slip from the beginning of the test, while no movement measured for the specimens which are initially uncracked until diagonal tension cracks start to appear crossing the shear plane. Typical shear stress-slip curves for the tested specimens with parallel reinforcement are illustrated in the following figure 2.15.

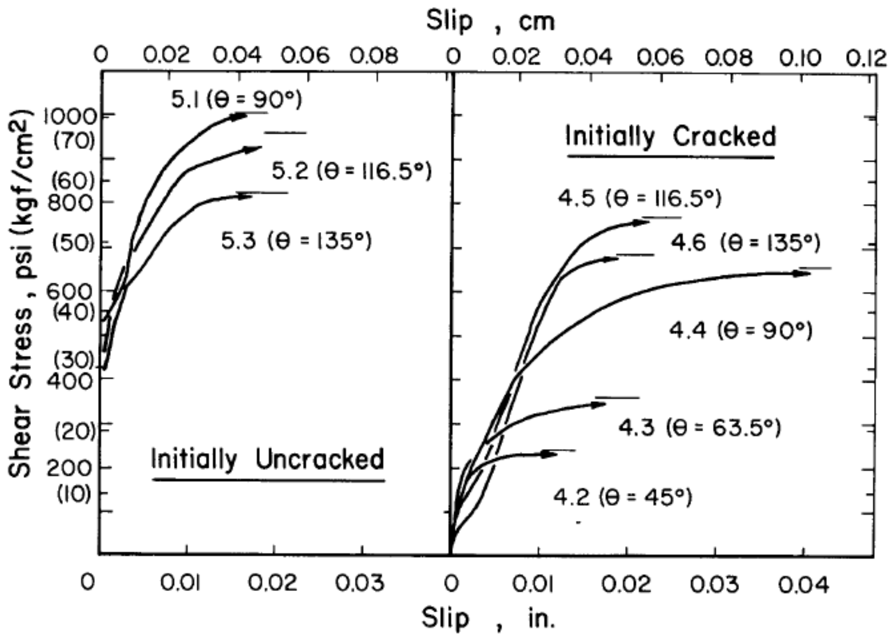

Fig. 2.15 – Typical shear stress-slip curves for specimens with parallel reinforcement, Mattock (1974)

Mattock developed an equation to estimate the ultimate shear stress v_u at the interface in case of inclined reinforcement as the following:

$$v_u = 2.76 \sin^2 \theta + \rho . f_s\,(0.8 \sin^2 \theta - 0.5 \sin 2\theta) \qquad (MPa)$$

Where, θ is the angle between the inclined steel and the shear plane.

The researcher made a comparison between the shear transfer strength by the above equation and the strengths measured in the push-off tests done for one of the series of specimens. Both calculated and experimented shear strength are very close.

The shear-friction hypothesis is proved by Mattock to be successfully applicable when having the case of reinforced concrete with inclined parallel or orthogonal reinforcement in an angle to the shear plane.

Walraven and Reinhardt, (1981) performed push-off tests on series of specimens with different geometry and stirrups arrangement and it is also supporting the theory of shear friction, sample of the tested specimens is shown in figure 2.16.

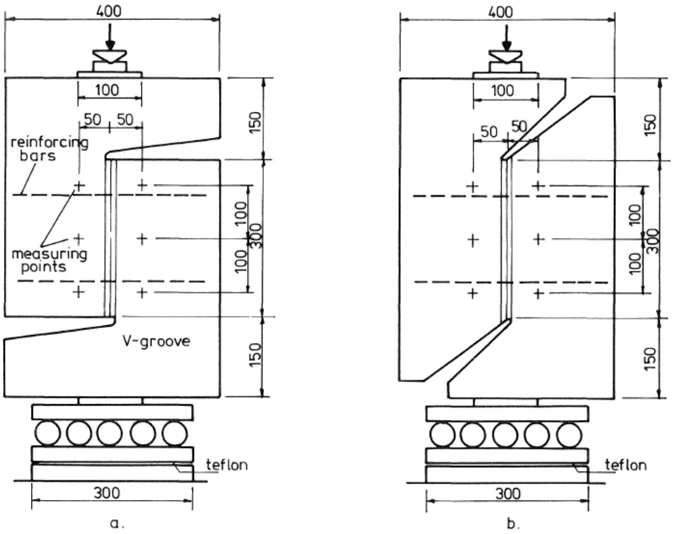

Fig. 2.16 – Geometry of the push-off specimens,
(Walraven and Reinhardt, 1981)

The setup for the push-off test machine and the electrical gauges fixed on the machine to measure the slip or the movement as shown in figure 2.17 as were used by Walraven and Reinhardt, 1981.

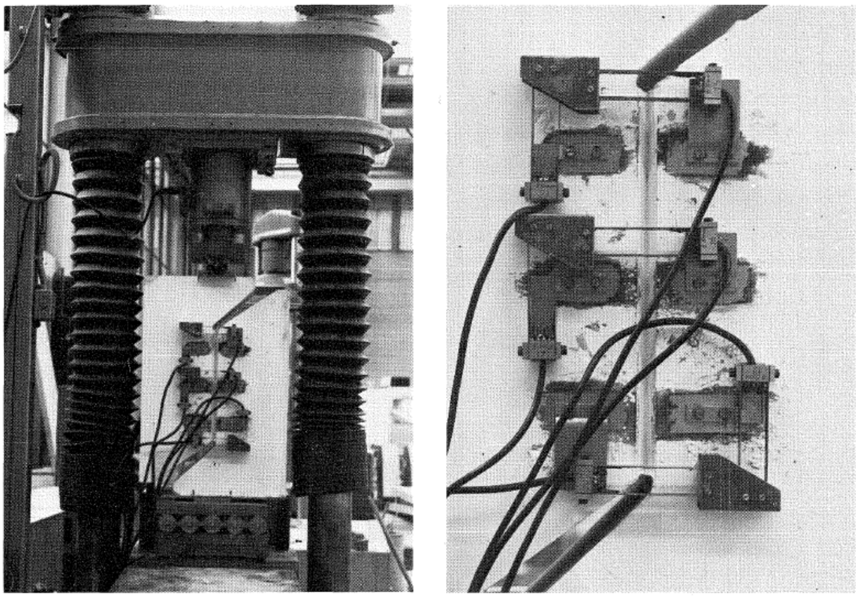

Fig. 2.17 – Push-off test setup, a loaded specimen to the left and the electrical strain gauges to the right,
(Walraven and Reinhardt, 1981)

Kahn and Mitchell, (2002) tested the shear friction at the interface of fifty specimens with high strength concrete (46.9 to 123.4 MPa). The specimens were designed to be identical to those done by Hofbeck *et al*. (1969) and Anderson (1960) but using high strength concrete. The interface was uncracked, precracked and cold joint. Figure 2.18 shows a specimen with a cold joint used at the test. Kahn and Mitchell recommended that the shear stress maximum limit of 0.2 f'_c to be maintained while the other limit of 5.5 MPa which was proposed for the normal strength concrete to be eliminated.

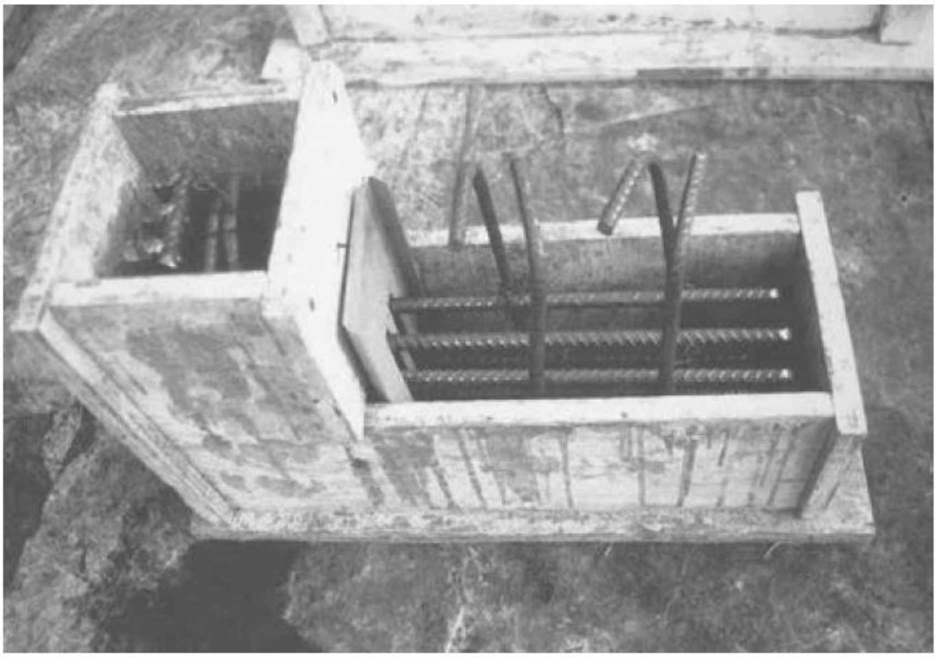

Fig. 2.18 – Cold joint specimen before concrete casting, Kahn & Mitchell (2002)

Sneed, Wermager and Krc, (2016) used the push-off test to study the shear friction at the interface of fifty-four specimens. Two of them were trials, the properties and results other fifty-two specimens were documented. The purpose was to test normal weight versus lightweight concrete specimens and give recommendations for the precast / prestressed concrete institute about the code factors related to the lightweight concrete. Figure 2.19 shows the steel used in one of specimens and the sensors and gauges which measure the strain are fixed to the steel bars which will be crossing the interface.

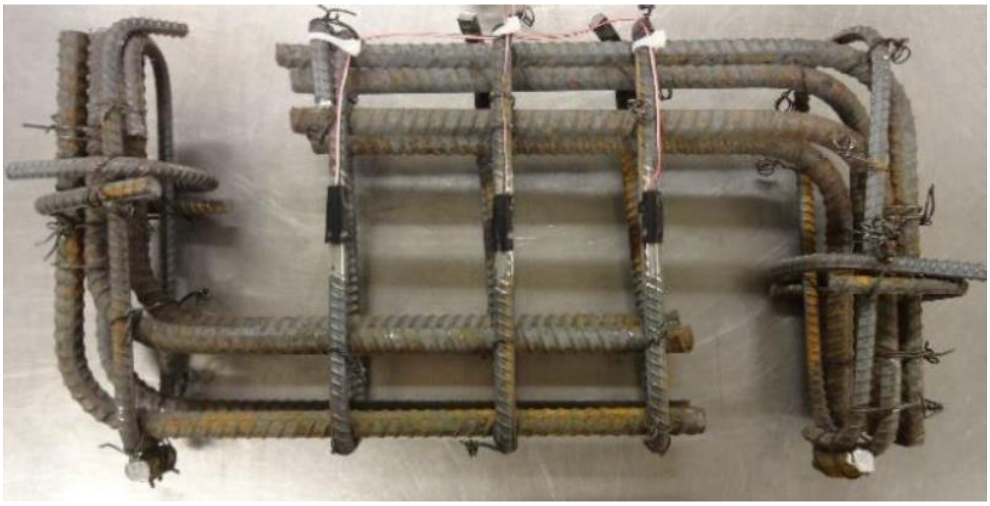

Fig. 2.19 – The steel cage with strain gauges fixed, Sneed et. al (2016)

2.4 Determination of the Horizontal Shear Failure

The horizontal shear failure of a composite concrete beam happens when a slip occurs between the two parts of the beam, and if that separation occurs before any flexural or vertical shear failure.

2.5 Maximum Slip

The maximum slip between the cast in place and the precast parts of the composite concrete beam as experimented and advised by Hanson (1960) was 0.13mm. However, bigger shear strengths will be considered if more slip values are allowed. Hall and Mast (1965) mentioned that no limits for the values of the slips should be considered.

2.6 Surface Preparation

The degree of roughness of the concrete surface has a big effect on the horizontal shear strength. There are many ways to have the concrete surface roughened such as wire brushing, sand blasting, shot blasting, hand scrubbing of the fresh concrete, formwork wavy shape and more. Figure 2.20 shows some of the roughening procedures that is usually used. Roughening the surface by the earlier researchers was done in different ways.

Hanson (1960) used the edge of a steel sheet to scrape the concrete to 9.5mm above and below the surface level. Saemann and Washa (1964) used retarding agents to allow for brushing the mortar between the aggregates and getting an intermediate rough surface with 3.2mm above and below the surface level. Evans and Chung (1969) used the wet brushing for the top surface of the webs to prepare the rough surface. Nosseir and Murtha (1971) used a wire brush to roughen the surface. The bond strength of the concrete-to-concrete interface increased with the increase of the surface roughness.

The provisions of the ACI 318-11 code of practice for getting full shear transfer is that the interface should be clean and free of laitance and the interface shall be roughened intentionally to a full amplitude of approximately 6mm regardless the way of roughening the surface.

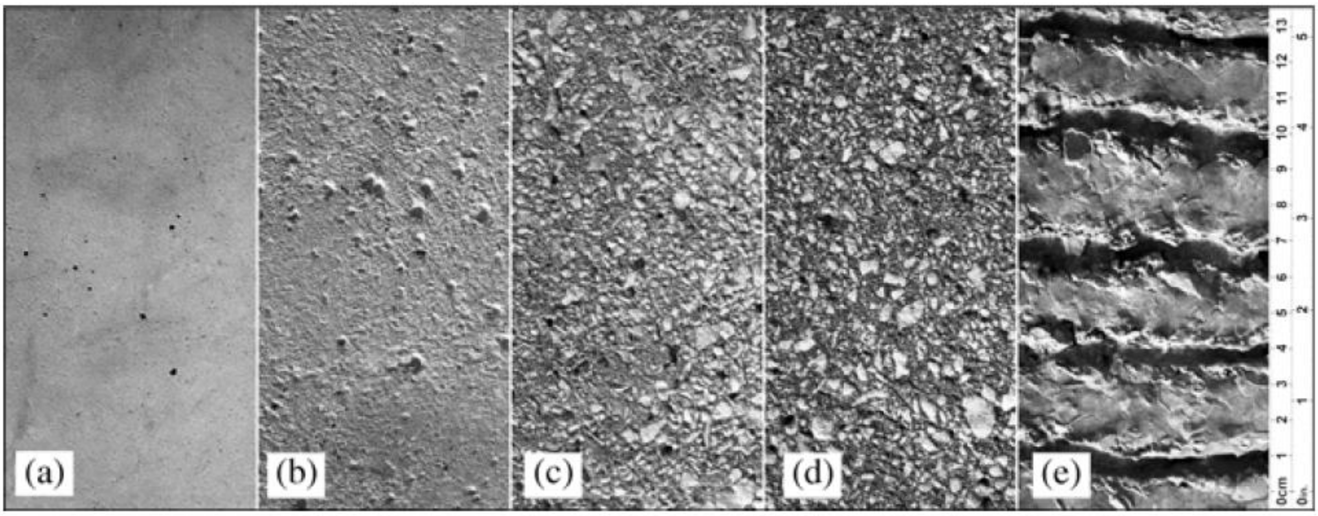

(a) Left as cast concrete surface.

(b) Wire brushing for the concrete surface.

(c) Sand blasting for the concrete surface.

(d) Shot blasting for the concrete surface.

(e) Hand scrubbing for the concrete surface.

Fig. 2.20 – Surface preparation & Roughness

2.7 Development Analysis of The Horizontal Shear Stresses

The development of beam horizontal shear stresses is illustrated in figure 2.21. If a beam is considered composed of layers or planks as per the explanation of Anil Patnaik, (1992). Those planks are of smooth surface from all sides, and a transversal force is applied. Those layers will bend separately as the smooth surfaces are frictionless, the layers slide above each other with no resistance as shown in figure 2.21b. This arrangement provides lower flexural strength than a monolithic beam of the same cross section. However, if those layers are clamped and well connected to each other, then sliding will be avoided and the beam strength should be the same as monolithic beam case. Shear stress is then developed at the interface in order to prevent any beam sliding, figure 2.21c. The stresses developed along the interface of the beam are known as the horizontal shear stresses. The composite concrete beam as shown in figure 2.21d can be categorized in between the previous two cases as it is not that smooth, and it is not perfectly connected beam layers or monolithic section.

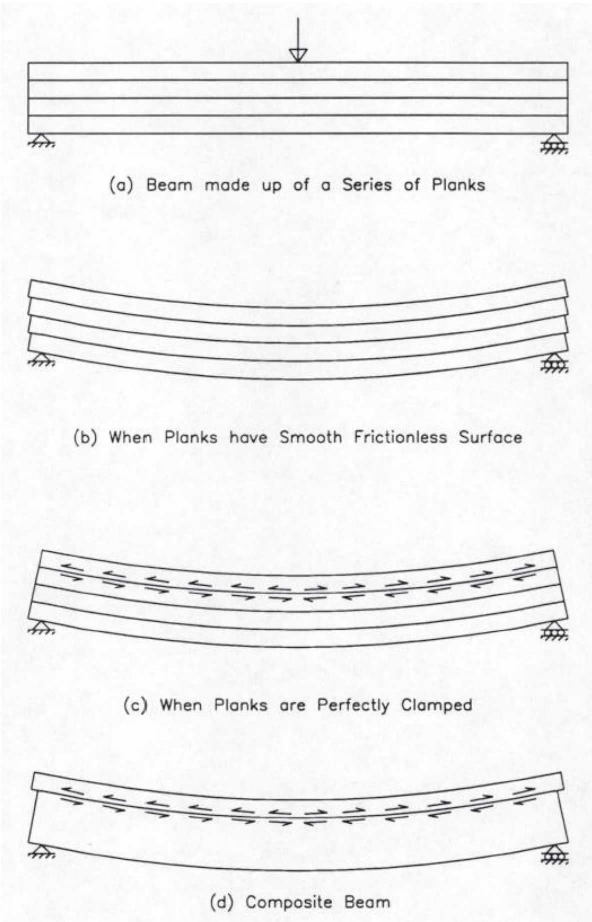

Fig. 2.21 – Development of horizontal shear stresses in concrete beams, Patnaik (1992)

Where the beam is in elastic and uncracked state when subject to transverse force, horizontal shear stress is determined by the equation (e.g., Gere and Timoshenko, 1984)

$$v_1 = \frac{V\,Q}{I\,b_v}$$

Where, V = shear force.

Q = first moment of area of the portion above the level under consideration with respect to the neutral axis.

I = moment of inertia of the whole section.

b_v = width of web at the level under consideration.

The above equation is only applicable to evaluate the shear stress at the linear elastic and uncracked condition. It can also be used for the cracked beams, but the moment of inertia and the first moment of area in this case are those used for the cracked section.

2.8 Shear-Friction Design Expressions – Historical Development

The shear-friction concept was brought to USA in 1958 and was continued for development by Hanson, Mast, Anderson, Birkeland & Birkeland, Mattock and other researchers. They introduced the shear-friction equation as the following:

$$v_u = \rho_v .\, f_y .\, \tan \phi$$

where, v_u is the horizontal shear strength at the interface of the composite concrete with two parts cast in different ages.

$\tan \phi$ is defined as a friction coefficient.

ρ_v is the ratio of steel crossing the interface of the composite concrete.

f_y is the steel yield strength.

This expression is simple to apply and easy to remember, it is being considered in many of the design standards and codes. It is proved by a lot of experimental studies and tests that it is safe and accurate for a certain degree. However, it is valid for low clamping stress only while it is unsafe for high values of clamping stresses. Continuous developments since then is happening to the shear-friction equation and the related studies of horizontal shear strength along the construction joints of the concrete beams cast in two stages at different ages.

2.8.1 Anderson (1960):

Anderson (1960) proposed an expression to calculate the ultimate horizontal shear strength at the interface of a composite beam. The equation is:

$$v_u = v_o + k.\rho$$

Where, v_u is the ultimate shear stress at the interface, ρ is the ratio of the reinforcement crossing the interface, v_o and k are parameters which are acquired from the push-off tests.

Anderson used two different concrete compressive strengths for each part of the beam, and each concrete has an equation to evaluate the shear stress as the following:

- When the compressive strength equals 20.7 MPa, $v_u = 4.41 + 229\ \rho$ (*MPa*).
- When the compressive strength equals 51.7 MPa, $v_u = 5.52 + 276\ \rho$ (*MPa*).

2.8.2 Hanson (1960):

Hanson (1960) also extracted the experimental results of the push-off tests similar to Anderson (1960) and he used one equation for the shear stress at the rough bonded interface of the composite beams, the equation is as follows:

$$v_u = 3.45 + 121\ \rho \quad (MPa).$$

The maximum slip at the interface of the tested specimens was 0.13mm. Hanson advised that this value should be the maximum allowed separation for composite concrete beams.

2.8.3 Mattock and Kaar (1961):

Mattock and Kaar (1961) included the effect of shear span depth ratio and determined the ultimate horizontal shear strength at the interface of the composite concrete beams by the following equation:

$$v_u = \frac{18.6}{\left(\frac{x}{d}+5\right)} + 121\ \rho \qquad (MPa).$$

Where, x is the shear span and d is the effective depth of the beam.

, and $\rho \geq 0.15\%$.

2.8.4 Grossfield and Birnstiel (1962):

Grossfield and Birnstiel (1962) experimented a total of eight beam, six of them are composite and the remaining two were monolithically casted. Different interface conditions were considered, some of them are rough, others are smooth, and others are of a smooth interface with applied adhesive material. The tested beams are of a span equal 3.05m. A fixed value of the clamping stress was considered for all beams, $\rho_v. f_y$ = 3.02 N/mm^2.

One beam only failed due to the shear friction and interface slip, all other beams failed due to flexural failure. The recorded slip for the beam failed in shear friction was 0.2mm. The authors concluded that the allowable slip limit of 13mm as advised by Hanson (1960) is not realistic and required to be reconsidered, specially that there is a doubt if those push-off specimens can be reliable to present real composite concrete beams.

2.8.5 Saemann and Washa (1964):

Saemann and Washa (1964) derived another equation to determine the interface ultimate horizontal shear strength of the composite concrete members as the following:

$$v_u = \frac{18.6}{X+5} + 207\,\rho\,\frac{33-X}{X^2+6X+5} \qquad (MPa).$$

Where,

X is the ratio between the shear span and section's effective depth.

The first term of the generated equation determines the shear stress without the effect of any reinforcing steel, and the second term of the equation considers the clamping stress when the steel reinforcement is provided across the interface of the beam.

2.8.6 Gaston and Kriz (1964):

Gaston and Kriz (1964) determined the ultimate shear stress in the scarf joints of the precast concrete elements.

The shear strength v_u for smooth unbonded interface is $v_u = 0.30 + 0.78\,\sigma_n$ (MPa).

The shear strength v_u for smooth bonded interface is $v_u = 0.76 + 0.70\,\sigma_n$ (MPa).

Where, σ_n is the normal stress at the interface due to external loads.

2.8.7 Birkeland and Birkeland, (1966):

Birkeland & Birkeland, (1966) introduced the shear-friction equation as the following:

$$v_u = \rho_v .\ f_y .\ \mu$$

where,

μ is the friction coefficient = tan ϕ.

ϕ is the angle of internal friction.

tan ϕ = 1.70 (monolithic concrete).

= 1.40 (intentionally roughened interfaces).

= 0.80 to 1.0 (ordinary construction joints and for concrete to steel interfaces).

$\rho_v .\ f_y$ is known as the clamping stress.

ρ_v is the ratio of steel reinforcement crossing the interface.

f_y is the yield strength of the steel reinforcement.

The application of the above equation is subject to the following limitations as per the researchers:

- The yield strength of the reinforcement crossing the interface should not exceed 350 *MPa*.
- Maximum reinforcing bar size = 19mm diameter.
- Well anchorage of the reinforcement at both parts of the beam should be done.
- The useful limit of steel ratio ρ_v = 0.015.
- The concrete is well confined.
- Concrete compressive strength, $f'_c \geq$ 27.6 MPa.
- Normal weight concrete is considered.
- The ultimate shear stress on the gross area of the interface $v_u \leq$ 5.52 MPa.
- Shear is developed by friction, not by bond.
- The interface is sound, clean and free from laitance, dust, paint or rust.

2.8.8 Badoux and Hulsbos (1967):

Badoux and Hulsbos (1967) studied the shear friction of the composite beams which include precast part and cast in place part using two types of surfaces. Rough surfaces and intermediate surfaces were tested. The intermediate surface was achieved by a steel brush in the next day of casting, while the rough surface was achieved either by a metal plate with sort of teeth or with a board having a popeyed pin.

The shear strength v_u at the interface of an intermediate finish surface is

$$v_u = \frac{13.79}{11+\left(\frac{a}{d}\right)} + 137.9 \qquad (MPa).$$

The shear strength v_u at the interface of rough finish surface is

$$v_u = \frac{24.14}{11+\left(\frac{a}{d}\right)} + 137.9 \qquad (MPa).$$

Where, a is the effective depth of the section and d is the shear span.

2.8.9 Birkeland (1968):

Birkeland (1968) was the first to determine the shear strength at the construction joint between the concrete parts using a nonlinear equation. This equation was derived from the research of Birkeland and Birkeland (1966). The horizontal shear stress of the parabolic function is obtained by:

$$v_u = 2.78\sqrt{\rho f_y} \qquad (MPa).$$

2.8.10 Mast (1968):

Mast (1968) used the same expression developed by Birkeland and Birkeland (1966), but he proposed maximum value for the ultimate shear strength equals 0.15 f'_c tan ϕ.

Mast tested concrete to concrete jointing with smooth and rough surfaces and concrete to steel composite beams. The following values of tan ϕ was considered:

tan ϕ = 1.40 (rough interface, concrete to concrete).

= 0.7 (smooth interface, concrete to concrete).

= 1.0 (concrete to steel interfaces, composite beams).

= 0.7 (concrete to steel interfaces, field-welded inserts).

2.8.11 Hofbeck, Ibrahim and Mattock (1969):

Hofbeck et al. (1969) discussed the proposals of previous researchers like Gaston and Kriz (1964), Birkeland and Birkeland (1966) and Mast (1968). Also studied the effect of some parameters on the shear strength at the interface between two concrete parts, such as concrete strength, steel strength, size of the shear reinforcement and the arrangement of the steel bars, dowel action, and the pre-cracked shear plane. The experiments showed that the existing cracks at the shear plane reduces the shear strength and increases the slip between the precast part and the cast in place part of the composite beam.

Changing the concrete strength affects the shear strength at the interface if the clamping stress $\rho.f_y$ is more than 4.14 MPa, while if the clamping stress value is lower, then the concrete strength will not affect the shear strength. Steel yield strength, size and arrangement of the steel crossing the interface affect the clamping stress $\rho.f_y$ and accordingly the shear strength. According to the tested samples, the dowel action affected significantly the shear strength of the beams with pre-cracked shear plane, while the effect is minor for the beams with previously uncracked shear plane.

2.8.12 Mattock and N.M. Hawkins (1972):

Mattock and Hawkins (1972) determined the ultimate horizontal shear strength at the interface of the composite concrete beams by derivation of the following equation:

$$v_u = 1.38 + 0.8\ (\rho.f_y + \sigma_n) \qquad (MPa)$$

Where,

σ_n is the normal stress at the interface.

As per the researchers' conclusion, the maximum value of v_u is the smaller between 10.34 MPa and $0.3f'_c$. $(\rho.f_y + \sigma_n)$ should be greater than or equal to 1.38 MPa. The coefficient of friction experimented specimen was 0.8.

2.8.13 Mattock (1974):

Mattock (1974) developed the proposal of Mattock and Hawkins (1972), and the updated shear strength design expression is as follows:

$$v_u = 2.76 + 0.8\,(\rho.f_y + \sigma_n) \qquad (MPa)$$

The shear strength and the clamping stresses limitations are similar to the previous research of Mattock and Hawkins (1972).

Mattock studied the shear transfer behavior of initially cracked concrete having reinforcement at an angle to the shear plane, figure 2.22.

The design expression presented was considering the effect of the reinforcement if inclined to the shear plane with an angle Θ, the ultimate shear strength then can be obtained from the following equation:

$$v_u = 2.76 \sin^2 \Theta + \rho.f_s\,(0.8 \sin^2 \Theta - 0.5 \sin 2\Theta) \qquad (MPa)$$

Where, Θ is the angle between the inclined steel and the shear plane. The maximum value of the ultimate shear strength is $0.3f'_c$.

f_s is a steel stress dependent on the angle Θ and can be determined with a friction coefficient equal 0.8 as the following:

$f_s = 0$, $0 \le \Theta \le 51.3^o$. (compression in the steel bars is small)

$f_s = -1.6\, f_y \cos(\Theta + 38.7^o)$, $51.3^o \le \Theta < 90^o$.

$f_s = f_y$, $90^o \le \Theta \le 180^o$.

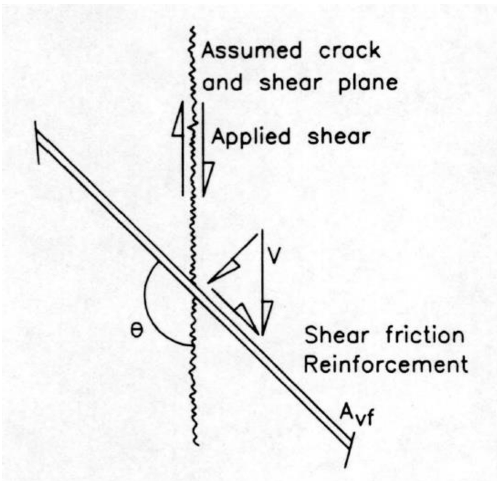

Fig. 2.22 - Shear-friction reinforcement inclined to the shear plane, Mattock (1974)

2.8.14 Hermansen and Cowan (1974):

Hermansen and Cowan (1974) performed number of push-off tests on specimens that was not precracked and proposed and equation similar to the design equation of Mattock (1974).

The equation considered to determine the ultimate horizontal shear strength v_u at the interface of monolithic section is as follows:

$$v_u = 4.0 + 0.8\ \rho.f_y \quad (MPa),$$

2.8.15 Cowan and Cruden (1975):

Cowan and Cruden (1975) continued the research done in 1974 by Hermansen and Cowan by testing more specimens that was not precracked as well.

They confirmed the previous results and adopted the same equation to determine the ultimate horizontal shear strength v_u at the interface of monolithic section is as follows:

$$v_u = 4.0 + 0.8\ \rho.f_y \quad (MPa),$$

2.8.16 Mattock, Li and Wang (1976):

Mattock *et al*. (1976) derived an equation to calculate the shear stress for lightweight concrete that is cracked at the shear plane.

The shear transfer strength v_u at the interface of all lightweight concrete - lightweight aggregate and lightweight sand - is as follows:

$$v_u = 1.38 + 0.8\ \rho.f_y \quad (MPa),$$

but not more than 0.2 f'_c nor 5.52 MPa.

The shear transfer strength v_u at the interface of sanded lightweight concrete is as follows:

$$v_u = 1.72 + 0.8\ \rho.f_y \quad (MPa),$$

but not more than 0.2 f'_c nor 6.90 MPa.

The above two design equations were achieved with a minimum value of clamping stress $\rho.f_y$ is not less than 1.38 *MPa*.

2.8.17 Raths (1977):

Raths (1977) presented an expression similar to the proposal of Birkeland (1968). He included the density of concrete to apply the equation on both normal weight and lightweight concrete.

The shear stress v_u for monolithic concrete beam is as follows:

$$v_u = 3.11\, C_s \sqrt{\rho f_y} \qquad (MPa).$$

The shear stress v_u for smooth concrete interface is as follows:

$$v_u = 2.03\, C_s \sqrt{\rho f_y} \qquad (MPa).$$

where,

the friction coefficient is considered equal to 0.60.

C_s is a constant related to the density of concrete, the typical values of C_s are as considered the following:

C_s = 1.0. (Normal weight concrete).

C_s = 0.85. (Sand lightweight concrete).

C_s = 0.75 (aggregate and sand lightweight concrete).

There is also a generated expression for the effective friction coefficient which is also related to the density of concrete as the following:

$\mu_e = 6.90 \frac{C_s^2 \mu}{v_u}$ (MPa).

2.8.18 Shaikh (1978):

Shaikh evaluated the ultimate shear stress at the interface of concrete to concrete or concrete to steel and the expression is as the following:

$$v_u = \phi.\rho.f_y.\mu_e$$

Where,

ϕ is a shear reduction factor equals 0.85.

μ_e is the effective coefficient of friction and can be obtained by the following equation:

$\mu_e = 6.90 \frac{C_s^2 \mu}{v_u}$ (MPa).

Where,

C_s is a constant related to the density of concrete, the typical values of C_s are as considered the following:

C_s = 1.0. (Normal weight concrete).

C_s = 0.85. (Sand lightweight concrete).

C_s = 0.75 (aggregate and sand lightweight concrete).

μ is the friction coefficient, and it is considered as the following:

μ = 1.4 (monolithically casting of concrete to concrete).

μ = 1.0 (concrete to concrete with roughened interface to amplitude of 6.4mm).

μ = 0.4 (concrete to concrete with smooth interface).

μ = 0.6 (concrete to steel interface).

2.8.19 Loov (1978):

Loov (1978) was the first to use the concrete strength in the evaluation of the ultimate shear strength as the following:

$$\frac{v_u}{f_c} = k\sqrt{\frac{\rho f_y + \sigma_n}{f_c}}$$

Where,

f_c is the concrete compressive strength.

K is a constant considered equals 0.50 for initially uncracked interface.

The ultimate shear strength is equal to the one proposed by Birkeland (1968) for a concrete compressive strength equals 30.89 MPa.

2.8.20 Mattock (1981):

Mattock (1981) experimented the effect of the cyclic loading on the behavior at the interfaces of the composite concrete beams. The reference for this research was the proposed design expressions of Mattock and Hawkins (1972) and Mattock *et al*. (1976) to evaluate the ultimate shear stress.

Mattock (1981) proposed that the ultimate shear strength at the interface between the two parts of the composite concrete beam under cyclic loading is equal to 0.80 of the shear strength due to monotonic loading of a normal weight composite concrete beam with roughened interface.

In case there is no bond between the concrete parts casted in different ages, then the shear strength under cyclic loading to be considered equal to 0.60 of the shear strength due to monotonic loading.

2.8.21 Vecchio and Collins (1986):

Vecchio and Collins (1986) experimented reinforced concrete elements considering previous researches, and proposed the following equation to evaluate the shear strength along the construction joint of the composite concrete sections:

$$v_u = 0.18\, v_{cimax} + 1.64\, f_{ci} - 0.82\, \frac{f_{ci}^2}{v_{cimax}} \qquad (MPa)$$

Where,

$$v_{cimax} = \frac{\sqrt{f_c'}}{0.31 + \frac{24\,w}{a + 16}} \qquad (MPa)$$

v_{cimax} = The maximum shear stress that can be resisted by the interface.

f_{ci} = compressive strength at the interface = $\rho . f_y + \sigma_n$ (MPa).

w = The average width of the interface, mm.

a = maximum size of the aggregate, mm.

The authors did not propose a maximum limit for the shear strength value of the above equation.

2.8.22 Walraven, Frenay and Pruijssers (1987):

Walraven *et al*. (1987) discussed the results of the push-off tests which were done by four separate researches on 88 specimens and then generated a non-linear equation to evaluate the shear strength of interface that is initially cracked. The design expression is as the following:

$v_u = C_1 \left(\rho f_y\right)^{C_2}$ (*MPa*).

$C_1 = 0.822 f_c^{0.406}$ (*MPa*).

$C_2 = 0.159 f_c^{0.303}$ (*MPa*).

The effect of concrete strength on the shear strength of the interface is illustrated in following figure 2.23.

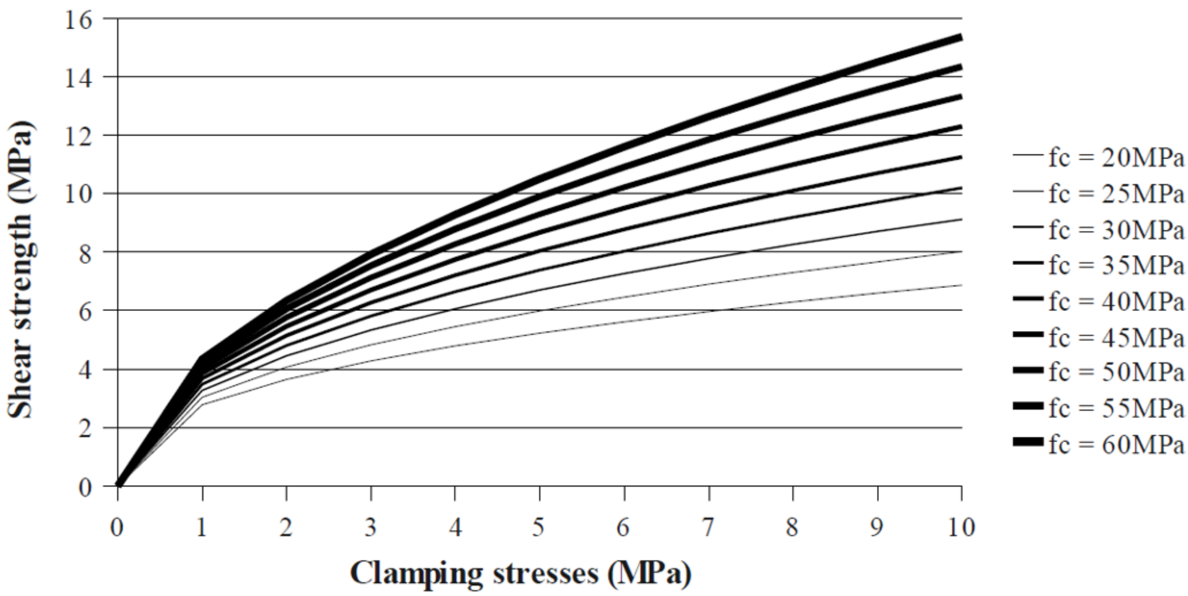

Fig. 2.23 – The effect of concrete compressive strength on the shear strength, Walraven *et al*. (1987)

The proposed shear strength equation is based on the model done by Walraven (1981), the composite concrete was assumed composed of paste and spheres representing aggregates and the interface represents the weakest part, so cracks develop in there. See figures 2.24 & 2.25.

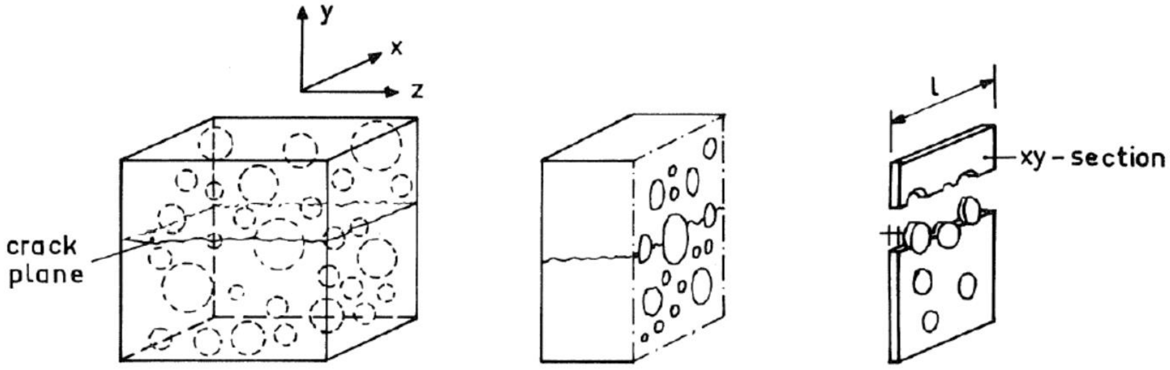

a. Cracked concrete body.

b. Z-plane of intersection.

c. Representative slice.

Fig. 2.24 – Cement matrix and aggregates effect, Walraven and Reinhardt (1981)

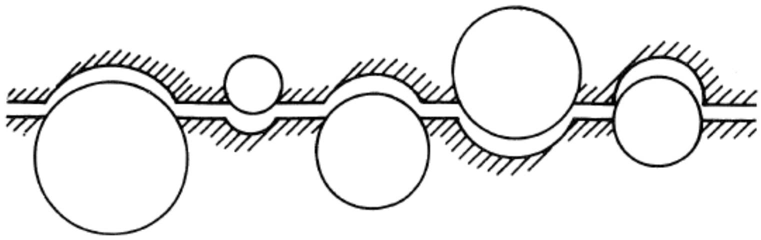

Fig. 2.25 – Generally observed structure of a crack plane (Sphere model), (Walraven and Reinhardt, 1981)

2.8.23 Mattock (1988):

Mattock (1988) studied and developed the proposal of Walraven *et al*. (1987) adding the effect of the normal force at the interface. The ultimate shear strength at the interface between the parts of the composite concrete beam is as the following:

$$v_u = 0.467 f_c^{0.545} + 0.8\left(\rho f_y + \sigma_n\right) \leq 0.3 f_c \qquad (MPa).$$

Where, σ_n is the normal stress at the interface.

2.8.24 Mau and Hsu (1988):

Mau and Hsu (1988) studied and discussed the paper of Walraven *et al*. (1987) and proposed the following expression to calculate the ultimate horizontal shear stress at the interface of the composite concrete beams:

$$\frac{v_u}{f_c} = k\left(\frac{\rho f_y}{f_c}\right)^{\alpha}$$

Where, k is constant similar to that proposed by Loov (1978) for the initially uncracked interface but Mau and Hsu (1988) considered the coefficient *k* equal to 0.66 for initially cracked and uncracked interface.

α is equal to 0.5, so the suggested shear strength expression is as the following:

$$\frac{v_u}{f_c} = 0.66\sqrt{\frac{\rho f_y}{f_c}} \leq 0.3$$

2.8.25 Anil Patnaik (1992):

Anil Patnaik (1992) tested sixteen beams of two parts casted at different stages, and proposed the following equation to evaluate the ultimate horizontal shear stress considering rough interface:

$$v_u = 0.6\sqrt{\left(0.1+\rho f_y\right) f_c} \leq 0.25 f_c \qquad (MPa).$$

2.8.26 Loov and Patnaik (1994):

Loov and Patnaik (1994) developed an expression to determine the shear strength based on the paper of Loov (1978). The suggested design expression considers the influence of the concrete strength, concrete density and the clamping stress for composite concrete beams with rough interface.

The ultimate shear strength at the interface where no steel crossing the beam interface is as the following:

$$v_u = 0.6\sqrt{0.1 f_c} \qquad (MPa).$$

The ultimate shear strength at the interface where steel crossing the beam interface is as the following:

$$v_u = k.\lambda\sqrt{\left(0.1+\rho f_y\right) f_c} \qquad (MPa).$$

Where, *K* is constant, and it is as the following:

K = 0.5 (composite concrete members).

K = 0.6 (monolithic reinforced concrete members).

λ is a correction factor related to the density of concrete and it is considered as the following:

λ = 1.00 (normal weight concrete).

λ = 0.85 (Sand lightweight concrete).

λ = 0.75 (aggregate and sand lightweight concrete).

The maximum horizontal shear strength should not exceed $0.25 f_c$.

2.8.27 Mattock (1994):

Mattock (1994) discussed the findings in the paper of Loov and Patnaik (1994), Mattock proposed that the shear strength at the joint of the composite beam not to be proportional with $f_c^{\,0.5}$. Mattock developed new expressions to determine the ultimate shear strength using the tests results by Loov and Patnaik (1994). The following equation determines the ultimate horizontal shear strength along a crack in a monolithic concrete beam with normal density:

$$v_u = \frac{\sqrt{\rho f_y}\ f_c^{0.73}}{4.536} \qquad (MPa).$$

The maximum ultimate horizontal shear strength is increased to $0.3 f_c$.

While for pre-cracked concreate beams with roughened interface, the following design expression was proposed:

$$v_u = \frac{\sqrt{\rho f_y}\ f_c^{0.73}}{4.536} - 0.02\, f_c \quad (MPa).$$

2.8.28 Valluvan, Kreger and Jirsa (1999):

Valluvan *et al*. (1999) proposed a modification to the provisions of the shear-frictions in the ACI 318 – 95 which they proved by their experiments that the code provisions are very conservative. The suggested equation to calculate the ultimate horizontal shear strength is as the following:

$$v_u = \mu\ (\rho.f_y + \sigma_n)$$

Where, σ_n is the normal stress due to external forces which acts at the interface.

The value of the shear strength using the above equation is applicable when the normal stress is equal or less than 5.52 MPa, and then the minimum value of the shear stress is between 0.25 f_c and 5.52 MPa.

The following equation calculates the ultimate shear strength at the interface when the normal stress at the interface is greater than 5.52 MPa.

$$v_u = \sigma_n.\ \mu$$

The minimum value of the shear stress due to external loads is between 0.6 f_c and 14.49 MPa.

2.8.29 Patnaik (2000):

Patnaik (2000) studied and discussed the paper and tests done by Valluvan *et al*. (1999), and suggested a modified equation to calculate the ultimate horizontal shear stress for monolithic concrete beams and composite concrete beams with roughened interface as the following:

$$v_u = 0.55\sqrt{\left(0.25+\rho\, f_y\right) f_c} \quad (MPa)$$

For beams with interface not intentionally roughened, the shear strength can be as the following:

$$v_u = 0.5\sqrt{\left(0.25+\rho f_y\right) f_c} \qquad (MPa)$$

The horizontal shear strength upper limit should not exceed the minimum between the following values:

1) 0.25 f_c and 7.93 MPa (Intentionally roughened interface).
2) 0.2 f_c and 5.52 MPa (Not intentionally roughened interface).
3) 0.2 f_c and 8.96 MPa (monolithic concrete).

2.8.30 Mattock (2001):

Mattock (2001) developed equations to calculate the shear strength for high strength and normal strength concrete. The applicable cases are monolithic concrete or a precast beam cast in two stages with interface that is either not intentionally roughened or intentionally roughened.

For concrete part cast against a precast concrete part with an interface not intentionally roughened, the ultimate horizontal shear strength is as follows:

$$v_u = 0.6\, \lambda.\rho.f_y$$

Where,

λ is a coefficient related to the density of concrete.

λ = 1.0 (normal weight concrete).

λ = 0.85 (sand lightweight concrete).

λ = 0.75 (sand and aggregate lightweight concrete).

The shear strength values are between 0.2f_c and 5.52 MPa.

While for monolithic cast concrete and composite concrete beams with intentionally roughened interface, where the normal stress at the interface ≥ k_1 /1.45, or when the ultimate shear stress ≥ 1.55k_1, the following design expression is used to calculate the ultimate horizontal shear strength at the interface:

$$v_u = k_1 + 0.8\ (\rho.f_y + \sigma_n)$$

The minimum value is between $K_2\ f_c$ and k_3, while if the normal stress < k_1 /1.45, or when the ultimate shear strength < 1.55k_1, the following design expression is used to calculate the ultimate horizontal shear strength at the interface:

$$v_u = 2.25\ (\rho.f_y + \sigma_n)$$

Where, σ_n is the normal stress at the interface.

k_1 is a coefficient related to the weight of concrete, k2 and k3 are parameters and can be determined as follows:

- For monolithic cast concrete with normal weight, the value of K_1 is between 0.1f_c and 5.52 MPa, k_2 = 0.3, k_3 = 16.55 MPa.
- For composite beams with intentionally roughened interfaces of normal weight concrete, k_1 = 2.76 MPa, k_2 = 0.3, and k_3 = 16.55 MPa.
- For sand lightweight concrete, k_1 = 1.72 MPa, k_2 = 0.2, and k_3 = 8.27 MPa.
- For sand and aggregate light weight concrete, k_1 = 1.38 MPa, k_2 = 0.2, and k_3 = 8.27 MPa.

2.8.31 Patnaik (2001):

Patnaik (2001) discussed the provisions of the shear friction for smooth interfaces which was proposed in the American code of practice ACI 318 – 99 and commented that is very conservative. Patnaik suggested the following equation to evaluate the ultimate horizontal shear strength for composite concrete beams with smooth interface:

$$v_u = 0.6 + \rho.f_y \quad (MPa).$$

The maximum horizontal shear strength should not exceed the minimum between 0.2 f_c and 5.5 MPa.

Patnaik suggested that shear strength can be utilized for smooth interface without crossing stirrups provided that the clamping stress is less than 0.35 MPa, although it is not recommended since there is an amount of uncertainty in depending on strength because of the friction of the cast in place slab part above the precast concrete web part alone in the designs. The following equation is then proposed:

$$v_u = 0,\ \ \rho.f_y < 0.35 \text{ MPa}$$

2.8.32 Kahn and Mitchell (2002):

Kahn and Mitchell (2002) proposed modifications to the provisions of the shear friction in ACI 318-99 to include the high strength concrete. A maximum upper limit of the shear strength of 0.2 $f'c$ is proposed and eliminating the other previously proposed upper limit of 5.5 MPa. The developed design expression as per the study is as the following:

$$v_u = 0.05\, f'_c + 1.4\, \rho.f_y$$

The considered friction coefficient is 1.4, which relates to monolithic concrete.

2.8.33 Gohnert (2003):

Gohnert (2003) tested ninety composite concrete specimen and then suggested an expression to calculate the ultimate horizontal shear strength at the interface between the precast concrete beam part and the cast in place part as the following:

$$v_u = 0.2090\, R_z + 0.7719 \quad (MPa;\ mm).$$

Where, R_z is a texture parameter that represent the distance between the peaks average height and valleys average height of the interface concrete surface. The tested precast parts of beams were produced by five different manufacturers, those ribs had different cross section geometry. The value of the interface surface amplitude parameter R_z varied between 0.89mm and 4.22mm and the used concrete strength was between 22.8 MPa and 56.2 MPa.

2.8.34 Mansur, Vinayagam and Tan (2008):

Mansur *et al*. (2008) studied the shear friction along the interface of composite concrete experimentally and analytically. A comparison was done between the expressions used in previous researches to calculate the horizontal shear strength. The design expressions developed by Walraven *et al*. (1987), Mau and Hsu (1988), Lin and Chen (1989), Mattock and co-workers (1972, 1976, 2001),

Loov and Patnaik (1994) were mainly discussed in addition to those proposed by the design codes of ACI 318 – 05 and PCI Design Handbook (1992).

Mansur *et al*. (2008) stated that the expressions proposed by Walraven *et al*. (1987), Mau and Hsu (1988), Loov and Patnaik (1994) are unsafe.

Based on the tests and the analytical model done by Mansur *et al*. (2008), and considering concrete strength for the tested specimens between 18 MPa and 100 MPa and the normalized clamping forces ($\rho.f_y/f_c$) are between 0.02 and 0.39. The developed expression to evaluate the ultimate horizontal shear strength at the interface of the composite concrete beams is as the following:

$$\frac{v_u}{f_c} = 0.566\sqrt{\frac{\rho f_y}{f_c}} \leq 0.3$$

Another design expression was proposed for normalized clamping forces ≤ 0.075 to evaluate the shear strength at the interface of the composite concrete beams as the following:

$$\frac{v_u}{f_c} = 2.5\,(\frac{\rho f_y}{f_c})$$

Also, the ultimate shear strength can be determined by the following equation for normalized clamping forces between 0.075 and 0.27 as follows:

$$\frac{v_u}{f_c} = \frac{0.56}{f_c^{\,0.385}} + 0.55\left(\frac{\rho f_y}{f_c}\right)$$

The ultimate shear strength can be obtained by the following equation for normalized clamping force ≥0.27:

$$\frac{v_u}{f_c} = 0.3$$

2.8.35 Harries, Zeno & Shahrooz (2012):

Harries *et al*. (2012) studied the interface shear resistance for number of specimens with different ratios of the steel reinforcement crossing the interface, and they compared the results of steel of yield stresses 414 MPa & 690 MPa. Each part of every specimen was cast after 14 days from the other interlocked part, and the concrete compressive strength is 40 MPa and 50 MPa at the time of test.

The authors found that the section ultimate capacity is not affected by the steel grade. Although, the specimens with lower rebar yield stress declined quickly after reaching the ultimate shear capacity, while those with higher steel grade sustained the ultimate shear load after reaching the peak of the curve.

It was suggested by the researchers that this behavior difference is because of the difference in bond characteristics of the steel bars of both grades. The illustration of the shear friction was done by separating concrete contribution from steel bars contribution to the shear strength as shown in figure 2.26. The authors found the steel does not yield for the specimen in figure 2.26b, and the shear capacity as per the following AASHTO equation cannot be reached.

$$V_{ni} = c\ A_{cv} + \mu\ (A_{vf}.f_y + P_c)$$

Where,

$C\ A_{cv}$ is the term account for effects of cohesion and aggregate interlock.

P_c is the applied load.

μ is the friction coefficient.

Harries *et al*., stated that the shear-friction provisions and equations of ACI 318-08 and AASHTO (2007) are very simplistic and misleading which is not represent the real behavior of the composite concrete cast in stages at different times. The authors proposed a modified equation for calculating the nominal horizontal shear strength V_{ni}.

$$V_{ni} = \alpha\ A_{cv}\ f'_c + 0.002\ A_{cv}.E_c \leq 0.20\ A_{cv}\ f'_c$$

Where,

α is interface coefficient, $\alpha = 0.075$ (monolithic uncracked interface).

, α = 0.04 (cold joint interface).

, α = 0.0 (monolithic pre-cracked interface).

, A_{cv} is the shear interface area = $b_v.L_{nh}$. b_v is the interface width & L_{nh} is the interface length.

, f'_c is the concrete compressive strength.

, E_c is the steel modulus of elasticity.

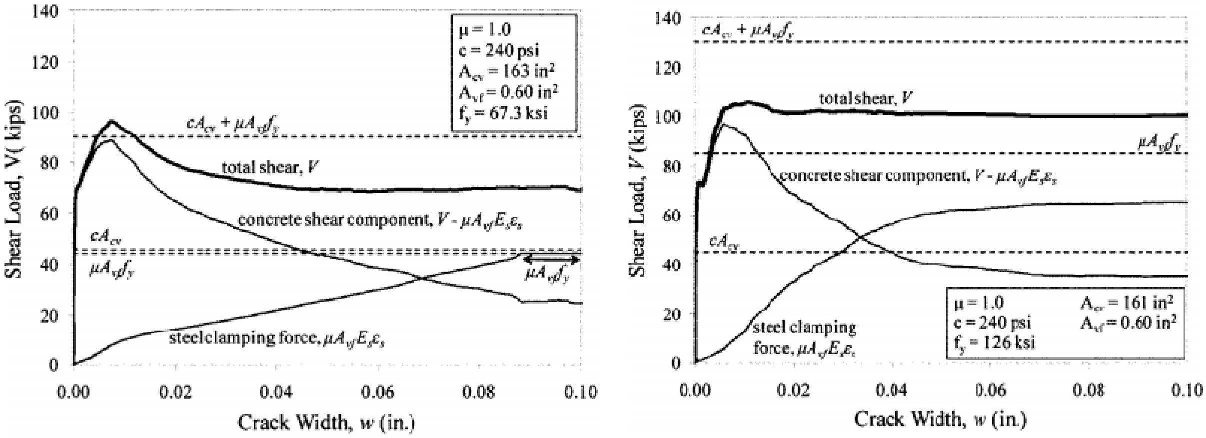

a) Specimen, with f_y = 414 MPa

b) Specimen, with f_y = 690 MPa

Fig.2.26 – Shear friction of concrete and steel components of two test specimens, with different steel grades.

2.8.36 Sneed, Wermager & Krc (2016):

Sneed *et al*. (2016) studied the shear friction along the interface of composite concrete experimentally. A total of 54 push-off specimens were tested. Two of them were just trials and the remaining 52 specimens were documented. Different conditions were considered, normal weight and light weight concrete of different light weight aggregates, different reinforcement ratios, both smooth and rough interfaces tested. Also, some of the specimens were uncracked at the time of experiment. Sneed *et al*., compared the results with the provisions of ACI 318-14 and the PCI Design Handbook (2010). The conclusion and recommendation are that the use of λ – the lightweight concrete factor – in the evaluation of the horizontal shear strength is so conservative and not required. Accordingly, the researcher recommended to remove λ from all the related equations regardless the interface surface preparation condition. This will end up with safe and economic design as per the research done.

2.9 Horizontal Shear Design Requirements - Code Provisions

2.9.1 Shear-Friction Provisions of ACI 318-11 Code of Practice

Horizontal shear forces are fully transferred between the parts of the composite concrete beams cast in more than one stage by the horizontal shear strength of the interface or by the well anchored stirrups, or by both of them. Surface preparation and the degree of roughness are considered important factor for determination of that shear strength.

The nominal horizontal shear strength at the shear plane or at the interface of concrete beam cast in two stages at different ages is: $\phi V_{nh} \geq V_u$

Where, ϕ is the shear reduction factor = 0.75 for shear.

There are three equations to calculate the nominal horizontal shear strength as listed in the ACI 318-11 code.

1) The case where no stirrups are used, the contact surface is clean, free of laitance and intentionally roughened. Then the maximum value of V_{nh} is to be considered 0.55 $b_v.l_{nh}$.
2) The case where minimum stirrups are crossing the interface between the two parts, and the contact surface is clean, free of laitance, and not intentionally roughened. Then the maximum value of V_{nh} is to be considered 0.55 $b_v.l_{nh}$.
3) The case where stirrups are provided, and contact surface is clean, free of laitance, and intentionally roughened to a full amplitude of approximately 6mm. Then the nominal horizontal shear V_{nh} is considered the lesser of the following:

- $(1.8 + 0.6\ \rho_v.f_y)\ \lambda\ b_v.l_{nh}$.
- 3.5 $b_v.l_{nh}$.

Where,

b_v is the width of the beam section at the interface.

l_{nh} is the interface beam length for horizontal shear design, taken between the inflection points.

In case the acting ultimate shear force V_u is greater than 3.5 $b_v.l_{nh}$, then the horizontal shear design shall be as the following:

The nominal shear strength at the shear plane or at the interface of concrete beam in case the stirrups are perpendicular to the shear plane is:

$$V_n = \mu . A_{vf} . f_y$$

$$\text{or, } v_u = \mu . \rho . f_y$$

and the area of shear friction reinforcement is:

$$A_{vf} = \frac{V_u}{\phi . f_y . \mu}$$

Where, ϕ is the shear reduction factor = 0.75.

μ is the friction coefficient and it depends on the weight of concrete and also the surface roughness at the shear plane. A variable that changes the value of the friction coefficient is λ, which is equal to 1.0 for normal weight concrete. While for light-weight concrete, λ is reduced and it is calculated with maximum value of 0.85. The following table 2.1 indicates the friction coefficient values as per the code.

2.9.1.1 Table (2.1) – Coefficient of friction as recommended by the (ACI 318-11)

Contact surface condition	Coefficient of friction μ [1]	
Concrete placed monolithically	1.4λ	(a)
Concrete placed against hardened concrete that is clean, free of laitance, and intentionally roughened to a full amplitude of approximately 6mm	1.0λ	(b)
Concrete placed against hardened concrete that is clean, free of laitance, and not intentionally roughened	0.6λ	(c)
Concrete placed against as-rolled structural steel that is clean, free of paint, and with shear transferred across the contact surface by headed studs or by welded deformed bars or wires	0.7λ	(d)

[1] λ=1.0 for normal weight concrete. For light weight concrete, λ is obtained from tables (2.2) & (2.3).

The maximum yield strength for the steel reinforcement crossing the interface between the two beam parts and which resist the horizontal shear is limited to 420 MPa.

When the reinforcement of shear friction is inclined by an angle α to the shear plane and tension is developed in the steel reinforcement by the shear force, the nominal shear strength along the shear plane / interface is calculated by the following equation:

$$V_n = A_{vf}.f_y.(\mu.\sin\alpha+\cos\alpha)$$

$$\text{or, } v_u = \rho.f_y.(\mu.\sin\alpha+\cos\alpha)$$

Where:

α is the angel between the shear plane and the provided shear-friction reinforcement.

ρ is the reinforcement ratio at the interface.

f_y is the yield strength of the steel reinforcement crossing the interface.

μ is the friction coefficient.

The inclined shear-friction reinforcement is explained in figure 2.27, the formula is extracted from the paper of Mattock 1974, the above equation is applicable if the component of shear force which is parallel to the reinforcing steel bar develops tension in the steel and the component parallel to the interface contributes to partial resistance of the shear force. While in case the component of shear force parallel to the reinforcing steel bar develops compression in the steel as shown in figure 2.28, then the shear friction is not applied (V_n = 0)

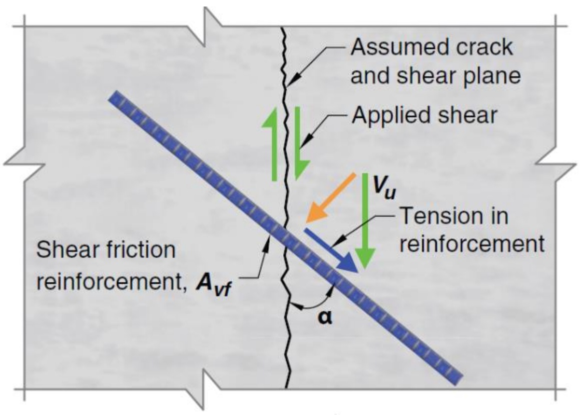

Fig. 2.27 – Tension in shear friction reinforcement according to Mattock, 1974

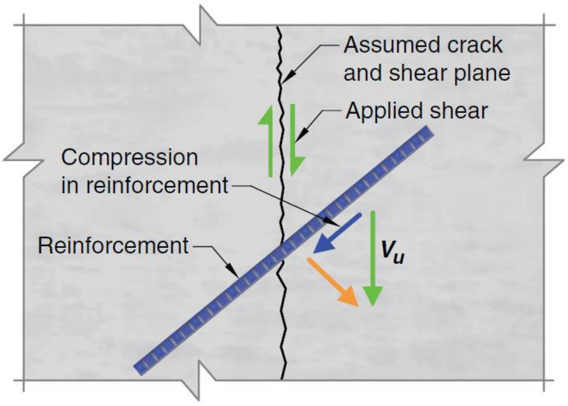

Fig. 2.28 – Compression in reinforcement where shear friction does not apply,

The values of λ for lightweight concrete based on equilibrium density and the composition of aggregates are obtained from the following tables 2.2 and 2.3 as proposed by the ACI 318-11 code.

2.9.1.2 Table (2.2) – Values of λ for lightweight concrete based on equilibrium density, (ACI 318-11)

w_c, kg/m³	λ	
≤ 1600	0.75	(a)
1600 < w_c < 2160	0.0075 w_c ≤ 1.0	(b)
≥ 2160	1.0	(c)

2.9.1.3 Table (2.3) – Values of λ for lightweight concrete based on composition of aggregates, (ACI 318-11)

Concrete Weight	Composition of aggregates	λ
All-lightweight	Fine: ASTM C330M Coarse: ASTM C330M	0.75
Lightweight, fine blend	Fine: Combination of ASTM C330M and C33M Coarse: ASTM C330M	0.75 to 0.85 [1]
Sand-lightweight	Fine: ASTM C33M Coarse: ASTM C330M	0.85
Sand-lightweight, coarse blend	Fine: ASTM C33M Coarse: Combination of ASTM C330M and C33M	0.85 to 1 [2]

[1] Linear interpolation from 0.75 to 0.85 is permitted based on the absolute volume of normal weight fine aggregate as a fraction of the total absolute volume of fine aggregate.

[2] Linear interpolation from 0.85 to 1 is permitted based on the absolute volume of normal weight coarse aggregate as a fraction of the total absolute volume of aggregate.

There are maximum values for shear friction as the equations become unconservative for some cases if exceeded the proposed upper limits as shown in the table 2.4, in case a concrete is cast on other concrete with different compressive strength, then the lesser value of f'_c should be considered:

2.9.1.4 Table (2.4) – Maximum shear strength v_u along the shear plane, (ACI 318-11)

Surface Condition	Maximum v_u		
Normal weight concrete placed monolithically or placed against hardened concrete intentionally roughened to a full amplitude of approximately 6mm	Least of (a), (b), and (c)	$0.2\, f'_c$	(a)
		$(3.3 + 0.08\, f'_c)$	(b)
		11 MPa	(c)
Other cases	Lesser of (d) and (e)	$0.2\, f'_c$	(d)
		5.5 MPa	(e)

2.9.2 Shear-Friction Provisions of Eurocode 2 (2004)

The shear strength at the shear plane or at the interface of concrete beam cast in two stages at different ages is $v_u = c.f_{ctd} + \mu\, \sigma_n + \rho.f_y.(\mu.\sin\alpha + \cos\alpha) \leq 0.5\, v\, f_{cd}$

Where:

σ_n is the stress caused by the minimum external normal stress acting on the interface.

f_{ctd} is the concrete tensile strength.

f_{cd} is the concrete compressive strength.

ρ is the reinforcement ratio at the interface.

f_y is the yield strength of the steel reinforcement crossing the interface.

v is the strength reduction factor.

α is the angle between the steel reinforcement and the interface shear plane, α is between 45 to 90.

c is the cohesion coefficient.

μ is the friction coefficient.

The value of σ_n is positive in case of compression and the upper limit is 0.6 f_{cd}, while it is negative at tension. The term $c.\ f_{ctd} = 0$ in case of tension.

The coefficients c and μ depend mainly on the surface roughness condition and can be obtained from table 2.5.

2.9.2.1 Table (2.5) – Coefficients of friction and cohesion, (EN 1992-1-1, 2004)

Contact surface condition	**Coefficient of friction μ**	**Coefficient of cohesion c**
Very smooth surface	0.50	0.025 to 0.10
Smooth surface	0.60	0.20
Rough surface with at least 3mm roughness at about 40mm spacing	0.70	0.40
Intended surface: Indentations as per the figure (2.29)	0.90	0.50

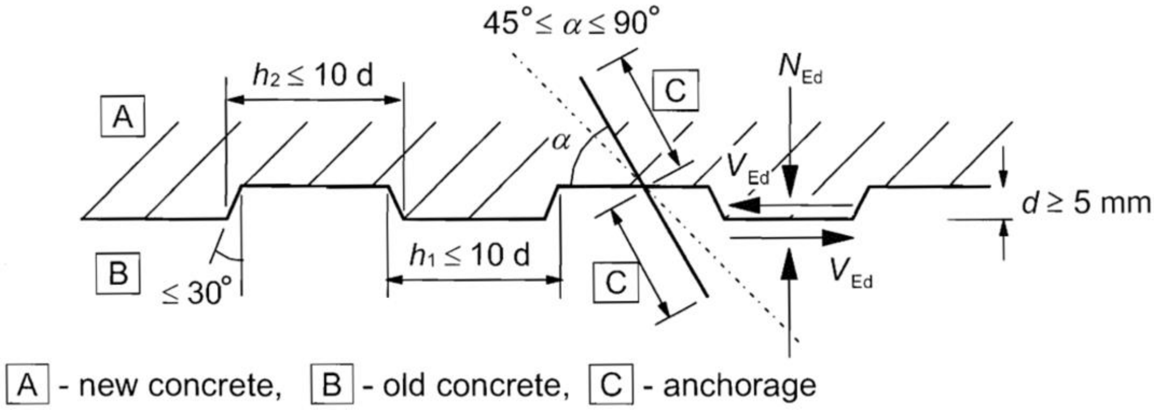

Fig. 2.29 – Intended surface at the joint between old and new concrete

2.9.3 Shear-Friction Provisions of PCI Design Handbook (2010)

As per the PCI Design Handbook which is a design code for the precast and prestressed concrete, shear-friction theory is considered the main tool to calculate the shear strength at the interface between the precast concrete and the topping cast in place slab part. The shear strength at the shear plane or at the interface of concrete beam cast in two stages at different ages is as the following:

$$v_u = \phi.\rho.f_y.\mu$$

or, if allowed, $v_u = \phi.\rho.f_y.\mu_e$

Where,

ϕ is constant is equal to 0.75.

ρ is the reinforcement ratio at the interface.

f_y is the yield strength of the steel reinforcement crossing the interface, $f_y \leq 420$ MPa.

μ_e is the effective friction coefficient, $\mu_e = (6.90\ \lambda\ \mu)/v_u$. The values of μ_e is categorized in the table 2.6.

μ is the coefficient of shear-friction, the values of μ depend on the weight and surface roughness condition of the interface. The values of μ are in accordance with the ACI 318-11 code of practice and are categorized in the table 2.6.

λ is a factor related the concrete density, it is equal to 1.0 for normal weight concrete, 0.85 for sand light weight concrete, and 0.75 for all aggregate and sand light weight concrete.

The maximum values of v_u are also mentioned in the table 2.6.

2.9.3.1 Table 2.6 – Recommended shear-friction coefficients, (PCI Design Handbook, 2010)

Crack interface condition	**Recommended μ**	**Maximum μ_e**	**Maximum v_u** (The lesser of)
Concrete to concrete, cast monolithically	1.4λ	3.4	0.30 λ f'_c 6.90 MPa
Concrete to hardened concrete, with roughened interface	1.0λ	2.9	0.25 λ f'_c 6.90 MPa
Concrete to concrete	0.6λ	Not allowed	0.20 λ f'_c 5.52 MPa
Concrete to steel	0.7λ	Not allowed	0.30 λ f'_c 5.52 MPa

2.9.4 Shear-Friction Provisions of AASHTO LRFD Bridge Design Specifications (2007)

According to the AASHTO code of bridge design, the shear-friction shall be studied for the following cases:

1) At Existing crack of a section.
2) At the interface between different materials.
3) At the interface between two concrete parts cast in two stages at different times.
4) At the interface between elements of different sections.

The ultimate shear resistance at the interface, V_{ri} is equal to the following:

$$V_{ri} = \phi \, V_{ni},$$

$$V_{ri} \geq V_{ui}$$

Where,

V_{ni} is the nominal interface resistance.

V_{ui} is the ultimate shear force at the interface due to the total load.

ϕ is shear resistance factor. The value of ϕ is as the following:

ϕ = 0.90. (Tension controlled reinforced concrete sections).

ϕ = 1.0 (Tension controlled prestressed concrete sections).

ϕ = 0.90. (Shear & Torsion in normal weight concrete sections).

ϕ = 0.70. (Shear & Torsion in lightweight concrete sections).

The nominal interface shear resistance is calculated from the following formula:

$$V_{ni} = c\ A_{cv} + \mu\ (A_{vf}\ f_y + P_c)$$

Where,

C = cohesion factor.

μ = friction coefficient.

P_c = permanent net compressive force normal to the shear plane.

A_{cv} = area of concrete section at the interface = $b_v.L_{vi}$.

A_{vf} = area of steel reinforcement crossing the interface.

f_y = yield stress of the steel reinforcement.

b_v = width of the section at the interface.

L_{vi} = Interface length.

The nominal shear strength V_{ni} shall not be more than the least of:

- $V_{ni} \leq k_1\ f'_c\ A_{cv}$
- $V_{ni} \leq k_2\ A_{cv}$

Where,

k_1 = fraction of concrete strength resisting the horizontal shear.

k_2 = Limiting horizontal shear strength.

The cohesion coefficient, friction coefficient, and the factors k_1 and k_2 depend on the conditions and the degree of roughness of the interface. That is summarized in the following table:

2.9.4.1 Table 2.7 – Recommended shear-friction coefficients, (AASHTO LRFD Specifications, 2007)

interface condition	Cohesion μ (MPa)	Coefficient of friction μ	K_1	K_2 (MPa)
Clean concrete surface, free of laitance and roughened to 6mm amplitude (Normal weight concrete)	1.90	1.0	0.30	12.5
Clean concrete surface, free of laitance and roughened to 6mm amplitude (Lightweight concrete)	1.90	1.0	0.30	9.0
Normal weight concrete placed monolithically	2.80	1.40	0.25	10.3
Lightweight concrete placed monolithically. Or non-monolithically cast on clean surface, free of laitance and roughened to amplitude of 6mm	1.70	1.0	0.25	6.9
Clean concrete surface, free of laitance and intentionally roughened to 6mm amplitude (Normal weight concrete)	1.70	1.0	0.25	10.3
Clean concrete surface, free of laitance but not roughened	0.52	0.60	0.2	5.5
Concrete anchored to steel by headed studs or steel reinforcement where all steel bars in contact with concrete are clean and paint free	0.17	0.70	0.2	5.5

3. RESEARCH METHODOLOGY

3.1 Introduction

In this chapter, I will summarize the proposed research strategy and method to achieve the objective.

Four composite concrete beams will be modeled and checked for shear friction using finite element software. These four beams are selected from the sixteen beams which were experimented and tested in lab and published in the research paper of Loov & Patnaik, 1994 and the PhD thesis of Anil Patnaik in 1992 in the of the title “Horizontal Shear Strength of Composite Concrete Beams With a Rough Interface”.

The selected beams have different web section, different reinforcement, and long and short flanges.

3.2 Research Approach & Strategy

Shear friction hand calculation for the selected composite concrete beams will be presented. The first beam is marked “Beam-2” as described in the thesis and research paper is of a T section with a total composite depth of 350mm. The width of the precast web is 150mm at the bottom and 75mm at the interface with the topping cast in situ flange which is 120mm in depth and 400mm in width, and the beam length is 3200mm which is supported on hinge & roller supports at 75mm distance from both edges. The interface between the two parts is clean, free of laitance and intentionally roughened to a full amplitude of 6mm. There are steel ties crossing the interface to increase the horizontal shear strength capacity, which is of 9.5mm diameter, spaced at 500mm. The second beam is marked “Beam-8”, is also a T section with a precast concrete web of a constant breadth equals 150mm and a cast in place topping flange. The stirrups crossing the interface are the same as those of Beam-2.

The third beam is marked “Beam-9”, it is similar to Beam-2, while there is no topping slab at distance 400mm towards the support at both ends of the beam.

The last beam is “Beam-10” and it is similar to Beam-8, while there is no topping slab at distance 400mm towards the support at both ends of the beam.

In this dissertation, 3D "solid" finite element models for the four beams at different loading stages are prepared. The solid elements of the four beams which are being studied have been meshed to a small divided mesh of 50mmx50mm size for more accurate results.

The advantage from using the solid element is the easy assignment of the small element as concrete or steel. In our case, using the solid element allowed us to model and mesh the composite beam with both parts cast in different times with interface and friction between both.

Figure 3.1 shows the first beam as modeled in the 3D model, the beam consists of a cast in situ flange slab of section 400mmx120mm above a precast web of a depth = 230mm and a variable width. The width of the web is 150mm at the bottom and 75mm at the interface with the topping slab. The flange is continuous all over the span of the beam between the supports.

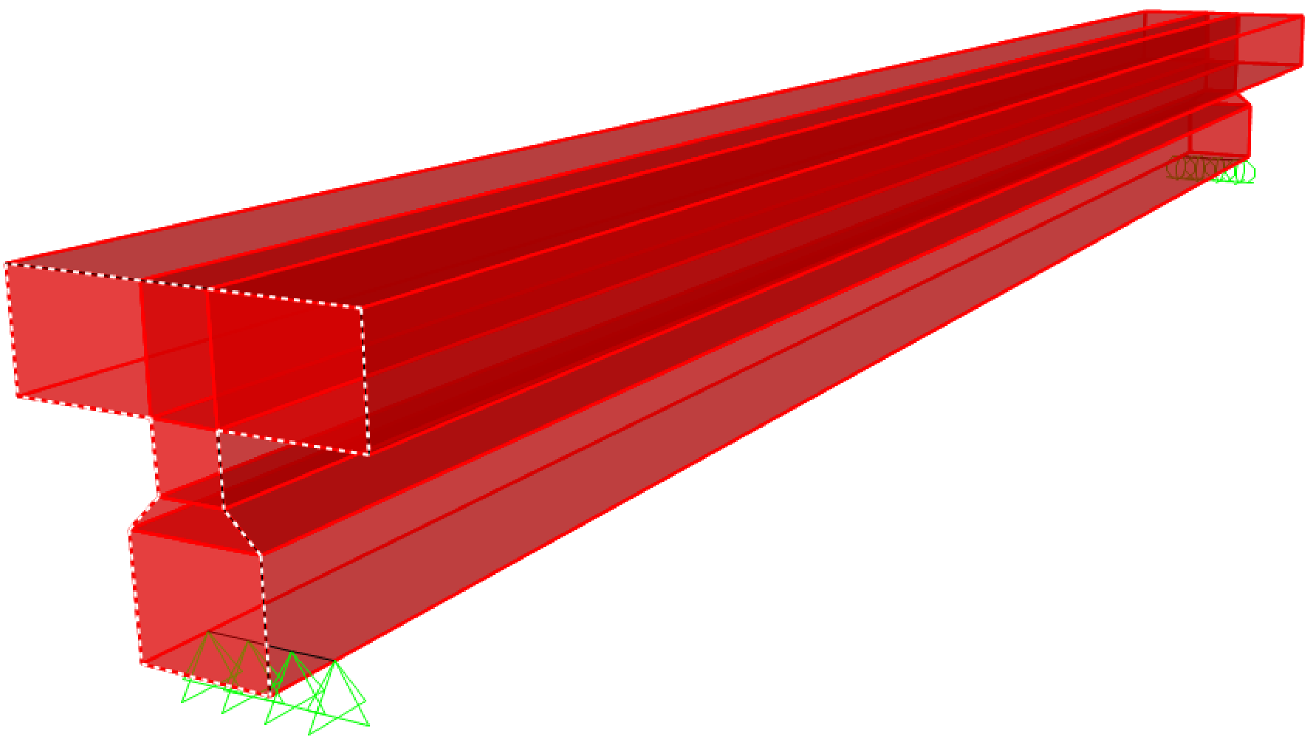

Fig. 3.1 – Modeling of the beam-2 by using the Solid element.

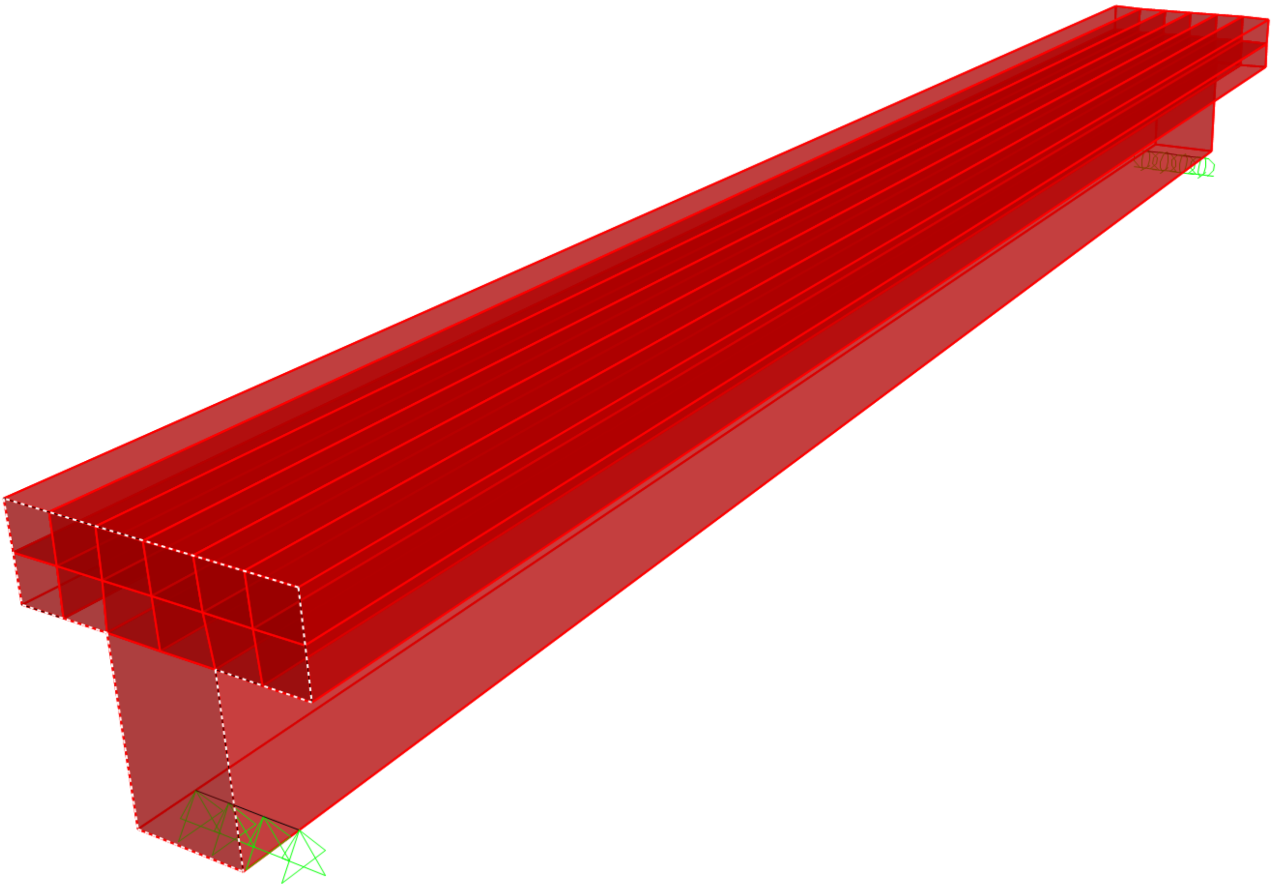

Fig. 3.2 – Modeling of the beam-8 by using the Solid element.

The supports of the beam are hinge and roller at the other end, and a concentrated load was assigned at the middle of the beam span. The horizontal shear failure occurred experimentally when reaching this load.

While in figure 3.2, an illustration of the second beam - 8. the beam consists of a web of uniform section 150mmx230mm and a topping cast in place flange slab of section 400mmx120mm which extends all over the beam length. It is also modeled as a solid element with small mesh size of 50mmx50mm. the smaller mesh size is required for more accurate results.

The third beam - B9 consists of a short-discontinued flange slab of section 400mmx120mm as shown in figure 3.3. The short flange is above a web of a depth = 230mm and a variable width. The width of the web is 150mm at the bottom and 75mm at the interface with the topping slab. It is also modeled as a solid element with small mesh size of 50mmx50mm.

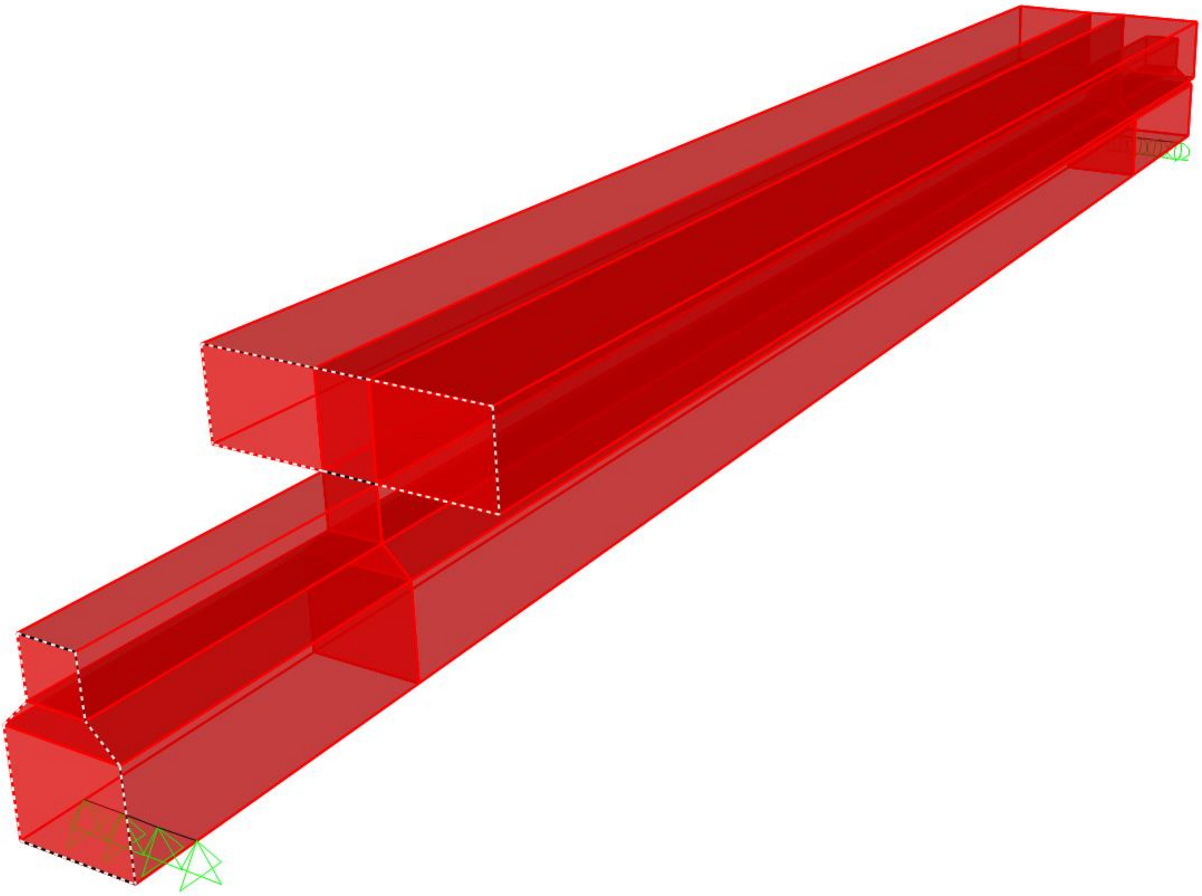

Fig. 3.3 – Modeling of the beam-9 by using the Solid element.

The last studied beam – B10 consists also of a short flange slab of section 400mmx120mm as shown in figure 3.4. The short flange is above a web of a section 150mmx230mm. It is also modeled as a solid element with small mesh size of 50mmx50mm.

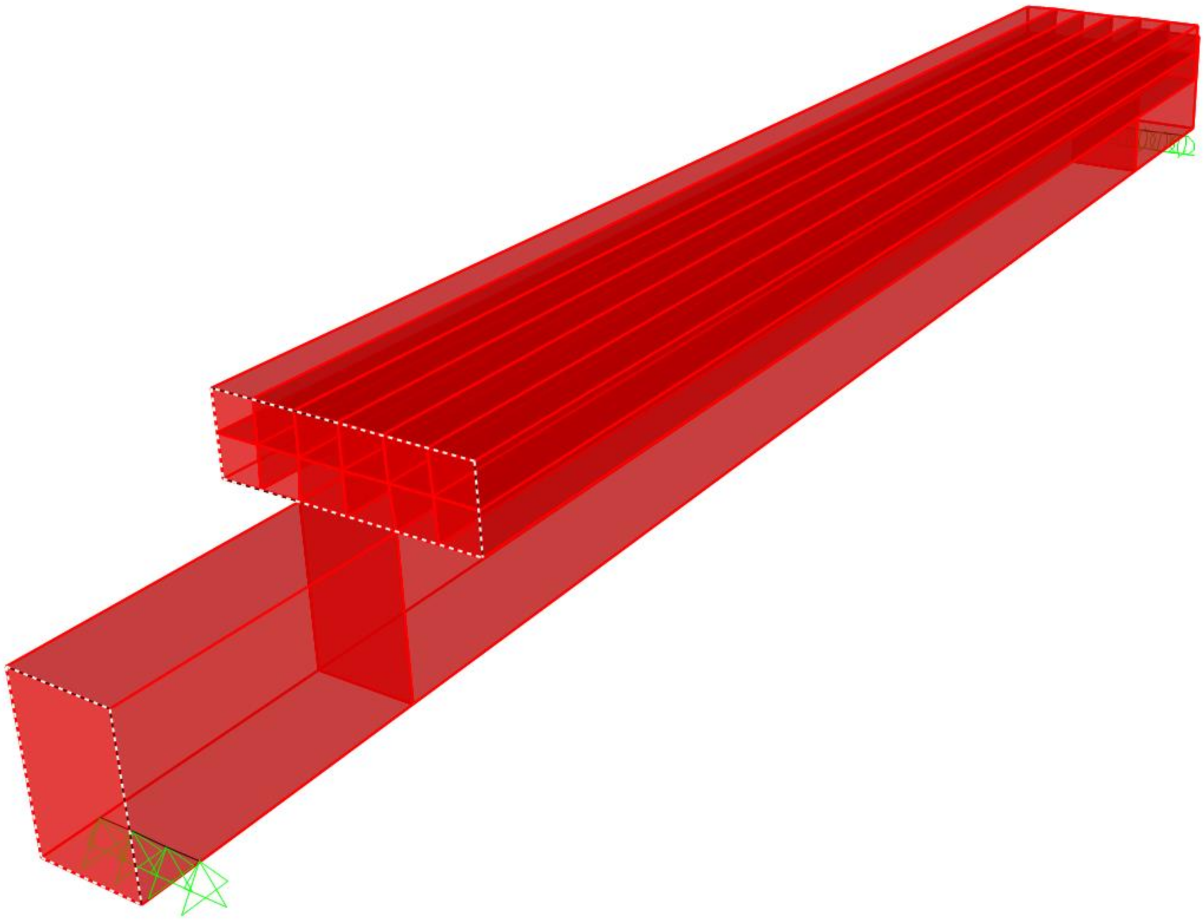

Fig. 3.4 – Modeling of the beam-10 by using the Solid element.

3.3 Long Flange and Short Flange

In the field testing of eight composite beams with flange extending all over the full beam length, it was observed that the interface at both end blocks of the beam was not effective. The end block rotates around the support to absorb the slip of the flange. Cracks at the interface are usually horizontal and the separation is visible, but as it comes closer to the support, then the horizontal cracks meets with diagonal cracks develops in the web at the end block which ended at the support as shown in figure 3.5.

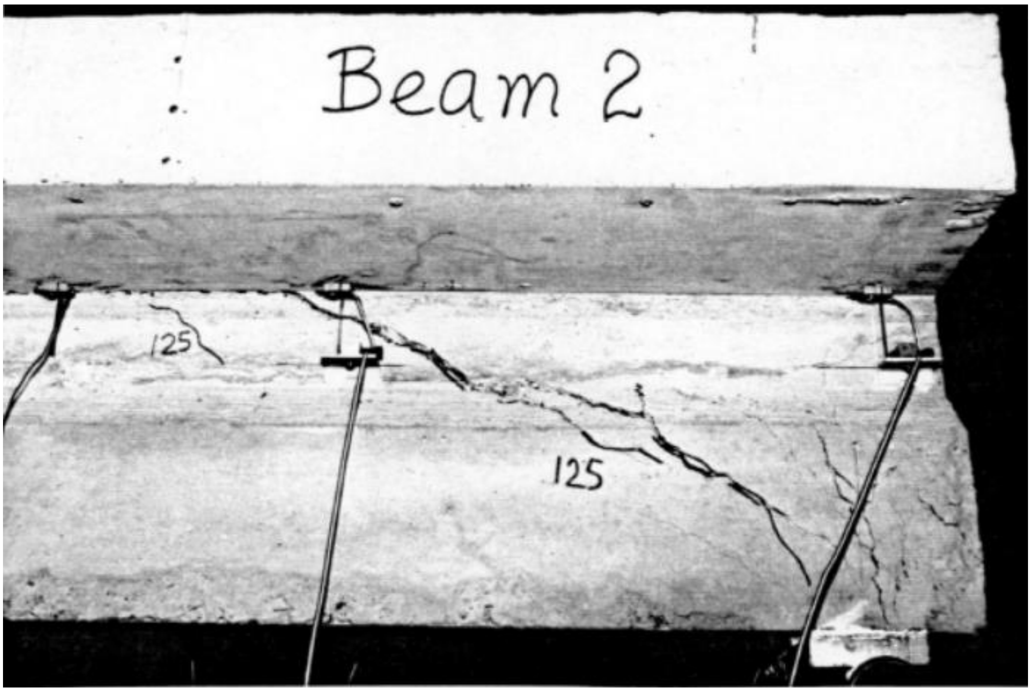

Fig. 3.5 – Horizontal shear failure mode for beams with full length flange.

Since the interface at the end block of the composite beam was noticed to be not effective, Patnaik then tested another eight beams with short and discontinued flanges for a distance of 400mm from the support.

The behavior was almost the same of the beams with full flanges which failed in the horizontal shear except that there were no observed diagonal cracks at the beam ends, refer to figure 3.6.

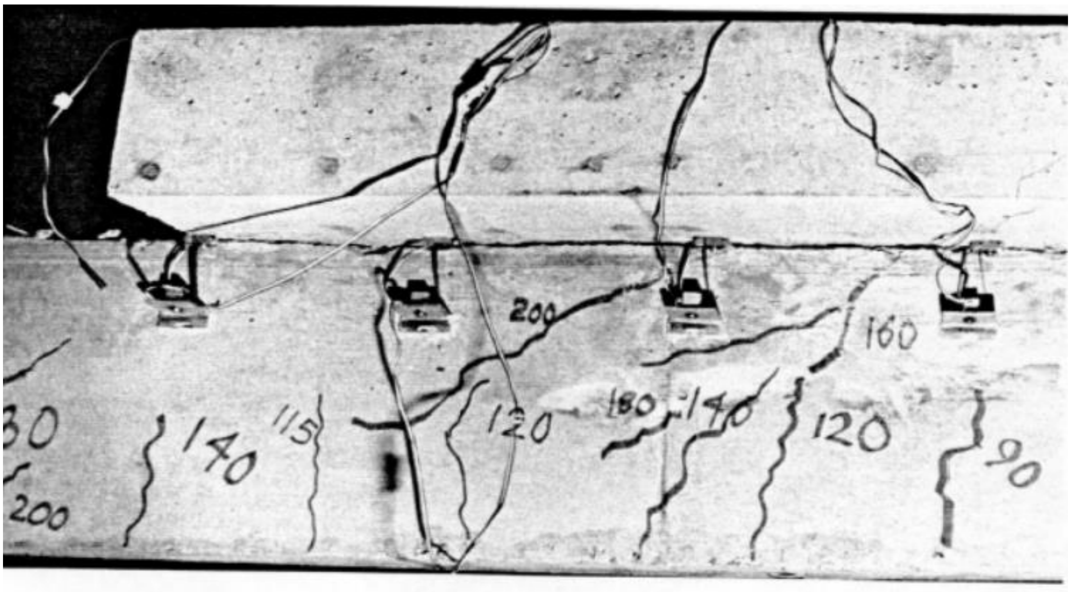

Fig. 3.6 – Horizontal shear failure mode for beams with short-discontinued flange.

The section dimensions of the composite concrete beam, including span, flange length, steel reinforcement and stirrups along with the clamping stress due to steel crossing the interface at the four tested beams are listed in the following table 3.1.

Table (3.1) – Properties of the Test Beams (Geometry and Reinforcement)

Beam No.	Interface width, mm	Width of the soffit, mm	Flange Length, mm	Total Depth, mm	Spacing of 9.5 mm stirrups crossing interface, mm	Bottom Steel (A_s), mm^2	Clamping stress, MPa $\sigma=\rho_v.f_y$
2	150	150	3200	350	500	1600	1.66
8	150	150	3200	350	500	1600	0.77
9	75	150	2400	350	500	2000	1.62
10	75	150	2400	350	500	2000	0.77

The concrete and steel material properties and the assigned concentrated loads at the middle of the four tested beams are listed in the following table 3.2.

Table (3.2) – Properties of the Test Beams (Material Strength and Loading)

Beam No.	f'_c, MPa	f_y, MPa Long steel	f_y, MPa Stirrup	Load (at 0.13mm slip), kN	Load (at 0.5mm slip), kN	Load (at failure), kN
2	34.9	454	438	120.6	151.0	161.7
8	35.6	454	407	177.9	220.3	238.0
9	37.1	431	428	130.9	166.8	170.8
10	37.6	431	409	180.8	256.1	256.1

In the next chapter, the analysis results of the finite element model for these four beams will be presented considering the concentrated loads at horizontal shear failure which were recorded in Patnaik research. Horizontal shear stress, displacements and other related needed output will be summarized along with manual shear friction calculations to compare with the experimental data extracted by Patnaik.

4. RESEARCH RESULTS

4.1 Introduction

In this chapter, I will summarize the horizontal shear output of the analysis for the studied beams from the 3D finite element model.

The beams were loaded with the same load at slip stations of 0.13mm, 0.5mm and at failure which are the same stations considered in the Patnaik experiment. Later a comparison will be done between them.

4.2 Shear Stresses

The horizontal shear stress values are extracted due to the stages of loading which resulted in slip values of 0.13mm, 0.5mm and at failure of the four tested beams 2, 8, 9 and 10. The basic solid element internal stress to be investigated is S13. The beam shear force and stress diagrams due to the concentrated forces are shown in figure 4.1.

According to the elastic method, the horizontal shear stress $v = \frac{V.Q}{I.b_v}$.

Where,

V = Shear force, kN.
I = Moment of inertia of the section, mm^4.
Q =
b_v = Width of the section at interface.

While as per the equilibrium method, the horizontal shear stress $v = \frac{2.C}{Lb_v}$.

Where,

C =
L = Beam Span.
b_v = Width of the section at interface.

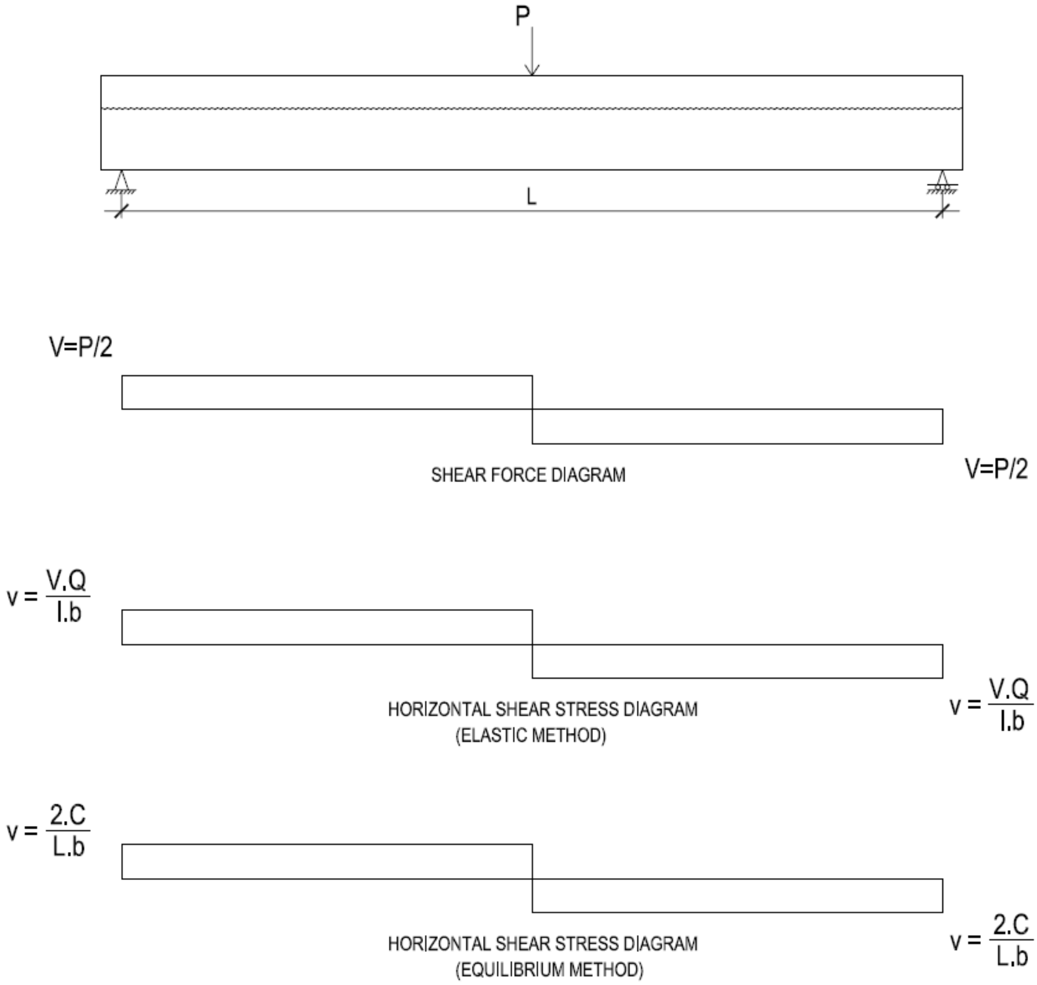

Fig. 4.1 – Horizontal shear stress Diagram for a simply supported beam subject to a concentrated load.

In the following section, a presentation for the contour values of S13 as extracted from the 3D finite element model of each of the four beams.

4.2.1 Beam 2 - Horizontal Shear Stress Contour Range (S13)

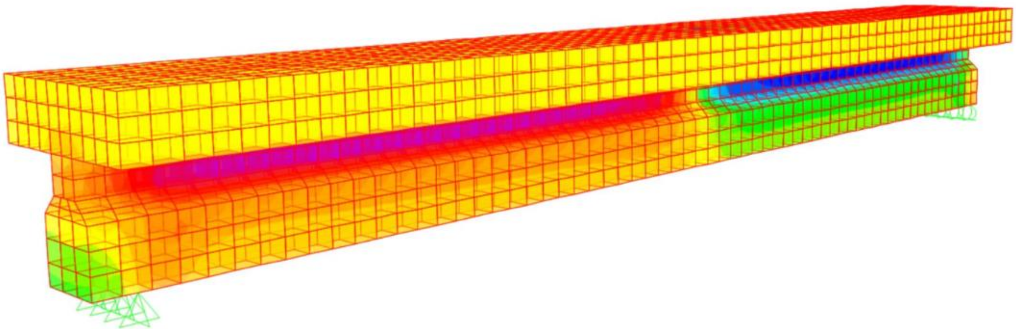

Fig. 4.2 – Horizontal shear stress contour S13 – Beam 2.

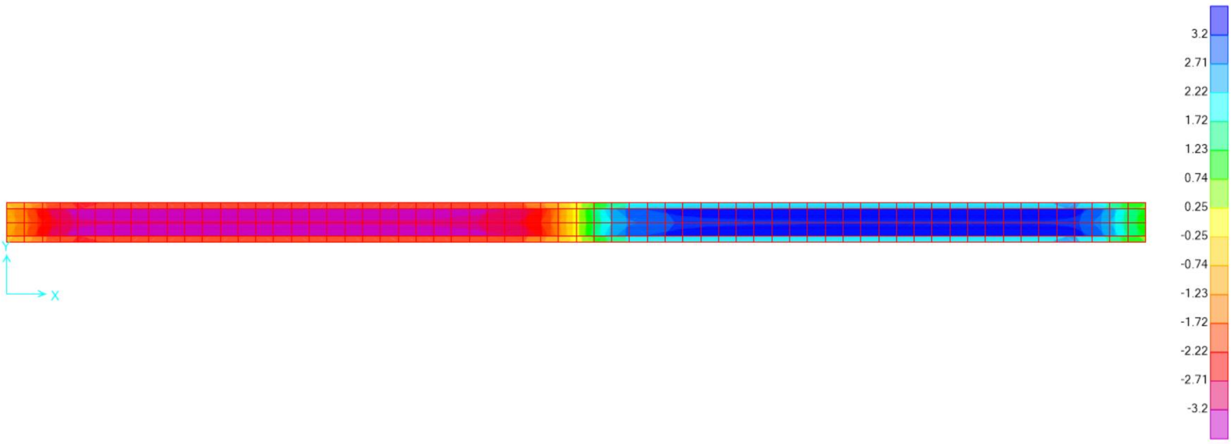

Fig. 4.3– Horizontal shear stress contour S13 at the interface of Beam 2 – (0.13mm slip).

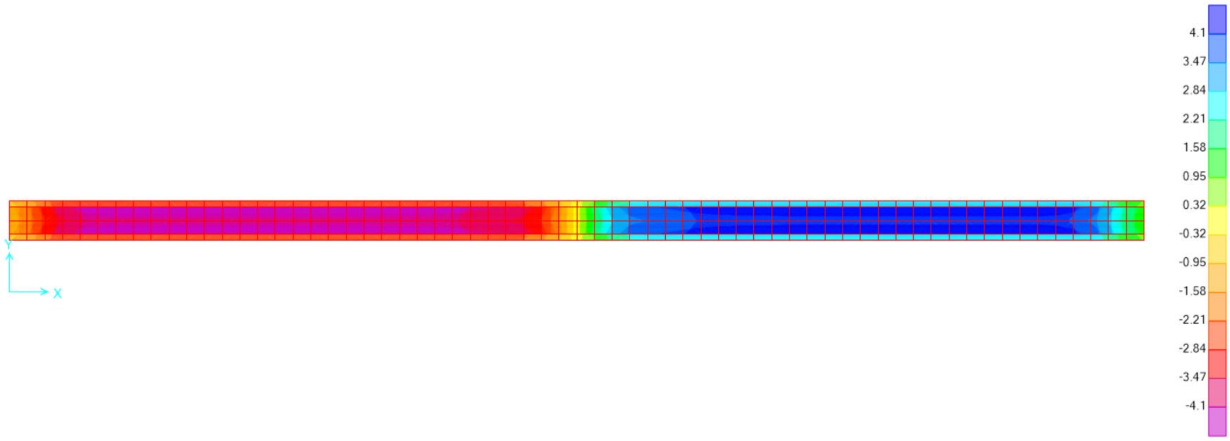

Fig. 4.4 – Horizontal shear stress contour S13 at the interface of Beam 2 – (0.5mm slip).

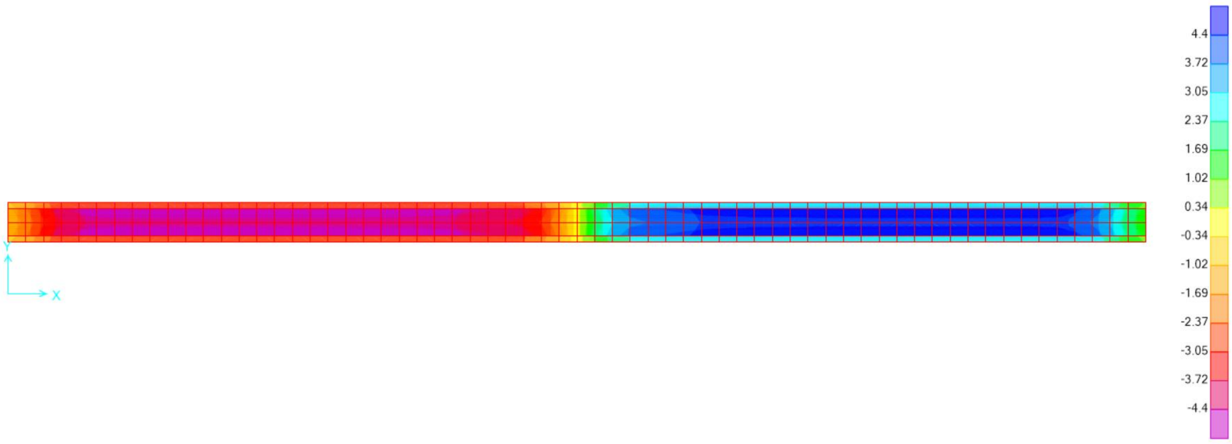

Fig. 4.5 – Horizontal shear stress contour S13 at the interface of Beam 2 – (failure slip).

4.2.2 Beam 8 - Horizontal Shear Stress Contour Range (S13)

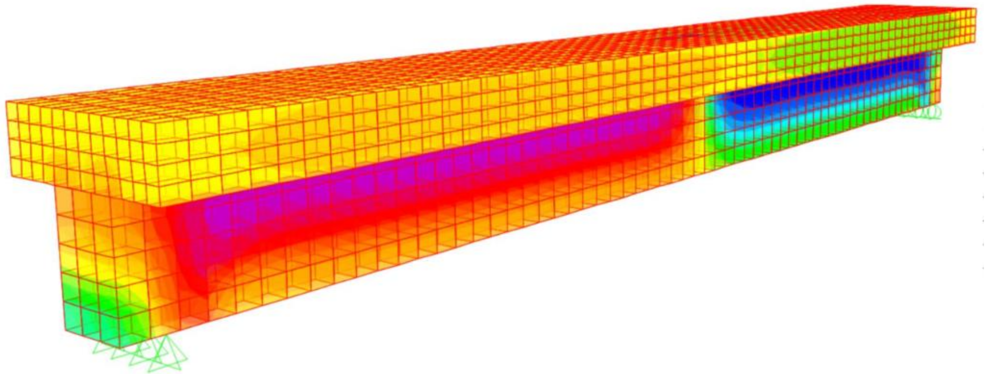

Fig. 4.6 – Horizontal shear stress contour S13 – Beam 8.

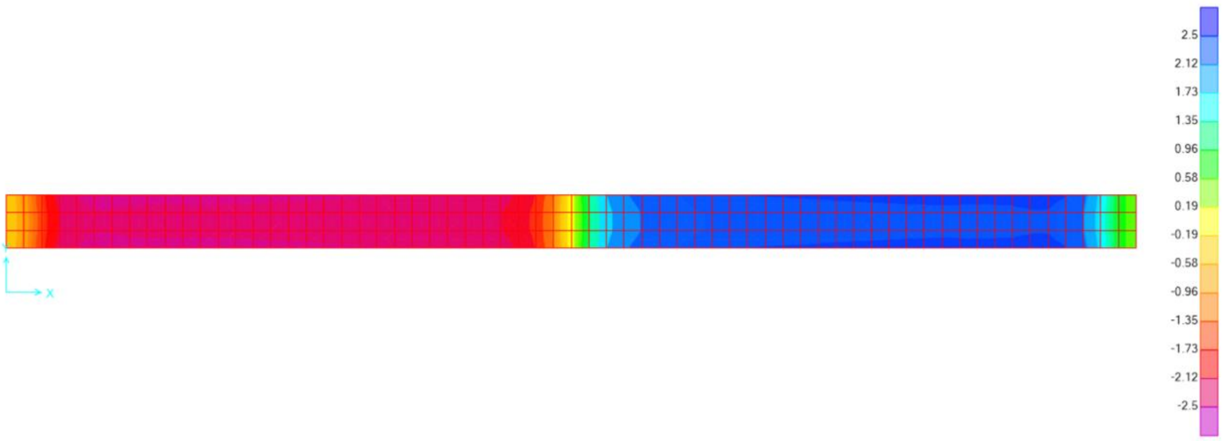

Fig. 4.7 – Horizontal shear stress contour S13 at the interface of Beam 8 – (0.13mm slip).

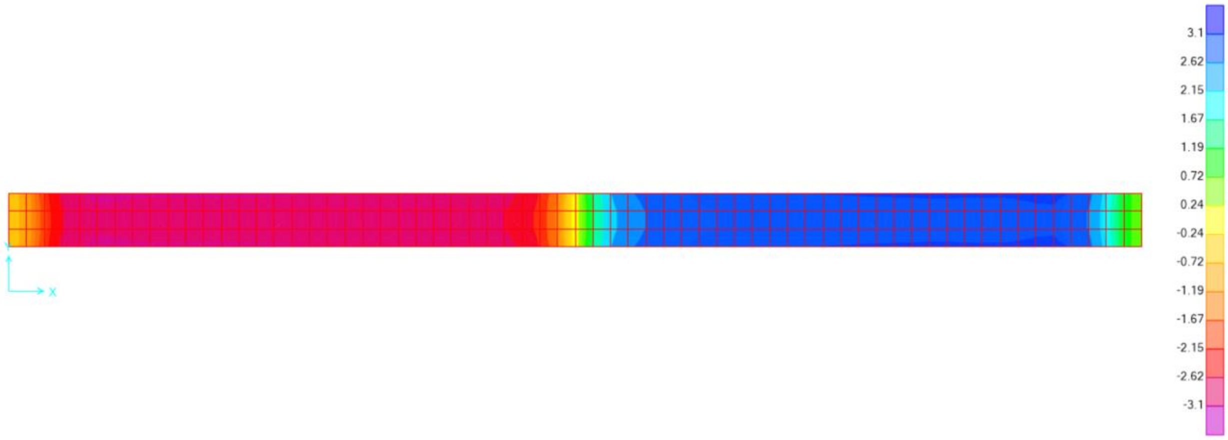

Fig. 4.8 – Horizontal shear stress contour S13 at the interface of Beam 8 – (0.5mm slip).

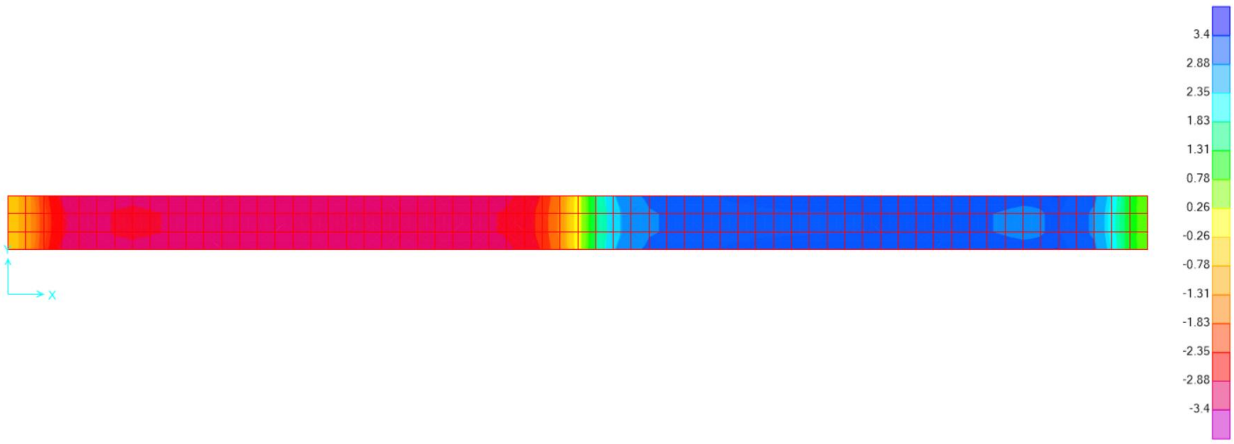

Fig. 4.9 – Horizontal shear stress contour S13 at the interface of Beam 8 – (failure slip).

4.2.3 Beam 9 - Horizontal Shear Stress Contour Range (S13)

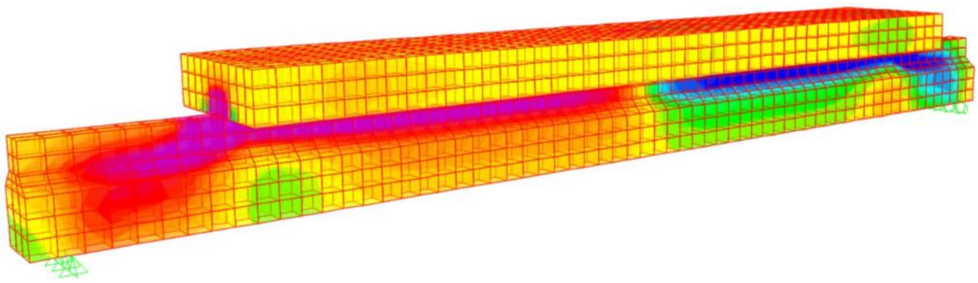

Fig. 4.10 – Horizontal shear stress contour S13 – Beam 9.

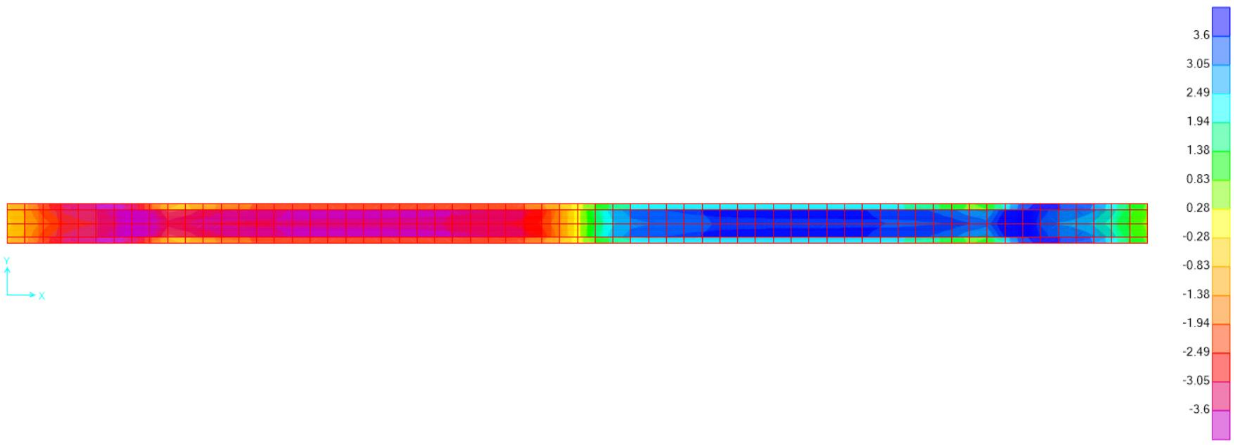

Fig. 4.11 – Horizontal shear stress contour S13 at the interface of Beam 9 – (0.13mm slip).

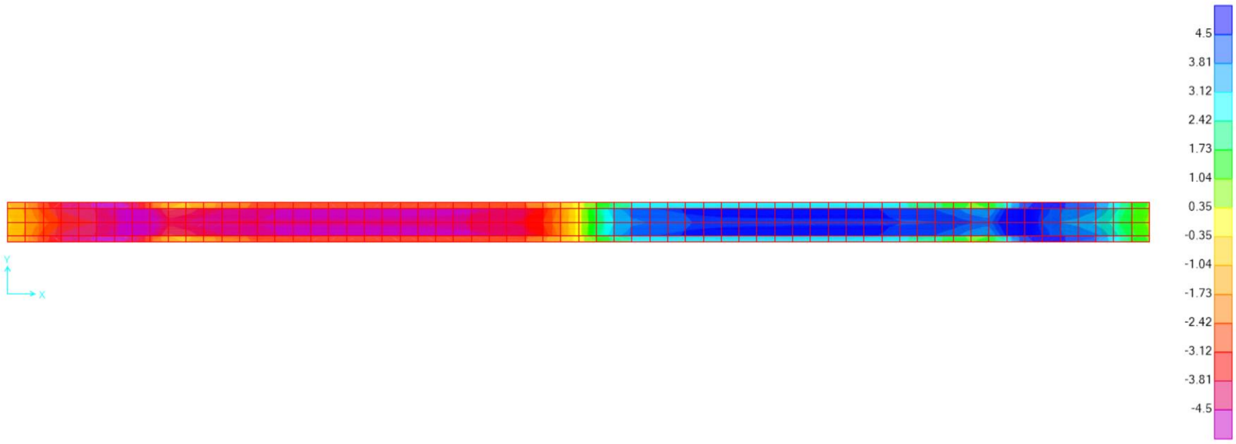

Fig. 4.12 – Horizontal shear stress contour S13 at the interface of Beam 9 – (0.5mm slip).

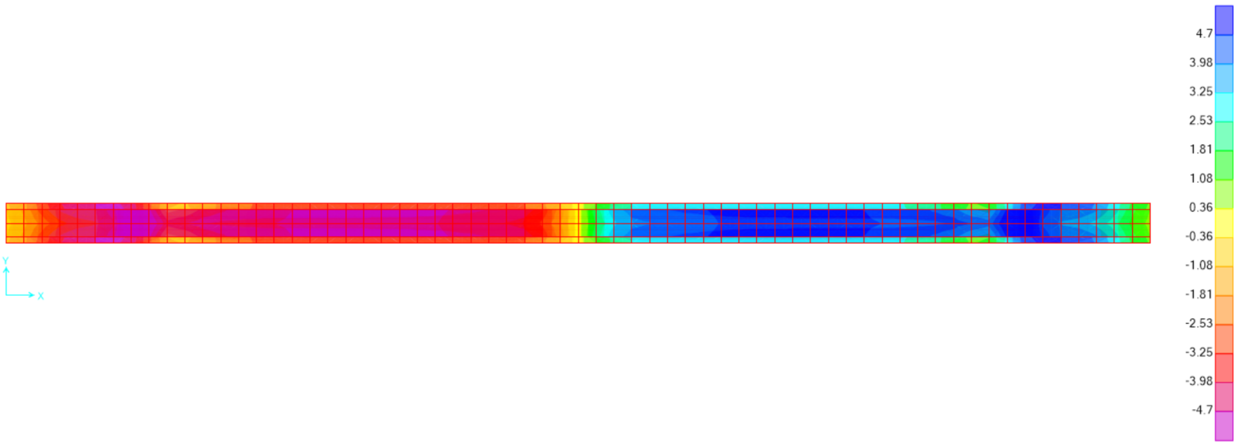

Fig. 4.13 – Horizontal shear stress contour S13 at the interface of Beam 9 – (failure slip).

4.2.4 Beam 10 - Horizontal Shear Stress Contour Range (S13)

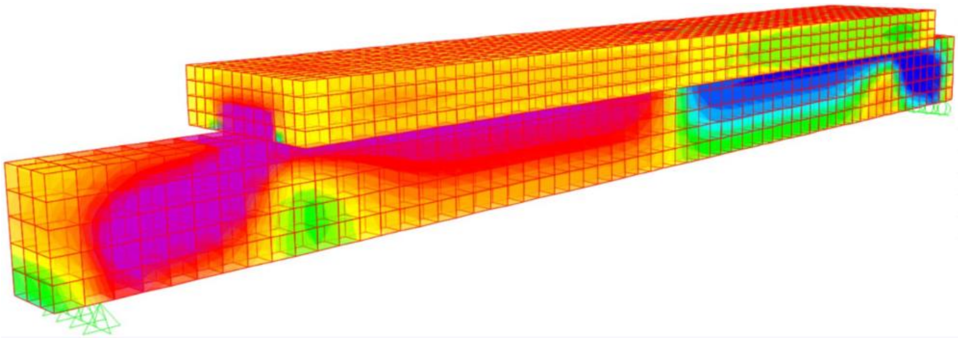

Fig. 4.14 – Horizontal shear stress contour S13 – Beam 10.

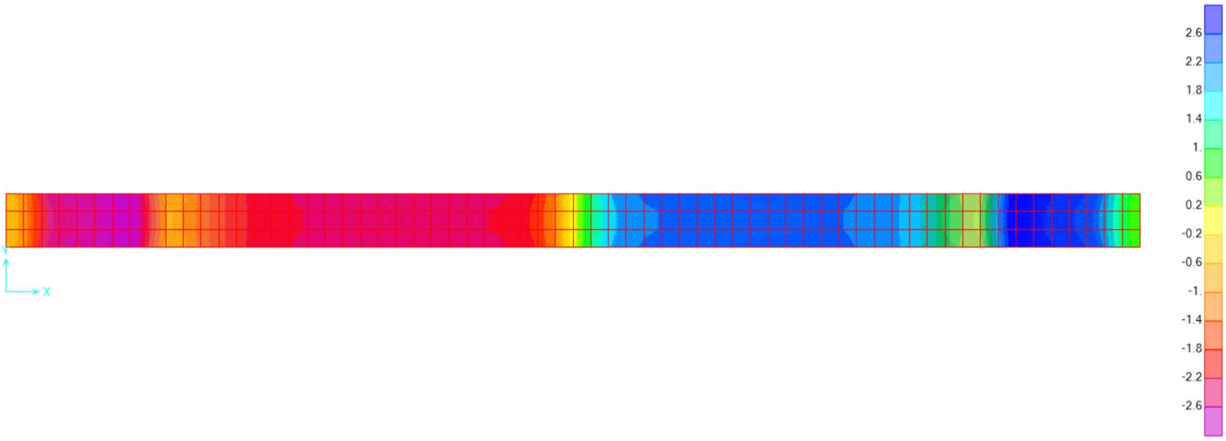

Fig. 4.15 – Horizontal shear stress contour S13 at the interface of Beam 10 – (0.13mm slip).

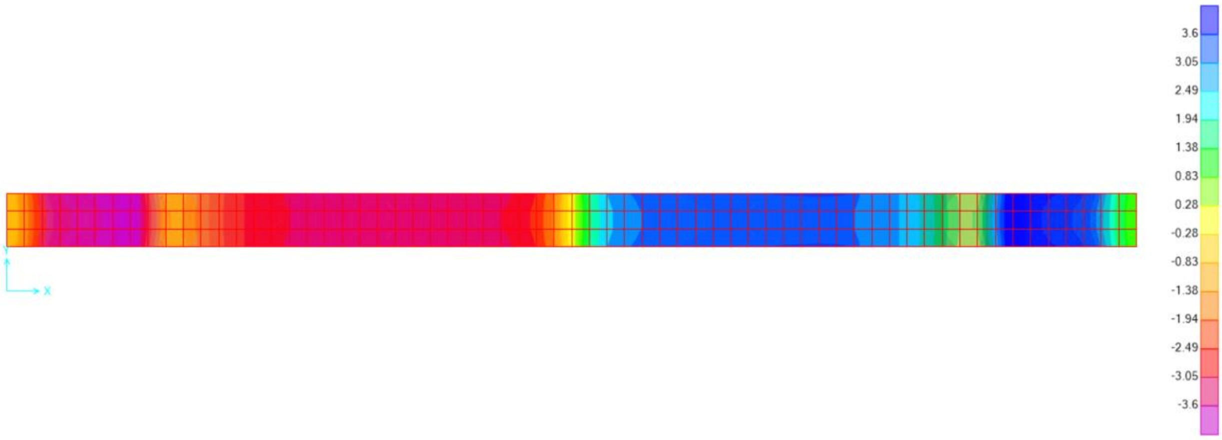

Fig. 4.16 – Horizontal shear stress contour S13 at the interface of Beam 10 – (0.5mm slip).

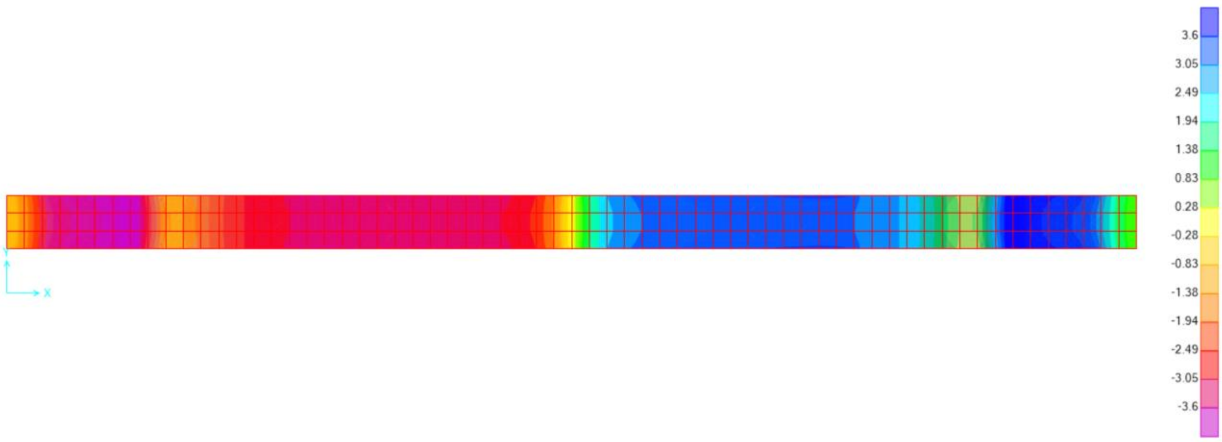

Fig. 4.17 – Horizontal shear stress contour S13 at the interface of Beam 10 – (failure slip).

4.3 Hand Calculation for the Beam Horizontal Shear

The following calculations for the shear friction follow the provisions, design equations and limits proposed by ACI 318-11 code of practice.

* <u>Shear Friction Calculation - Beam-2:</u>

The geometry of the web of beam-2 is not uniform as shown in figure 4.19, a full flange is provided along the span of the beam as drawn at the beam elevation, figure 4.18.

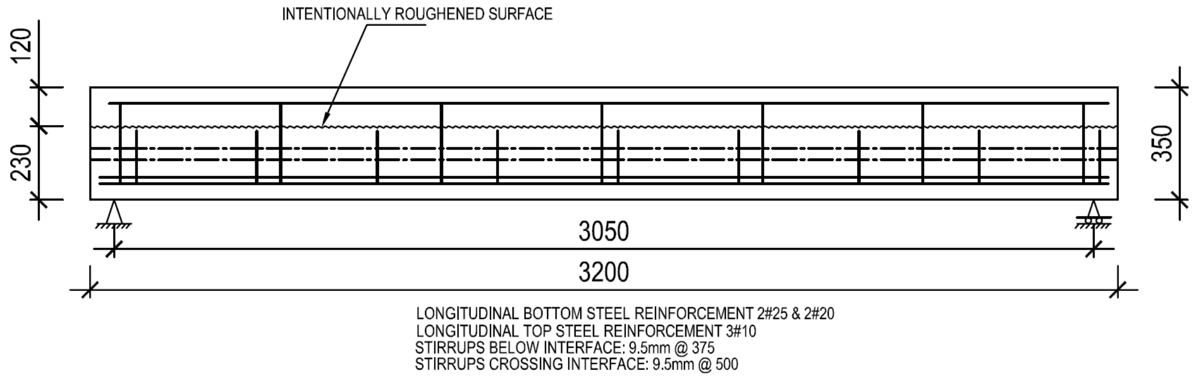

Fig. 4.18 – Reinforcement elevation of Beam-2.

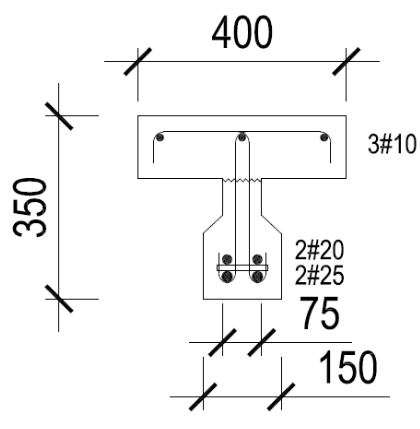

Fig. 4.19 – Reinforcement section of Beam-2.

The interface width b = 75mm.

The beam clear span = 3050mm.

The interface beam length for HL shear design l_{nh} = 0.5*3050mm 1525mm. (simply supported beam, no inflection points).

The provided bottom reinforcement area (A_s) = 2*300 + 2*500 = 1600 mm^2.

The provided top reinforcement area (A_s') = 3*71= 213mm^2.

Stirrups crossing the interface = 2 legs, 9.5mm dia @ 500mm.

f'_c = 34.9 N/mm^2.

E_c = 4100 * √34.9 = 24221 N/mm^2.

E_s = 200 GPa.

Longitudinal reinforcement f_y = 454 N/mm^2.

Stirrups f_{ys} = 438 N/mm^2.

The horizontal bottom force V_{ub} = A_s * f_y = 1600 * 454 /1000 = **727 kN**

The horizontal top force V_{ut} = 0.85 * width*depth of CIP flange * f_c' + (A_s'*f_y) = [0.85*400*120*34.9 + (213*454)]/1000 = **1521 kN**

V_u is the smaller of the top and the bottom horizontal forces, so V_u = **727 kN.**

- $\phi V_{nh} \geq V_u$

The interface shear capacity without ties, with clean surface free of laitance and intentionally roughened =

V_{nh} = (0.55 $b_v.l_{nh}$) ……. (Clause 17.5.3.1)

V_{nh} = 0.55*75*1525/1000 = 62.9 kN.

ϕ V_{nh} = 0.75*62.9 = 47.18 kN.

The interface shear capacity with ties provided, clean surface free of laitance and intentionally roughened to a full amplitude of 6mm =

V_{nh} = (1.8 + 0.6 $\rho_v.f_{ys}$) λ b_v l_{nh}. not greater than 3.5 b_v l_{nh}……… (Clause 17.5.3.3)

The provided stirrups at interface are of 9.5mm dia and spaced @ 500mm, the area is:

Two branches, 9.5mm diameter = 2*71 = 142 mm^2.

V_{nh} = [1.8 + (0.6*142/ (75*500)) * 438] * 1 * 75 * 1525 / 1000 = 319.7 kN.

ϕ V_{nh} = 0.75*319.7 = **239.77 kN**.

3.5 b_v l_{nh} = 3.5*75*1525/1000 = 400.3 kN.

ϕ (3.5 b_v l_{nh}) = 0.75* 400.3 = **300.23 kN < V_u = 727 kN**

The section requires more shear friction reinforcement crossing the interface.

The design for horizontal shear shall be in accordance with clause 11.6.4 & 11.6.5.

The maximum capacity at friction interface = The minimum of

1) ϕ * 0.2 * f'_c * b_v * l_{nh} = 0.75*0.2*34.9*75*1525/1000 = 598.75 kN.
2) ϕ * (3.3+0.08f'_c) *b_v*l_{nh} = 0.75(3.3+0.08*34.9) *75*1525/1000 = 522.58 kN.
3) ϕ * 11 * b_v * l_{nh} = 0.75*11*75*1525/1000 = 943.6 kN.

, **The interface ultimate capacity = 522.58 kN, < V_u = 727 kN.**

The ultimate shear force V_u resulted from the provided bottom reinforcement is greater than the capacity of the section at the interface, so maximum stress is to be limited to the capacity of the section.

The horizontal shear strength at the interface = $\frac{522.58*1000}{75*1525}$ = **4.56 N/mm².**

The required stirrups considering the section capacity are as the following:

$A_{vf} = \phi\ V_n / (f_{ys}\ \mu)$

ϕ V_n = 522.58 kN

f_{ys} = 438 N/mm^2

μ = 1

A_{vf} = 522580/ (438*1) = 1193.1 mm^2

Each stirrup of 2 legs, then the required area per leg = 1193.1/2 = 596.55 mm^2.

Distributing those stirrups over the interface length, consider 400mm spacing.

Then, 596.55/8 = 74.57 mm^2.

10mm dia @ 400mm stirrups are required to cross the interface.

For the purpose of comparison between the results of the experimental work, the 3D finite element model and the manual calculation, we may get the horizontal shear stress corresponding to the slip values recorded in the field work at 0.13mm and 0.5mm by approximation from the calculated shear-friction capacity.

The horizontal shear corresponding to a concentrated load of 120.6 kN, v=3.40 kN/mm^2.

The horizontal shear corresponding to a concentrated load of 151 kN, v=4.26 kN/mm^2.

* **<u>Shear Friction Calculation - Beam-8:</u>**

The geometry of the section of beam-8 is different than beam-2, it has a web of a constant width and different arrangement of the top reinforcement. The bottom reinforcement and stirrups are the same as beam-2. Concrete strength and steel grades were very close.

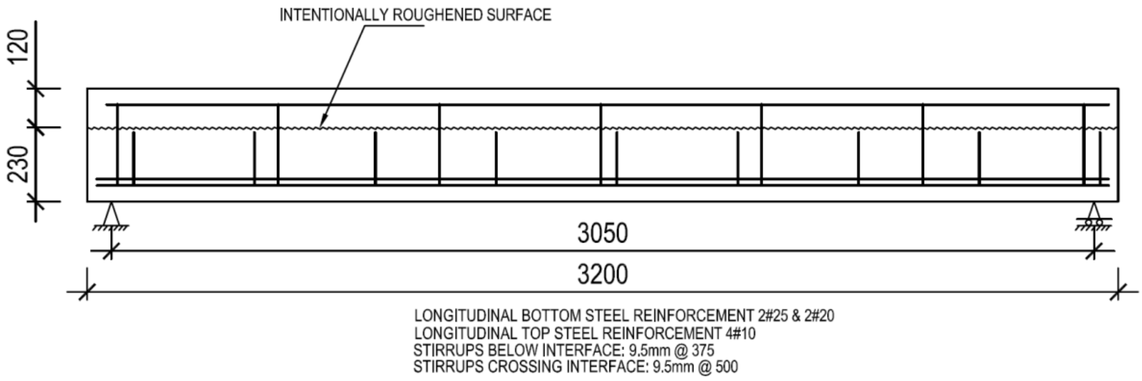

Fig. 4.20 – Reinforcement elevation of Beam-8.

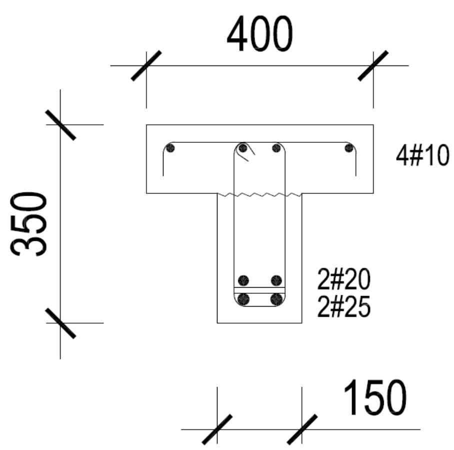

Fig. 4.21 – Reinforcement section of Beam-8.

The interface width b = 150mm.

The beam clear span = 3050mm.

The interface beam length for HL shear design l_{nh} = 0.5*3050mm 1525mm. (simply supported beam, no inflection points).

The provided bottom reinforcement area (A_s) = 2*300 + 2*500 = 1600 mm^2.

The provided top reinforcement area (A_s') = 4*71= 284mm^2.

Stirrups crossing the interface = 2 legs, 9.5mm dia @ 500mm.

f'_c = 35.6 N/mm^2.

E_c = 4100 * √35.6 = 24463 N/mm^2.

E_s = 200 GPa.

Longitudinal reinforcement f_y = 454 N/mm^2.

Stirrups f_{ys} = 407 N/mm^2.

The horizontal bottom force V_{ub} = A_s * f_y = 1600 * 454 /1000 = **727 kN**

The horizontal top force V_{ut} = 0.85 * width*depth of CIP flange * f_c' + (A_s'*f_y) = [0.85*400*120*35.6 + (284*454)]/1000 = **1581 kN**

V_u is the smaller of the top and the bottom horizontal forces, so V_u = **727 kN.**

- $\phi V_{nh} \geq V_u$

The interface shear capacity without ties, with clean surface free of laitance and intentionally roughened =

V_{nh} = (0.55 $b_v.l_{nh}$) ……. (ACI 318-11, Clause 17.5.3.1)

V_{nh} = 0.55*150*1525/1000 = 125.8 kN.

ϕ V_{nh} = 0.75*125.8 = 94.4 kN.

The interface shear capacity with ties provided, clean surface free of laitance and intentionally roughened to a full amplitude of 6mm =

V_{nh} = (1.8 + 0.6 $\rho_v.f_{ys}$) λ b_v l_{nh}. not greater than 3.5 b_v l_{nh}……… (Clause 17.5.3.3)

The provided stirrups at interface are of 9.5mm dia and spaced @ 500mm, the area is:

Two branches, 9.5mm diameter = 2*71 = 142 mm^2.

V_{nh} = [1.8 + (0.6*142/ (150*500)) * 407] * 1 * 150 * 1525 / 1000 = 517.4 kN.

ϕ V_{nh} = 0.75*517.4 = **388 kN**.

3.5 b_v l_{nh} = 3.5*150*1525/1000 = 800.6 kN.

ϕ (3.5 b_v l_{nh}) = 0.75* 800.6 = **600.45 kN < V_u = 727 kN**

The section requires more shear friction reinforcement crossing the interface.

The design for horizontal shear shall be in accordance with clause 11.6.4 & 11.6.5.

The maximum capacity at friction interface = The minimum of

4) ϕ * 0.2 * f'_c * b_v * l_{nh} = 0.75*0.2*35.6*150*1525/1000 = 1200.9 kN.
5) ϕ * (3.3+0.08f'_c) *b_v*l_{nh} = 0.75(3.3+0.08*35.6) *150*1525/1000 = 1045.5 kN.
6) ϕ * 11 * b_v * l_{nh} = 0.75*11*150*1525/1000 = 1887.2 kN.

, **The interface ultimate capacity = 1045.5 kN, > V_u = 727 kN**

so, the horizontal shear stress at the interface of the section = $\frac{727*1000}{150*1525}$ = **3.18 N/mm².**

The required stirrups are as the following:

$A_{vf} = V_u / (\phi\ f_{ys}\ \mu)$

V_u = 727 kN

ϕ = 0.75

f_{ys} = 407 N/mm^2

μ = 1

A_{vf} = 727000/ (0.75*407*1) = 2453.7 mm^2

Each stirrup of 2 legs, then the required area per leg = 2453.7/2 = 1226.86 mm^2.

Distributing those stirrups over the interface length, consider 200mm spacing.

Then, 1226.86/16 = 76.68 mm^2.

10mm dia @ 200mm stirrups are required to cross the interface.

For the purpose of comparison between the results of the experimental work, the 3D finite element model and the manual calculation, we may get the horizontal shear stress corresponding to the slip values recorded in the field work at 0.13mm and 0.5mm by approximation from the calculated shear-friction capacity.

The horizontal shear corresponding to a concentrated load of 177.9 kN, v=2.37 kN/mm^2.

The horizontal shear corresponding to a concentrated load of 220.3 kN, v=2.94 kN/mm^2.

*** Shear Friction Calculation - Beam-9:**

The geometry of the section of beam-9 is similar to beam-2, but the change in the flange length and the provided bottom reinforcement. Concrete strength and steel grades are very close.

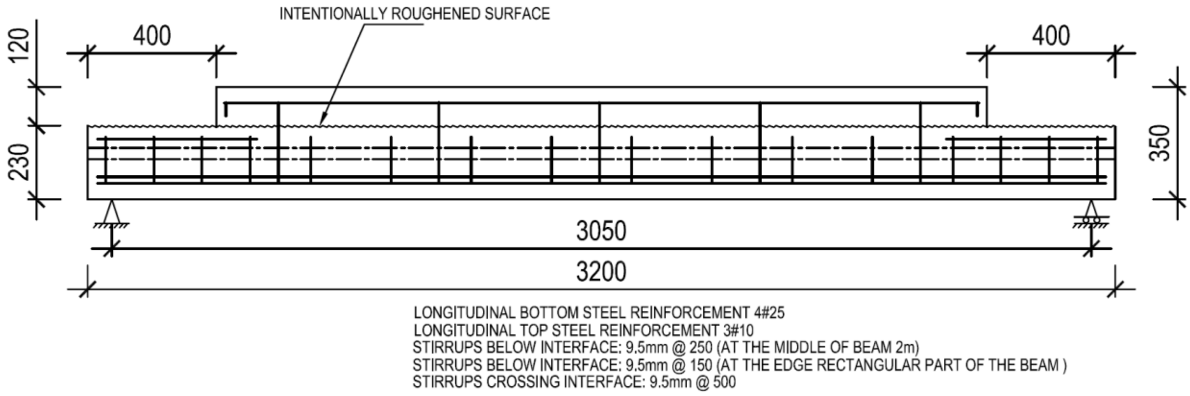

Fig. 4.22 – Reinforcement elevation of Beam-9.

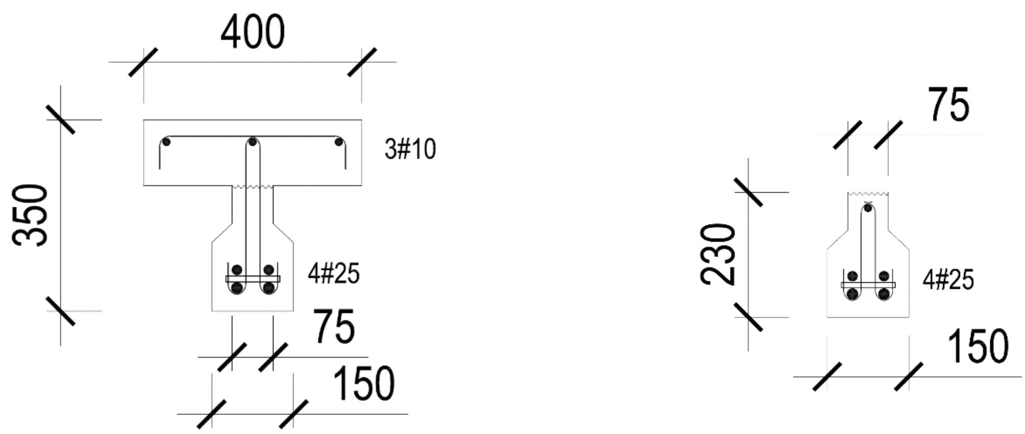

Fig. 4.23 – Beam-9 sections with and without a topping flange.

The interface width b = 75mm.

The beam clear span = 3050mm.

The interface beam length for HL shear design l_{nh} = 0.5*3050mm 1525mm. (simply supported beam, no inflection points).

The provided bottom reinforcement area (A_s) = 4*500 = 2000 mm^2.

The provided top reinforcement area (A_s') = 3*71= 213mm^2.

Stirrups crossing the interface = 2 legs, 9.5mm dia @ 500mm.

f'_c = 37.1 N/mm^2.

E_c = 4100 * √37.1 = 24973 N/mm^2.

E_s = 200 GPa.

Longitudinal reinforcement f_y = 431 N/mm^2.

Stirrups f_{ys} = 428 N/mm^2.

The horizontal bottom force V_{ub} = A_s * f_y = 2000 * 431 /1000 = **862 kN**

The horizontal top force V_{ut} = 0.85 * width*depth of CIP flange * f_c' + (A_s'*f_y) = [0.85*400*120*37.1 + (213*431)]/1000 = **1605.5 kN**

V_u is the smaller of the top and the bottom horizontal forces, so V_u = **862 kN.**

- $\phi V_{nh} \geq V_u$

The interface shear capacity without ties, with clean surface free of laitance and intentionally roughened =

V_{nh} = (0.55 $b_v.l_{nh}$) ……. (Clause 17.5.3.1)

V_{nh} = 0.55*75*1525/1000 = 62.9 kN.

ϕ V_{nh} = 0.75*62.9 = 47.18 kN.

The interface shear capacity with ties provided, clean surface free of laitance and intentionally roughened to a full amplitude of 6mm =

V_{nh} = (1.8 + 0.6 $\rho_v.f_{ys}$) λ b_v l_{nh}. not greater than 3.5 b_v l_{nh}……… (Clause 17.5.3.3)

The provided stirrups at interface are of 9.5mm dia and spaced @ 500mm, the area is:

Two branches, 9.5mm diameter = 2*71 = 142 mm^2.

V_{nh} = [1.8 + (0.6*1.62)] * 1 * 75 * 1525 / 1000 = 317.05 kN.

ϕ V_{nh} = 0.75*317.05 = **237.79 kN**.

3.5 b_v l_{nh} = 3.5*75*1525/1000 = 400.3 kN.

ϕ (3.5 b_v l_{nh}) = 0.75* 400.3 = **300.23 kN < V_u = 862 kN**

The section requires more shear friction reinforcement crossing the interface.

The design for horizontal shear shall be in accordance with clause 11.6.4 & 11.6.5.

The maximum capacity at friction interface = The minimum of

1) ϕ * 0.2 * f'_c * b_v * l_{nh} = 0.75*0.2*37.1*75*1525/1000 = 636.5 kN.
2) ϕ * (3.3+0.08f'_c) *b_v*l_{nh} = 0.75(3.3+0.08*37.1) *75*1525/1000 = 537.68 kN.
3) ϕ * 11 * b_v * l_{nh} = 0.75*11*75*1525/1000 = 943.6 kN.

, **The interface ultimate capacity = 537.68 kN, < V_u = 862 kN.**

The ultimate shear force V_u resulted from the provided bottom reinforcement is greater than the capacity of the section at the interface, so maximum stress is to be limited to the capacity of the section.

The horizontal shear strength at the interface = $\frac{537.68*1000}{75*1525}$ = **4.71 N/mm².**

The required stirrups considering the section capacity are as the following:

$A_{vf} = \phi V_n / (f_{ys}\,\mu)$

ϕV_n = 537.68 kN

f_{ys} = 428 N/mm^2

μ = 1

A_{vf} = 53768/ (428*1) = 1256.3 mm^2

Each stirrup of 2 legs, then the required area per leg = 1256.3/2 = 628.13 mm^2.

Distributing those stirrups over the interface length, consider 250mm spacing.

Then, 628.13/9 = 69.8 mm^2.

10mm dia @ 250mm stirrups are required to cross the interface.

For the purpose of comparison between the results of the experimental work, the 3D finite element model and the manual calculation, we may get the horizontal shear stress corresponding to the slip values recorded in the field work at 0.13mm and 0.5mm by approximation from the calculated shear-friction capacity.

The horizontal shear corresponding to a concentrated load of 130.9 kN, v=3.61 kN/mm^2.

The horizontal shear corresponding to a concentrated load of 166.8 kN, v=4.60 kN/mm^2.

*** Shear Friction Calculation - Beam-10:**

The geometry of the section of beam-10 is similar to beam-8, but the change in the flange length and the provided bottom reinforcement. Concrete strength and steel grades are very close.

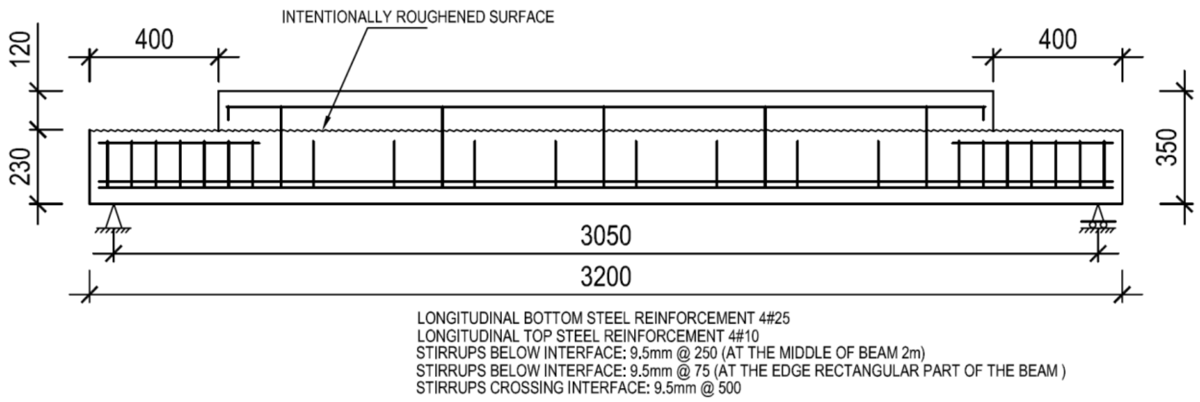

Fig. 4.24 – Reinforcement elevation of Beam-10.

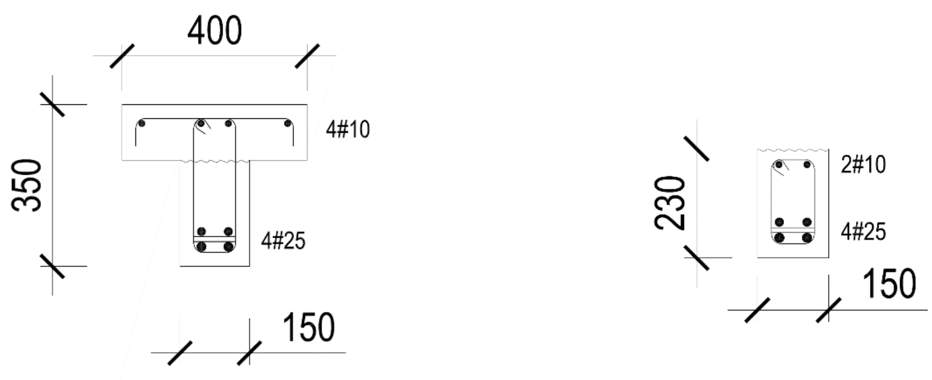

Fig. 4.25 – Beam-10 sections with and without a topping flange.

The interface width b = 150mm.

The beam clear span = 3050mm.

The flange length = 2400mm.

The interface beam length for HL shear design l_{nh} = 0.5*3050mm 1525mm. (simply supported beam, no inflection points).

The provided bottom reinforcement area (A_s) = 4*500 = 2000 mm^2.

The provided top reinforcement area (A_s') = 4*71= 284mm^2.

Stirrups crossing the interface = 2 legs, 9.5mm dia @ 500mm.

f'_c = 37.6 N/mm^2.

E_c = 4100 * √37.6 = 24463 N/mm^2.

E_s = 200 GPa.

Longitudinal reinforcement f_y = 431 N/mm^2.

Stirrups f_{ys} = 409 N/mm^2.

The horizontal bottom force V_{ub} = A_s * f_y = 2000 * 431 /1000 = **862 kN**

The horizontal top force V_{ut} = 0.85 * width*depth of CIP flange * f_c' + (A_s'*f_y) = [0.85*400*120*37.6 + (284*431)]/1000 = **1652 kN**

V_u is the smaller of the top and the bottom horizontal forces, so V_u = **862 kN.**

- $\phi V_{nh} \geq V_u$

The interface shear capacity without ties, with clean surface free of laitance and intentionally roughened =

V_{nh} = (0.55 $b_v.l_{nh}$) ……. (ACI 318-11, Clause 17.5.3.1)

V_{nh} = 0.55*150*1525/1000 = 125.8 kN.

ϕ V_{nh} = 0.75*125.8 = 94.4 kN.

The interface shear capacity with ties provided, clean surface free of laitance and intentionally roughened to a full amplitude of 6mm =

V_{nh} = (1.8 + 0.6 $\rho_v.f_{ys}$) λ b_v l_{nh}. not greater than 3.5 b_v l_{nh}……… (Clause 17.5.3.3)

The provided stirrups at interface are of 9.5mm dia and spaced @ 500mm, the area is:

Two branches, 9.5mm diameter = 2*71 = 142 mm^2.

V_{nh} = [1.8 + (0.6*0.77)] * 1 * 150 * 1525 / 1000 = 517.4 kN.

ϕ V_{nh} = 0.75*517.4 = **388 kN**.

3.5 b_v l_{nh} = 3.5*150*1525/1000 = 800.6 kN.

ϕ (3.5 b_v l_{nh}) = 0.75* 800.6 = **600.45 kN < V_u = 862 kN**

The section requires more shear friction reinforcement crossing the interface.

The design for horizontal shear shall be in accordance with clause 11.6.4 & 11.6.5.

The maximum capacity at friction interface = The minimum of

1) ϕ * 0.2 * f'_c * b_v * l_{nh} = 0.75*0.2*37.6*150*1525/1000 = 1290.15 kN.
2) ϕ * (3.3+0.08f'_c) *b_v*l_{nh} = 0.75(3.3+0.08*37.6) *150*1525/1000 = 1082.22 kN.
3) ϕ * 11 * b_v * l_{nh} = 0.75*11*150*1525/1000 = 1887.19 kN.

, **The interface ultimate capacity = 1082.22 kN, > V_u = 862 kN**

so, the horizontal shear stress at the interface of the section = $\frac{862*1000}{150*1525}$ = **3.77 N/mm^2.**

The required stirrups are as the following:

$A_{vf} = V_u / (\phi f_{ys} \mu)$

V_u = 727 kN

ϕ = 0.75

f_{ys} = 409 N/mm^2

μ = 1

A_{vf} = 862000/ (0.75*409*1) = 2810.11 mm^2

Each stirrup of 2 legs, then the required area per leg = 2810.11/2 = 1405.1 mm^2.

Distributing those stirrups over the interface length, consider 150mm spacing.

Then, 1405.1/15 = 93.67 mm^2.

12mm dia @ 150mm stirrups are required to cross the interface.

For the purpose of comparison between the results of the experimental work, the 3D finite element model and the manual calculation, we may get the horizontal shear stress corresponding to the slip values recorded in the field work at 0.13mm and 0.5mm by approximation from the calculated shear-friction capacity.

The horizontal shear corresponding to a concentrated load of 180.8 kN, v=2.66 kN/mm^2.

5. DISCUSSION OF THE RESULTS

5.1 Introduction

The results of the research will be presented and summarized in this section. A comparison between the simplified code approach, 3D fiber (solid) finite element model and results from the experimental work will be clarified, the related horizontal shear stress values is provided in tables and a comparison charts is to be illustrating the difference between the three different approaches.

5.2 Composite Concrete Beams – Horizontal Shear Stress Comparative Tables and Charts

The following tables show the values of the horizontal shear stress for the four beams which were the case study of this dissertation. In table 5.1, the stress values are considered as a result of loading beam 2 with a certain concentrated load that was previously applied on the real test beam and caused interface slip at three stages; 0.13mm, 0.50mm and 7.44mm at the ultimate failure stage. The same loads are considered in this research using the fiber (solid) finite element model and in the hand calculations.

Table (5.1) – Beam2 – Horizontal Shear Values Comparison

Slip, mm	Load, kN	Horizontal shear stress (Experiment), MPa	Horizontal shear stress (3D FEM Model), MPa	Horizontal shear stress (Code Equations), MPa
0.13	120.6	3.22	3.29	3.40
0.5	151.0	4.0	4.17	4.26
7.44 - failure	161.7	4.27	4.46	4.56

For more clarification of the tabulated results and the relation between the field work, finite element modeling and the code approach, the charts in figure 5.1 illustrates the shear-friction of beam 2 at the different slip stages considering the three approaches; experimental work, 3D model and code hand calculations.

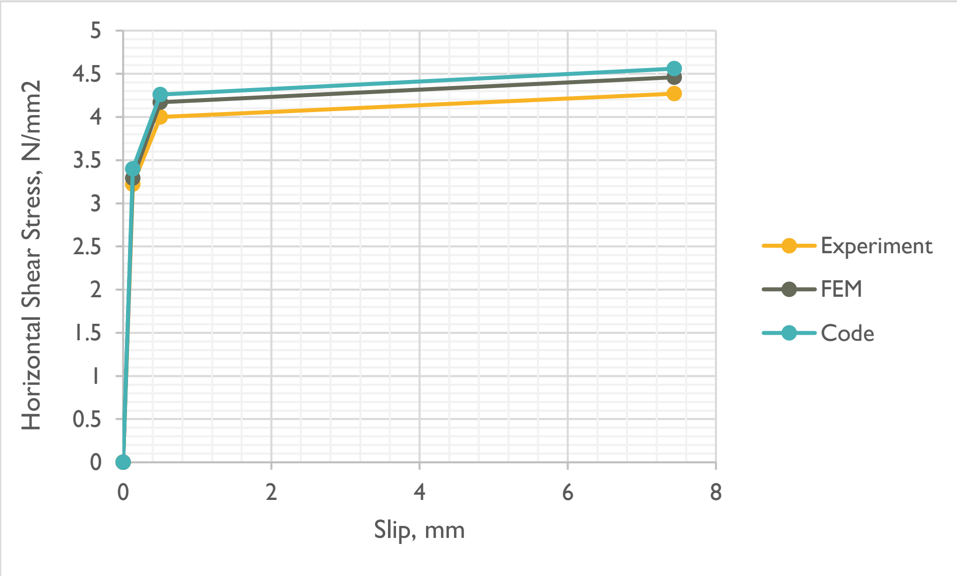

Fig. 5.1 – Horizontal shear stress / slip approach comparison - Beam-2.

Table 5.2 shows the horizontal shear stress values that are considered as a result of loading beam 8 with a certain concentrated load that was previously applied on the real test beam and caused interface slip at three stages; 0.13mm, 0.50mm and 1.09mm at the ultimate failure stage. The same loads are considered in this research using the fiber (solid) finite element model and in the hand calculations.

Table (5.2) – Beam 8 - Horizontal Shear Values Comparison

Slip, mm	Load, kN	Horizontal shear stress (Experiment), MPa	Horizontal shear stress (3D FEM Model), MPa	Horizontal shear stress (Code Equations), MPa
0.13	177.9	2.35	2.59	2.37
0.5	220.3	2.89	3.14	2.94
1.09 - failure	238.0	3.12	3.43	3.18

For more clarification of the tabulated results and the relation between the field work, finite element modeling and the code approach, the charts in figure 5.2 illustrates the shear-friction of beam 8 at the different slip stages considering the three approaches; experimental work, 3D model and code hand calculations.

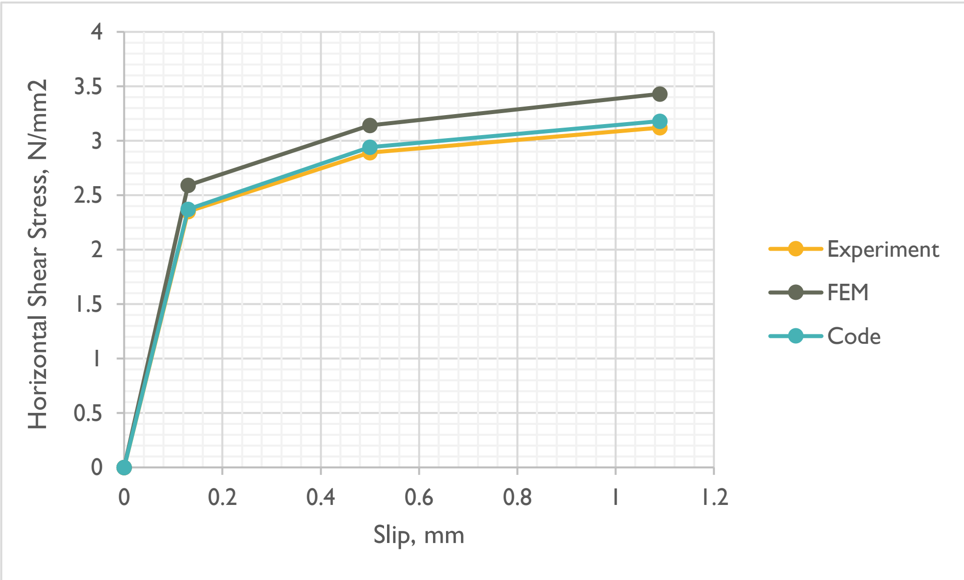

Fig. 5.2 – Horizontal shear stress / slip approach comparison - Beam-8.

Table 5.3 shows the horizontal shear stress values that are considered as a result of loading beam 9 with a certain concentrated load that was previously applied on the real test beam and caused interface slip at three stages; 0.13mm, 0.50mm and 5.54mm at the ultimate failure stage. The same loads are considered in this research using the fiber (solid) finite element model and in the hand calculations.

Table (5.3) – Beam 9 - Horizontal Shear Values Comparison

Slip, mm	Load, kN	Horizontal shear stress (Experiment), MPa	Horizontal shear stress (3D FEM Model), MPa	Horizontal shear stress (Code Equations), MPa
0.13	130.9	3.59	3.64	3.61
0.5	166.8	4.54	4.58	4.60
5.54 - failure	170.8	4.64	4.76	4.71

For more clarification of the tabulated results and the relation between the field work, finite element modeling and the code approach, the charts in figure 5.3 illustrates the shear-friction of beam 9 at the different slip stages considering the three approaches; experimental work, 3D model and code hand calculations.

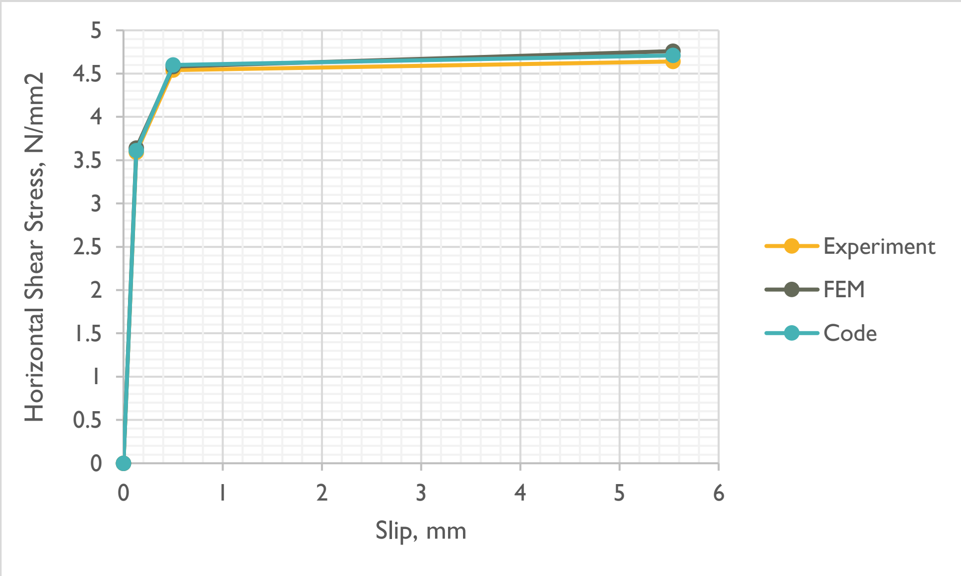

Fig. 5.3 – Horizontal shear stress / slip approach comparison - Beam-9.

Table 5.4 shows the horizontal shear stress values that are considered as a result of loading beam 10 with a certain concentrated load that was previously applied on the real test beam and caused interface slip at three stages; 0.13mm, 0.50mm and 5.74mm at the ultimate failure stage. The same loads are considered in this research using the fiber (solid) finite element model and in the hand calculations.

Table (5.4) – Beam 10 - Horizontal Shear Values Comparison

Slip, mm	Load, kN	Horizontal shear stress (Experiment), MPa	Horizontal shear stress (3D FEM Model), MPa	Horizontal shear stress (Code Equations), MPa
0.13	180.8	2.46	2.61	2.66
0.5	256.1	3.46	3.67	3.77
5.74 - failure	256.1	3.46	3.67	3.77

For more clarification of the tabulated results and the relation between the field work, finite element modeling and the code approach, the charts in figure 5.4 illustrates the shear-friction of beam 10 at the different slip stages considering the three approaches; experimental work, 3D model and code hand calculations.

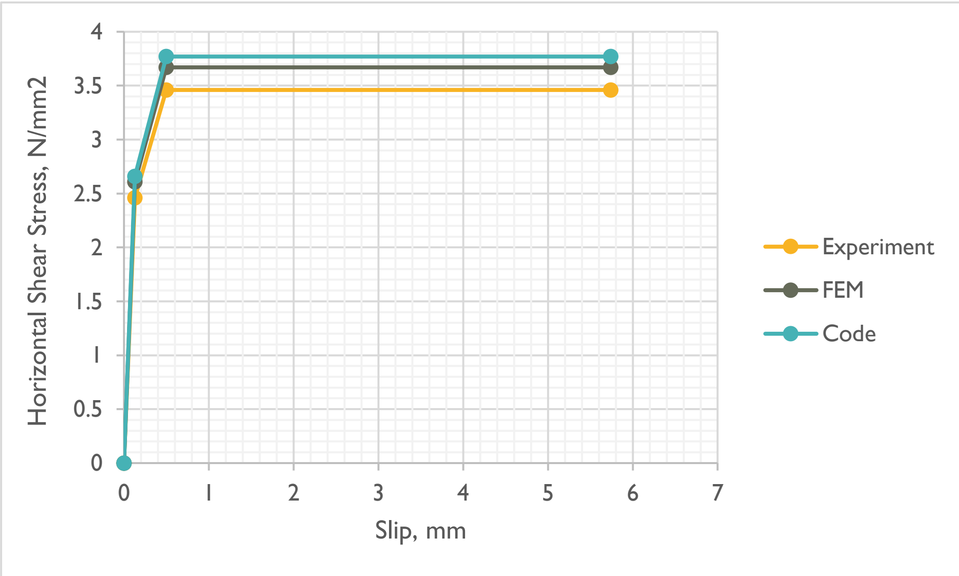

Fig. 5.4 – Horizontal shear stress / slip approach comparison - Beam-10.

6. SUMMARY AND CONCLUSION

This research was about the shear-friction for the composite concrete beams which are cast in two time stages. There are many advantages from using those composite beams as explained earlier, and that is why it is an interesting topic to search about it and try to prove the related theories and the codes provisions.

The research was done on four composite beams of intentionally roughened interface, different section and material properties and different reinforcement but all have the same span of 3200mm, those beams were tested and loaded incrementally to failure in a separate research published by Anil Patnaik in 1992 and later by Loov and Patnaik in 1994.

The scale of the tested beams is small compared to those real beams needed to be produced by this composite way, and that was because of the capacity limitation of the testing laboratory, even though it is still dependable, and the results are quite reasonable.

In this dissertation, the four beams were modeled using a 3D finite element software and also hand calculations were prepared to determine the horizontal shear stress for the beams when subject to different concentrated loads. That hand calculations considered the provisions and equations proposed by ACI 318-11 code.

A comparison then was done between the three approaches of the four beams in a shape of tables and charts.

6.1 Composite Concrete Beams – Horizontal Shear Stress Comparison Conclusion

From the comparison done in the previous chapter, it was noticed that the horizontal shear stress values were very close at the three different methods. However, it was always the least in the experimental case. While the higher stress values were recorded in beam 2 and 10 due to code equations and the higher stresses in beams 8 and 9 were due to the 3D finite element models. These records express that the results are quite accurate, the finite element is a great tool to get horizontal shear results and composite beams cast in two time stages can modeled easily while the hand calculation is also dependable and give the exact area and number of the required stirrups crossing the interface to help the concrete section to resist the horizontal shear stresses and the interface slip.

There is a safety margin in both finite element and the code equations, and that is why the stresses were a bit higher that the lab experiment test.

Finite element analysis is pretty conservative as the beams are modeled in solid sections, and the small divided meshes show a fairly smooth stress pattern.

Design codes also apply safety margin, because it is based on the assumption that the user is doing hand calculations, so extra margin is taken in case of wrong assumptions or some secondary effects are missing out.

6.2 Design Recommendations

In the design of composite concrete beams cast in stages, it is important to take care of the following points:

- Surface condition; should be clean and free of laitance. To get the maximum effective section then the interface surface should also be intentionally roughened to a full amplitude.
- Higher concrete strength has better performance and increase the shear strength.
- The higher ratio of the reinforcement crossing the interface, the higher clamping stress and accordingly higher horizontal shear strength.
- The higher yield strength of the steel, the higher resistance to shear stresses.
- The reinforcement detailing and the anchorage of the steel in both parts of the beam.
- The quality of the concrete mix and the aggregate interlock is very important to enhance the shear-friction.
- Construction sequence is to be considered in the design of the partial precast elements.

6.3 Recommendation for Future Research

- An experimental work with appropriate scale beams is vital to display the research approach and to compare the theoretical results vs experimental results.

- Future researches should be conducted by adopting different concrete compressive strength, and shear-friction comparison is then to be done.

- Future researches should be conducted by adopting different steel yield strength, and shear-friction comparison is then to be done.

7. REFERENCES

- Birkeland, P.W., and Birkeland, H. W., 1966, "Connections in Precast Concrete Construction," ACI Journal Proceedings, V.63, No. 3, March, 1966, pp. 345-368.
- Hofbeck, J.A., Ibrahim, I.O., and Mattock, A.H., 1969, "Shear Transfer in Reinforced Concrete," ACI Journal, Vol. 66, No. 2, February, 1969, pp. 119-128.
- Mattock, A. H., and Hawkins, N. M., 1972, "Shear Transfer in Reinforced Concrete-Recent Research," PCI Journal, V. 17, No. 2, March-April, 1972, pp. 55-75.
- Anderson, A.R., 1960, "Composite Designs in Precast and Cast in Place Concrete," Progressive Architecture, Vol. 41, No. 9, September, 1960, pp. 172-179.
- Mattock, A. H., 1974, "Shear Transfer in Concrete Having Reinforcement at an Angle to the Shear Plane," American Concrete Institute Publication SP-42, Shear in Reinforced Concrete, pp. 17-42.
- Norman W. Hanson, 1960, "Precast-Prestressed Concrete Bridges 2. Horizontal Shear Connections" Journal of the PCA Research and Development Laboratories, Vol. 2, No. 2, 38-58 (May, 1960).
- Mast, R. F., 1968, "Auxiliary Reinforcement in Concrete Connections," Journal of the Structural Division, V. 94, June, pp. 1485-1504.
- Patnaik, Anil Kumar, 1992, "Horizontal Shear Strength of Composite Concrete Beams With a Rough Interface," PhD thesis, Department of Civil Engineering, University of Calgary, Alberta, Canada, December 1992.
- Loov, Robert E., and Patnaik, Anil K., 1994, "Horizontal shear strength of composite concrete beams with a rough interface," PCI Journal, V. 39, No. 1, January-February 1994, pp. 48-69.
- Pedro Miguel Duarte dos Santos, 2009, "Assessment of the shear strength between concrete layers" PhD thesis, University of Coimbra, Portugal, July 2009.
- Kupfer, H., Hilsdorf, H.K. and Rusch, H., 1969, "Behavior of Concrete Under Biaxial Stresses," ACI Journal, Vol. 66, No. 8, August 1969, pp.656-666.
- Mohannad Al-Sherrawi, "Shear and Moment Behavior of Composite Concrete Beams," PhD Thesis, University of Baghdad, Iraq, December 2000.

- Revesz, S., 1953, “Behavior of Composite T-Beams with Prestressed and Unprestressed Reinforcement.” ACI Journal., 49(2), 585-593.
- Saemann, J. C., and Washa, G. W. (1964). “Horizontal Shear Connections between Precast Beams and Cast-in-Place Slabs.” ACI Journal., 61(11), 1383-1409.
- Walraven, J.C & H.W. Reinhardt, 1981, “Theory and Experiments on the Mechanical Behaviour of Cracks in Plain and Reinforced Concrete Subjected to Shear Loading”, Heron, Vol. 26, No. 1A, 1981, pp.2.
- Walraven, J, J. Frenay & A. Pruijssers, 1987, “Influence of Concrete Strength and Load History on Shear Friction Capacity of Concrete Members”, PCI Journal, January-February 1987, pp. 66-84.
- Badoux, J. C., and Hulsbos, C. L., 1967, “Horizontal Shear Connection in Composite Concrete Beams under Repeated Loads.” ACI Journal., 64 (12), 811-819.
- Mattock, A. H.; Johal, L.; and Chow, H. C., 1975, “Shear Transfer in Reinforced Concrete with Moment or Tension Acting Across the Shear Plane,” PCI Journal, V. 20, No. 4, July-August, pp. 76-93.
- Mattock, A. H.; Li, W. K.; and Wang, T. C., 1976, “Shear Transfer in Lightweight Reinforced Concrete,” PCI Journal, V. 21, No. 1, January-February, pp. 20-39.
- Mattock, A. H., 1977, discussion of “Considerations for the Design of Precast Concrete Bearing Wall Buildings to Withstand Abnormal Loads,” by PCI Committee on Precast Concrete Bearing Wall Buildings, PCI Journal, V. 22, No. 3, May-June, pp. 105-106.
- Patnaik, A. K., 2001, “Behavior of Composite Concrete Beams with Smooth Interface,” Journal of Structural Engineering, April 2001.
- Jonathan D. Kovach and Clay Natio, “Horizontal shear capacity of composite concrete beams without interface ties,” PCI / PITA Research project, Lehigh University, June 2008, ATLSS Report No. 08-05.
- Valluvan, R., Kreger, M. E. and Jirsa, J. O., 1999, “Evaluation of ACI 318-95 Shear-Friction Provisions,” ACI Structural Journal, Vol. 96, No. 4, pp. 473-483, July-August 1999.
- Mattock, A.H., 2001, “Shear Friction and High-Strength Concrete,” ACI Structural Journal, V. 98, No. 1, January-February, pp. 50-59.
- Vecchio, F.J. & Collins M.P., 1986, “The Modified Compression-Field Theory for Reinforced Concrete Elements Subjected to Shear,” ACI Journal, March-April 1986, pp. 219-231.

- Katrin Marie Wieneke, 2019, “Horizontal Shear Design of Concrete Interfaces in Beam and Slab Structures”, PhD Thesis, Aachen University of Applied Sciences.
- David Darwin, Charles W. Dolan & Arthur H. Nilson, 2016, “Design of Concrete Structures, Fifteenth Edition” Published by McGraw-Hill Education, ISBN 978-0-07-339794-8, MHID 0-07-339794-6.
- Pedro M. Santos & Eduardo N. Julio, 2011, “Factors Affecting Bond between New and Old Concrete,” ACI Material Journal, July-August 2011.
- Pedro M. Santos & Eduardo N. Julio, 2014, “Interface Shear Transfer on Composite Concrete Members,” ACI Structural Journal, January-February 2014.
- L. F. Kahn & A. D. Mitchell, 2002, “Shear Friction Tests with High-Strength Concrete,” ACI Structural Journal, January-February 2002.
- Kent A. Harries, Gabriel Zeno, and Bahram Shahrooz, 2012, “Toward an Improved Understanding of Shear-Friction Behavior,” ACI Structural Journal, November-December 2012.
- Lesley H. Sneed, Samantha Wermager & Kristian Krc, 2016, “Interface Shear Transfer of Lightweight Aggregate Concretes with Different Lightweight Aggregates”, research report submitted to The Precast/Prestressed Concrete Institute, Chicago, IL60606.
- Zhuangcheng Fang, Haibo Jiang, Airong Liu, Jiahui Feng and Yuanhang Chen, 2018, “Horizontal Shear Behaviors of Normal Weight and Lightweight Concrete Composite T-Beams”, a research published by the International Journal of Concrete Structures and Materials.
- Samantha Lynn Wermager, 2015, “Shear-friction of sand-lightweight Clay and Slate Aggregate Concretes with Varied Reinforcement Ratios”, thesis, Missouri University of Science and Technology, US.
- K.H. Tan, L. W. Guan, X. Lu, and T. Y. Lim, 1999, “Horizontal Shear Strength of Indirectly Loaded Composite Concrete Beams”, ACI Structural Journal, July-August 1999.
- ACI 318-11, “Building Code Requirements for Reinforced Concrete” and commentary, American Concrete Institute, Farmington Hills, MI 48331.
- PCI Design Handbook, 2010, “Precast and Prestressed Concrete”, 7th Edition, Prestressed Concrete Institute, 200 West Adams Street, Chicago, IL 60606-5230.

- EN 1992-1-1, 2004 – Eurocode 2 – "Design of Concrete Structures – Part 1-1": General Rules and Rules for Buildings, European Standard (Incorporating Corrigenda January 2008 and November 2010).
- AASHTO LRFD Bridge Design specifications, American Association of State Highway and Transportation Officials, 4th edition, SI units edition, 2007, ISBN 1-56051-354-3, 1526 P.
- CIRSOC 201 – Argentinian Design Code for Concrete Structures, National Institute of Industrial Technology, Buenos Aires, Argentinian Republic, July 2005, 642 p.